

UNIVERSIDADE ESTADUAL DE CAMPINAS

Faculdade de Engenharia Química



ALEXANDRO BARBOSA DE SOUZA

ESTUDOS *IN VITRO* E *IN VIVO* DA ADMINISTRAÇÃO ORAL DO ÁCIDO
HIALURÔNICO NAS FORMAS LIVRES E NANOESTRUTURADAS

CAMPINAS

2019



ALEXANDRO BARBOSA DE SOUZA

ESTUDOS *IN VITRO* E *IN VIVO* DA ADMINISTRAÇÃO ORAL DO ÁCIDO
HIALURÔNICO NAS FORMAS LIVRES E NANOESTRUTURADAS

*Tese apresentada à Faculdade de
Engenharia Química da Universidade
Estadual de Campinas como parte dos
requisitos exigidos para a obtenção do título
de Doutor em Engenharia Química*

Orientadora: Prof^a. Dr^a. Maria Helena Andrade Santana
Coorientador: Prof. Dr. Marco Vinicius Chaud

ESTE EXEMPLAR CORRESPONDE À VERSÃO FINAL
DA TESE DEFENDIDA PELO ALUNO ALEXANDRO
BARBOSA DE SOUZA E ORIENTADA PELA PROF^A. DR^A.
MARIA HELENA ANDRADE SANTANA.

A handwritten signature in black ink, which appears to read "M.H. Santana", is written over a horizontal line.

CAMPINAS

2019

Agência(s) de fomento e nº(s) de processo(s): CAPES, 33003017034P8

ORCID: <https://orcid.org/0000-0002-0332-0830>

Ficha catalográfica
Universidade Estadual de Campinas
Biblioteca da Área de Engenharia e Arquitetura
Elizangela Aparecida dos Santos Souza - CRB 8/8098

Souza, Alexandre Barbosa de, 1989-
So89e Estudos *in vitro* e *in vivo* da administração oral do ácido hialurônico nas formas livres e nanoestruturadas / Alexandre Barbosa de Souza. – Campinas, SP: [s.n.], 2019.

Orientador: Maria Helena Andrade Santana.

Coorientador: Marco Vinicius Chaud.

Tese (doutorado) – Universidade Estadual de Campinas, Faculdade de Engenharia Química.

1. Ácido hialurônico. 2. Adesão. 3. Permeação. 4. Absorção. I. Santana, Maria Helena Andrade, 1951-. II. Chaud, Marco Vinicius. III. Universidade Estadual de Campinas. Faculdade de Engenharia Química. IV. Título.

Informações para Biblioteca Digital

Título em outro idioma: *In vitro* and *in vivo* studies of oral administration of hyaluronic acid in free and nanostructured forms

Palavras-chave em inglês:

Hyaluronic acid

Adhesion

Permeation

Absorption

Área de concentração: Engenharia Química

Títuloção: Doutor em Engenharia Química

Banca examinadora:

Maria Helena Andrade Santana [Orientador]

Gisella Maria Zanin

Reinaldo Gaspar Bastos

Giuliana Piovesan Alves

Carolina Caliari Oliveira

Data de defesa: 26-02-2019

Programa de Pós-Graduação: Engenharia Química

FOLHA DE APROVAÇÃO

Tese de doutorado defendida por Alexandro Barbosa de Souza e aprovada em 26 de fevereiro de 2019 pela banca examinadora constituída pelos doutores:

Prof^a. Dr^a. Maria Helena Andrade Santana

FEQ/UNICAMP

Dr^a. Gisella Maria Zanin

UEM

Dr. Reinaldo Gaspar Bastos

UFSCar

Dr^a. Giuliana Piovesan Alves

Cristália Produtos Químicos Farmacêuticos Ltda

Dr^a. Carolina Caliarí Oliveira

In Situ Terapia Celular

A Ata da Defesa, assinada pelos membros da Comissão Examinadora, consta no SIGA/Sistema de Fluxo de Tese e na Secretaria do Programa da Unidade.

DEDICATÓRIA

À minha querida e amada família.

AGRADECIMENTOS

À minha querida orientadora Profa. Dra. Maria Helena Andrade Santana pelas orientações acadêmicas e ensinamentos para a vida. Ao meu querido coorientador Prof. Dr. Marco Vinicius Chaud, pela colaboração e constante presteza. Ambos são excepcionais instrutores, um exemplo para a minha vida profissional.

À Fernanda Bortolazzo, que se faz presente em minha vida, e veio para ficar.

Aos meus colegas Rhelvis de Oliveira, André Delano e Gilson Maia do Laboratório de Desenvolvimento de Processos Biotecnológicos pelo companheirismo e bons momentos.

Às doutorandas Thais Francine e Juliana Ferreira e também ao Denicezar do Laboratório de Biomateriais e Nanotecnologia do Parque Tecnológico de Sorocaba pela presteza e amizade.

À Isabel Janet e Gabriela Pérez pelo carinho e pela amizade.

À Coordenação de Aperfeiçoamento de Pessoal de Nível Superior (CAPES) pelo apoio financeiro.

Even if you had completed your third year . . . in the University, and were perfect in the theory of the subject, you would still find that there was need of many years of experience, before you could move in a fashionable crowd without jostling against your betters.

From Abbott's Flatland

RESUMO

O ácido hialurônico (AH) é um glicosaminoglicano com ampla distribuição tecidual. A administração do AH exógeno tem sido objeto de intensos estudos na biologia articular, mucosal e patofisiologia porque possui propriedades anti-inflamatória e restauradora dos níveis endógenos. O AH oral tem ganhado atenção para propósitos preventivos e terapêuticos de doenças articulares e das mucosas, adquirindo uma crescente aceitação devido aos baixos custos de administração. Apesar deste avanço, o efeito da estrutura do AH na sua captação intestinal não é investigado. Neste contexto, o objetivo deste trabalho foi estudar os fenômenos de adesão e de permeação intestinal e a absorção do AH nas formas livres e nanoestruturadas, em modelos *ex vivo* e *in vivo* de mucosa intestinal de ratos. Um estudo da força e do trabalho de adesão do AH em mucina tipo III de estômago de porco e em mucosa intestinal de ratos selecionou as melhores formulações para o estudo de permeação intestinal e de absorção *in vivo*. A força de destacamento e o trabalho de adesão, a taxa de captação intestinal e o *clearance* vascular do AH exógeno foram variáveis responsivas aos seus aspectos estruturais (tamanhos de partículas, distribuição e potencial zeta), influenciados pela pureza, distribuição de massa molar, concentração e estabilidade química. AH livre com fração 10^5 Da e nanoparticulado com tamanhos inferiores a 200 nm foram adequadas para atender simultaneamente o metabolismo da microbiota e a reposição dos níveis de concentrações teciduais. Estes resultados mostram a relevância dos aspectos estruturais do AH para o entendimento fenomenológico da captação intestinal, impactando na escolha de estruturas mais favoráveis para compor formulações orais.

Palavras-chave: Ácido hialurônico; Arquitetura estrutural; Mucoadesão; Permeação; Absorção.

ABSTRACT

Hyaluronic acid (HA) is a glycosaminoglycan with wide tissue distribution. The administration of exogenous HA has been the object of intense studies in the articular and mucosal biology and pathophysiology because it has anti-inflammatory and restorative properties of the endogenous levels. Oral HA has gained attention for preventive and therapeutic purposes of joint and mucosal diseases, acquiring a growing patient compliance due to the low administration costs. Despite this advancement, the effect of the HA structure on its intestinal uptake is not investigated. In this context, the objective of this thesis was to study the adhesion and intestinal permeation phenomena and the absorption of HA in free and nanoparticulate forms, in *ex vivo* and *in vivo* models of intestinal mucosa of rats. A study of the detachment force and work of adhesion of HA on the Type III mucin of porcine stomach and intestinal mucosa of rats selected the best formulations for the study of intestinal permeation and absorption *in vivo*. The detachment force and the work of adhesion, the rate of intestinal uptake and the vascular clearance of exogenous HA were variable responsive to their structural aspects (particle sizes, distribution and zeta potential), influenced by the purity, distribution molar mass, concentration and chemical stability. Free HA with fraction 10^5 Da and nanoparticulated of sizes less than 200 nm are adequate to meet both the metabolism of the microbiota and the replacement of tissue concentration levels. These results show the relevance of the structural aspects of HA for the phenomenological understanding of intestinal uptake, impacting on the choice of more favorable structures to compose oral formulations.

Keywords: Hyaluronic acid; Structural architecture; Mucoadhesion; Permeation; Absorption.

LISTA DE ILUSTRAÇÕES

FIGURA 1. (A) DISSACARÍDEO DE AH (B) CONFIGURAÇÃO TRIDIMENSIONAL DO AH	16
FIGURA 2. FLUXOGRAMA MOSTRANDO ADMINISTRAÇÃO ORAL DO AH.....	18
FIGURA 3. ESQUEMA DE APARATO EXPERIMENTAL PARA ESTUDO DE MUCOADESÃO.	22
FIGURA 4. ILUSTRAÇÃO DE RATO VIVO E ALIMENTAÇÃO DE INTESTINO COM FORMULAÇÃO DE AH.....	22

LISTA DE TABELAS

TABELA 1 – RESUMO DE ALGUMAS FORMULAÇÕES ORAIS CONTENDO AH	20
--	----

SUMÁRIO

1	INTRODUÇÃO	15
1.1	ÁCIDO HIALURÔNICO	15
1.2	ÁCIDO HIALURÔNICO ORAL	17
1.3	MERCADO	18
1.4	ESTUDOS DE ADESÃO E ABSORÇÃO INTESTINAL	21
1.4.1	<i>Objetivo</i>	21
2	FUNDAMENTAÇÃO TEÓRICA	25
2.1	HYALURONIC ACID BEHAVIOR IN ORAL ADMINISTRATION AND PERSPECTIVES FOR NANOTECHNOLOGY-BASED FORMULATIONS	26
3	RESULTADOS E DISCUSSÃO	61
3.1	PENETRATION OF FREE AND NANOPARTICLE HYALURONIC ACID IN MUCIN TABLETS AND IN RAT INTESTINAL MUCOSA	62
3.2	INTESTINAL UPTAKE ASSESSMENT OF THE ORAL HYALURONIC ACID IN RATS	107
4	CONCLUSÕES E SUGESTÕES PARA PRÓXIMOS TRABALHOS	134
5	REFERÊNCIAS BIBLIOGRÁFICAS	136
	APÊNDICE	143
	ANEXO I	144
	ANEXO II	145
	ANEXO III	146

APRESENTAÇÃO

Este manuscrito foi estruturado em capítulos. No capítulo 1 são introduzidos o tema, a justificativa e o objetivo do presente estudo. No capítulo 2 é apresentado a fundamentação teórica na forma de artigo de revisão. O capítulo 3 é composto pelas metodologias, os resultados e as discussões, apresentados na forma de artigos científicos. No capítulo 4 são apresentadas a conclusão geral e específicas e as sugestões para trabalhos futuros.

CAPÍTULO 1: INTRODUÇÃO

1 INTRODUÇÃO

1.1 Ácido Hialurônico

Breve Histórico

Karl Meyer e John Palmer identificaram em membrana hialóide de vítreo cortical bovino uma substancia gelatinosa que recebeu o nome de ácido hialurônico (AH) (Meyer e Palmer, 1934). Nos anos seguintes, o AH foi isolado da crista de galo que se tornou uma promissora fonte de obtenção de origem animal. Entretanto, a contaminação de origem proteica trazia efeitos indesejáveis em humanos e os custos de purificação oneravam o produto comercializado (Boas, 1949).

Desde a década de 80, a produção microbiana tem substituído a extração de fonte animal com benefícios na qualidade e segurança nas aplicações biológicas (Akasaka et al., 1988). Bio-HA é a designação dada ao AH produzido por rota microbiana. O produto comercial é comumente produzido por streptococcus, um microrganismo fastidioso, que requer meio de cultura rico em nutrientes. A fonte de nitrogênio pode ser de origem animal, como o Brain Heart Infusion (BHI) (Kogan et al., 2007), porém, na maioria das vezes, a produção é realizada com extrato de levedura, glicose e sais no meio de cultivo (Chong e Nielsen, 2003). Pires e Santana (2010) mostraram que os sais podem ser removidos do meio de cultivo sem prejuízos para a produção. Com a evolução dos trabalhos, as peptonas vegetais assumiram posição de destaque para a obtenção de um AH livre de determinantes antigênicos de origem animal ou microbiana (Heenan et al., 2002; Liu et al., 2005; Patel et al., 2008; Benedini e Santana, 2013; Oliveira e Santana, 2014), atendendo às exigências das indústrias farmacêutica e de cosmético.

Os estudos sobre a purificação do AH a partir do caldo fermentado envolvem a combinação de diferentes técnicas pós - separação celular, como micro- e ultrafiltração, adsorção em carvão ativado e cromatografia de separação por tamanho, entretanto, a precipitação bulk com etanol é a estratégia mais empregada (Sousa et al., 2009; Santosh et al., 2007).

Aspectos Moleculares, Distribuição Tecidual e Funções

O AH é um polímero aniônico linear constituído por unidades dissacarídeas repetidas de ácido glucurônico e N-acetilglicosamina unidos por ligações glicosídicas do tipo β . As áreas coloridas na Figura 1a representam regiões de maior (azul) e menor (vermelho) densidades eletrônicas que aparecem repetidas em lados alternados ao longo do comprimento da molécula. A repulsão mútua entre regiões de mesma natureza química favorece o ganho de volume hidrodinâmico em uma solução fisiológica (Figura 1b).

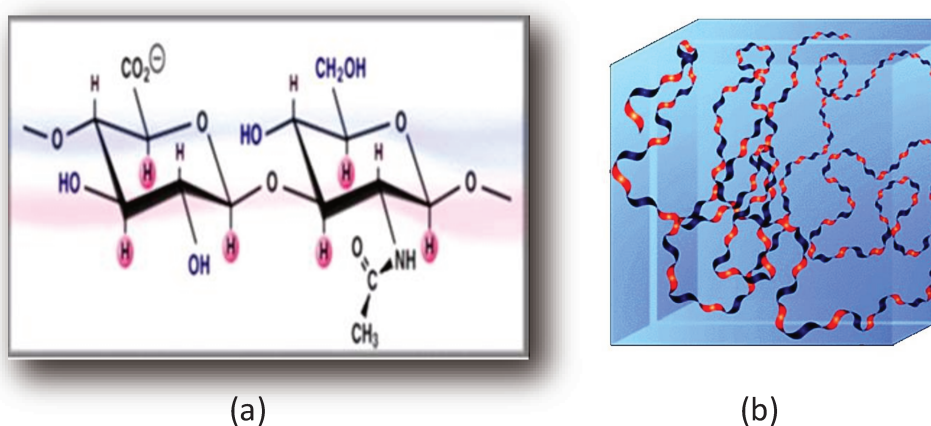


Figura 1. (a) Dissacarídeo de ácido glucurônico e N-acetilglicosamina, bloco constitutivo da molécula de AH (b) Configuração tridimensional do polímero em solução aquosa. Fonte: Adaptado de Hascall et al., 1997

Altas concentrações de AH - $\mu\text{g/ml}$ a mg/ml - aparecem associadas a diferentes tecidos e fluidos biológicos de mamíferos (de la Motte e Kessler, 2015). Aproximadamente 50% da massa do AH corporal está presente na pele de humanos (Hascall et al., 1997). Aparece ainda em áreas imuno-privilegiadas como no humor vítreo e cordão umbilical formando um colt com fibras de colágeno (Meyer e Palmer, 1934; 1936). Uma alta massa molar (MM) 10^5 - 10^7 Da é necessária para a formação das agreganas na cartilagem articular (Alberts et al., 2014).

Concentração e MM são variáveis que afetam as funções estrutural e lubrificante do AH porque alteram a viscoelasticidade e a capacidade de retenção hídrica (Balazs e Denlinger, 1989). Sinalização celular é também uma função atribuída ao AH, que através de receptores específicos, como CD44, TLR4, RHAMM mantem

a integridade e organização da matriz extracelular de tecido mesenquimal de origem mesodérmica (de la Motte, 2011). Esta sinalização também fornece um mecanismo de controle do sistema imune (Asari et al., 2010).

O AH exógeno possui atividade modificadora de matriz extracelular de cartilagem e fluido sinovial, estimulando a síntese de AH endógeno por condrócitos, fibroblastos e sinoviócitos (Smith e Ghosh, 1987). Além disso, possui propriedades antioxidantes, reduzindo a inflamação e acelerando a cicatrização de feridas (Fukuda et al, 1997; Balazs e Band, 2008). O AH é aplicado nas áreas médicas de ortopedia, oftalmologia, cardiologia, periodontia, dermatologia (Balazs e Denlinger, 1989; Hällgren et al, 1990; Neo et al., 1997; Barbucci et al., 2002; Pinnix et al, 2012; Dahiya e Kamal, 2013).

1.2 Ácido hialurônico Oral

A administração oral de AH ganhou credibilidade nas duas últimas décadas, sendo considerada a molécula da juventude (Sardi, 2004; 2007).

Os testes de segurança alimentar em ratos (Akasaka et al., 1988; Balogh et al., 2008; Canut et al., 2012) e em humanos (Möller et al., 2009; Nagaoka et al., 2010; Yoshimura et al., 2012; Tashiro et al., 2012; Martinez-Puig et al., 2013; Moriña et al., 2013) confirmam a não-toxicidade e a não mutagenicidade do AH oral.

Estudos conduzidos sob diferentes dosagens orais (48-240 mg/dia) e por diferentes períodos de tempo de uso (2 semanas-12 meses) comprovam os benefícios para o alívio da dor nas articulações (Kalman et al., 2008; Sato e Iwaso, 2009), melhorando diferentes outros aspectos na qualidade de vida, sem registros de efeitos colaterais.

Por tratar-se de um β -glicano, o AH pode ser empregado como terapia complementar de doenças que tem a sua origem na disbiose (Di Cerbo et al., 2013; Koropatkin et al., 2012). O AH administrado oralmente reduz a expressão do receptor TLR4, do fator de transcrição NF- κ B e da proteína cinase C pelas células do epitélio intestinal, e promove a proliferação de células-tronco, o crescimento dos vilos e das criptas intestinais, estimulando a produção de prostaglandina E2 (Cario et al, 2000; Zheng et al, 2009; Gareau et al, 2010; Riehl et al, 2012; Li et al., 2013).

Os benefícios intestinais refletem na saúde sistêmica quando desordens imunes e metabólicas (Ley et al., 2006; de Goffau et al., 2013; Smith et al., 2013) e, desordens inflamatórias crônicas das articulações e das mucosas (O'Neill, 2003; Moreland, 2003; Keely et al, 2012) são o resultado de vias envolvidas em um crosstalk multifatorial, incluindo o desequilíbrio da microbiota, o mau funcionamento da barreira intestinal e a autoimunidade (Figura 2).

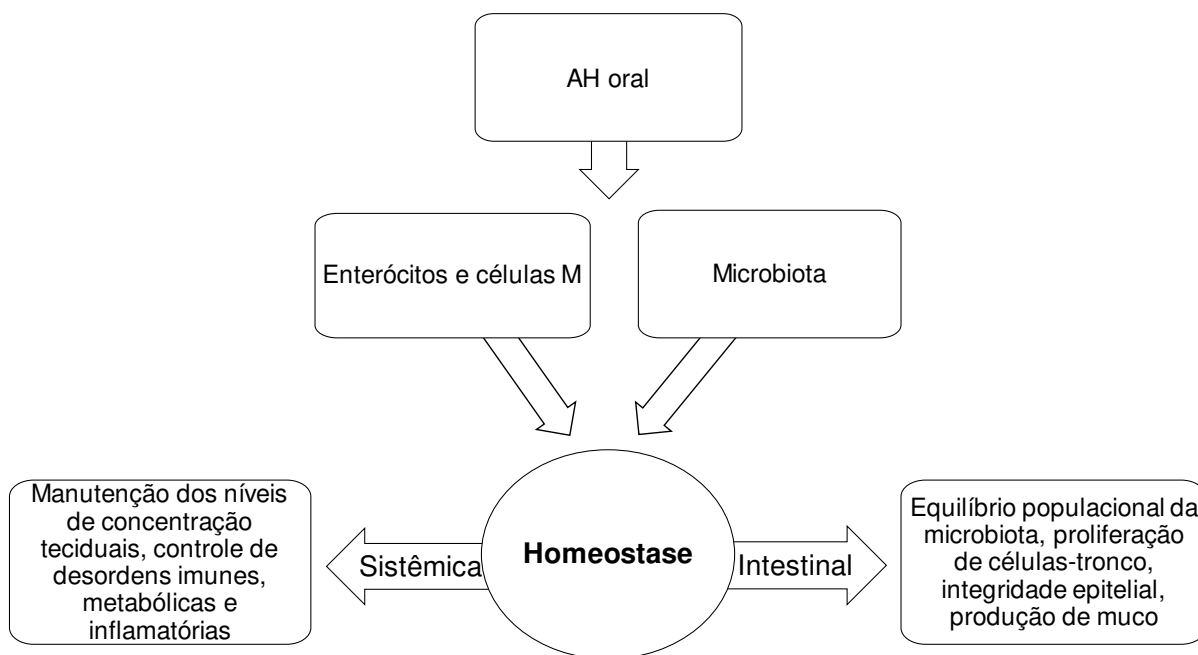


Figura 2. Fluxograma mostrando que o AH administrado oralmente é utilizado pelas células intestinais (enterócitos, células M) e também pela microbiota para a manutenção da homeostase. Os principais benefícios nos níveis intestinal e sistêmico são listados.

1.3 Mercado

Produtos de AH de grau alimentar movimentaram no Japão um valor de mercado estimado em 250 milhões de dólares, em 2014 (Fuji Keizai Co. Ltd., 2014). Previsões de mercado para o período 2016-2024 apontam um aumento no volume de comercialização de AH de grau farmacêutico e alimentar, a uma taxa de crescimento anual de 6,1% com um valor de mercado estimado em 13,4 bilhões de dólares em 2024 (Grand View Research, Inc., 2016).

Apesar da evolução do mercado, algumas formulações orais são comercializadas sem a identificação da fonte de obtenção e outras informações indispensáveis para uma avaliação criteriosa do AH comercial, como massa molar

(MM), pureza e concentração (Tabela 1). Estas variáveis afetam a captação intestinal e a sinalização celular MM-dependente em outros tecidos.

Tabela 1 – Resumo de algumas formulações orais contendo AH. Produtos comercializados como pó encapsulado ou na forma líquida.

Suplemento alimentar (Fabricante)	Fonte	MM (kDa)	(%) Pureza	g/L	Dose (mg/dia)	Preço (\$)	Referências
Food Grade Hyaluronic Acid (Stanford Chemicals)	<i>Streptococcus equi</i> , subsp. <i>zooepidemicus</i>	<10 - 1800	≥ 91	--	100	--	--
Regenerix Gold - Fast Acting Tissue Repair (MD Therapeutics)	Hidrolizado de colágeno tipo III	Baixo	--	--	100	80	Clark et. al, 2008
Vegan Hyaluronic Acid (Deva)	*Microbiano	--	--	--	100	30	Price et. al, 2007
Hyaluronic Acid BioCell Collagen® with OptiMSM® (Nature's Lab™)	Extrato de cartilagem de esterno de frango	< 500	< 10	--	100	32	Schwartz and Park, 2012
Synthovial Seven® (Hyalogic™)	--	Alto	--	0,1	3	40	Bucci and Turpin, 2004
Play Again Now® (Viscos LLC)	Microbiano	Alto	--	0,1	75	62	Jensen et al, 2015

* AH proveniente de fermentação em meio de cultivo 100% vegetal, segundo o fabricante.

-- Informações não disponibilizadas pelo fabricante.

1.4 Estudos de Adesão e Absorção Intestinal

A literatura não tem sido conclusiva sobre a captação intestinal do AH de alta MM ($\geq 10^5$ Da) (Oe et al., 2016; Kawada et al., 2014; Schultz et al., 1989), apesar de resultados qualitativos baseados em métodos fluorescentes confirmarem o trânsito intestino-tecidos do AH (Balogh et al., 2008; Kawada et al., 2014). Adicionalmente, a influência das propriedades físico-químicas e estruturais do AH sobre os limiares de absorção intestinal (concentração, tempo) não são investigados.

Resultados de estudos preliminares com o modelo animal *ex vivo* (Barthe et al., 1999), obtidos pela nossa equipe de pesquisa, revelaram uma inconsistência no balanço de massas nos lados da serosa e da mucosa, após o período incubatório. Concluímos que o AH estava aderido à mucosa. A partir desta constatação decidimos estudar a adesão intestinal do AH como primeira etapa do processo absorptivo.

1.4.1 Objetivo

O objetivo desta tese foi estudar os fenômenos observados em modelos *ex vivo* e *in vivo* de mucosa intestinal de ratos, a partir da administração do AH nas formas livres e nanoestruturadas, como uma avaliação prospectiva de sua adesão e permeação intestinal e absorção.

Metas

A produção tecnológica do AH nanoparticulado, a caracterização físico-química, reológica, mucoadesiva e absorptiva das formulações avaliadas constituíram as principais metas desenvolvidas.

A adesão do AH em mucina e mucosa intestinal foi investigada com o texturômetro. Trata-se de um procedimento simples, barato e rápido de obtenção de mucoadesividade (Jones et al., 1996). Para a análise, o probe é revestido com o substrato biológico (mucina de estômago de porco ou o intestino invertido de ratos) e a formulação de AH é depositada em um recipiente a um volume fixo, que entra em contato com o substrato biológico durante o movimento

descendente do probe. Durante o movimento ascendente, ocorre o registro de informações de distância versus força (Figura 3).

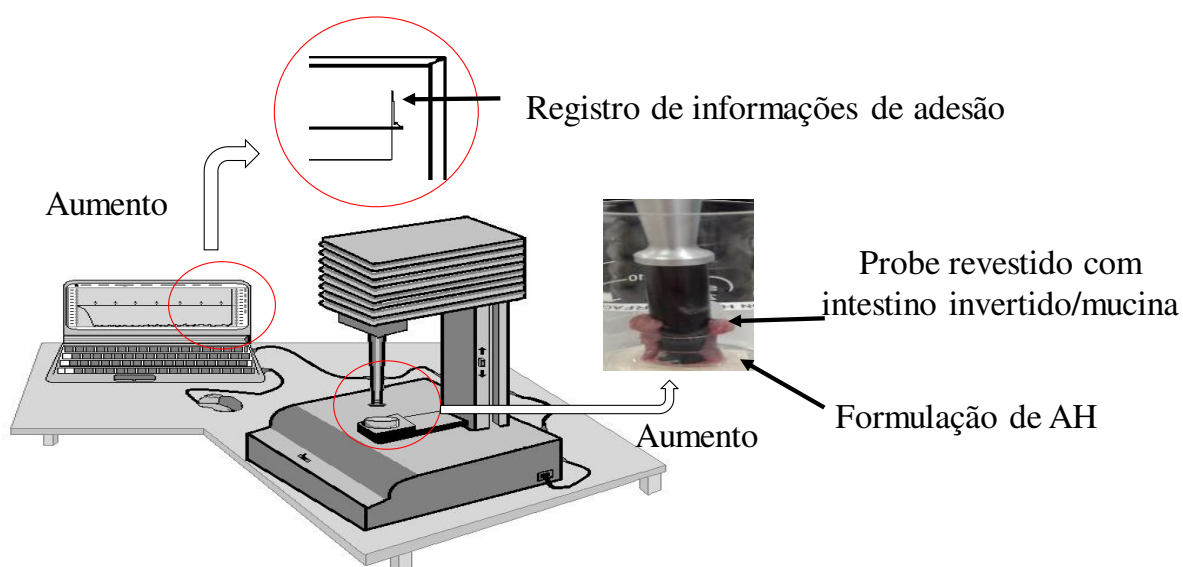


Figura 3. Esquema de aparato experimental para estudo de mucoadesão.

Na etapa seguinte, a permeação intestinal e absorção de formulações de AH pré-selecionadas foram investigadas em modelos de ratos pelo método *single-pass intestinal perfusion*. Neste método, as funções vitais do animal permanecem intactas durante o estudo (Versantvoort et al., 2000).

O intestino delgado é perfundido pela formulação de AH (Figura 4), a fração não permeada e a fração permeada pelo epitélio são quantificadas e o balanço de massas fornecem uma previsão da permeabilidade intestinal.

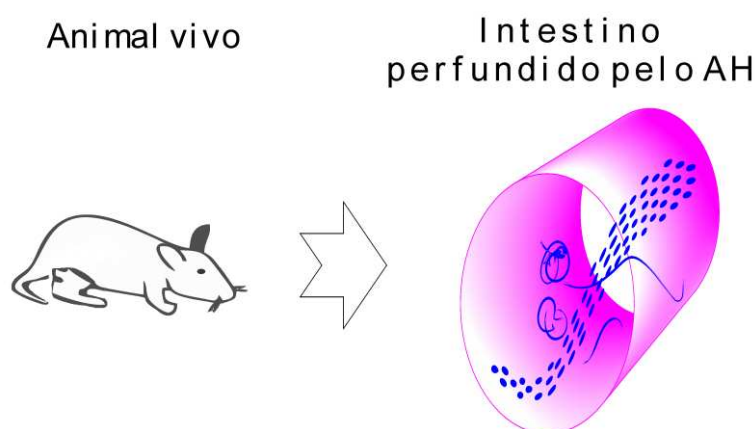


Figura 4. Ilustração mostrando que o intestino delgado do rato vivo é alimentado com a formulação de AH durante estudos de permeabilidade e cinética de captação.

CAPÍTULO 2: FUNDAMENTAÇÃO TEÓRICA

2 FUNDAMENTAÇÃO TEÓRICA

Esta seção é composta pelo artigo “*Hyaluronic acid behavior in oral administration and perspectives for nanotechnology-based formulations*”. O artigo revisou o AH no trato gastrointestinal, uma abordagem nanotecnológica foi apresentada e discutida com perspectivas para futuros desenvolvimentos de formulações orais para atender simultaneamente o metabolismo microbiano e a captação intestinal na forma de alta MM.

2.1 Hyaluronic acid behavior in oral administration and perspectives for nanotechnology-based formulations

Hyaluronic acid behavior in oral administration and perspectives for nanotechnology-based formulations

Alexandro B. de Souza¹, Marco V. Chaud² & Maria H. Andrade Santana^{1*}

¹Department of Materials and Bioprocesses Engineering, School of Chemical Engineering, University of Campinas, P.O. Box 6066, 13083-852, Campinas, SP, Brazil ² Laboratory of Biomaterials and Nanotechnology, University of Sorocaba, 18300-000, Sorocaba, SP, Brazil.

*Correspondence should be addressed to mariahelena.santana@gmail.com

ABSTRACT

Hyaluronic acid (HA) is a ubiquitous polysaccharide present at the various tissues with diverse biological functions. It is known that in the intestinal epithelium, the exogenous HA of molar mass $\geq 10^5$ Da orally administered antagonizes TLR4 overexpression resulting from dysbiosis and promotes immunomodulation in a multifactorial crosstalk, thus helping to treat or to prevent injuries. As the cell signaling is mediated by macromolecules, the three-dimensional structure of HA plays an important role in those intestinal functions. Introducing HA in terms of its molecular structure, its spatial architecture as dependent on pH, concentration and molar mass, occurrence, biological functions and turnover in the tissues, this review addresses the HA in the gastrointestinal system, the molecular dynamics of intestinal uptake and signaling, immunomodulation at intestinal and systemic levels and HA fate to other tissues. Finally, at the light of these behaviors, a nanotechnological approach is presented as a progress in the field of the oral HA administration, and discussed with perspectives for future developments.

Keywords: Oral hyaluronic acid, Dysbiosis, Intestinal immunomodulation, Systemic homeostasis.

Abbreviations: HA-NPs, hyaluronic acid nanoparticles; ECM, extracellular matrix; GAG, glycosaminoglycan; HA, hyaluronic acid; LMM-HA, low molar mass hyaluronic acid; HAS, hyaluronic acid synthase; HMM-HA, high molar mass hyaluronic acid; TLR4, toll-like receptor 4; CD44, cluster of differentiation 44; MHC, major histocompatibility complex; NF- κ B, factor nuclear kappa B; PKC, protein kinase C; IgA, Immunoglobulin A; PTEN, phosphatase and tensin homolog; PI3K, phosphatidylinositol 3-kinase; Akt, protein kinase B; ROS/RNS, reactive oxygen/nitrogen species.

1. Introduction

Hyaluronic acid (HA) is a linear non-sulphated glycosaminoglycan composed of β (1-4) linked disaccharide units of D-glucuronic acid and N-acetyl-D-glucosamine which are β (1-3) bounded. The disaccharide units have molar mass (MM) 400 Da, while the entire polymer molecule can reach 10^7 Da (Necas et al., 2008). HA also is an amphiphilic with the hydrophobic CH patches and the abundant hydrophilic domains provided by its COOH and OH groups (Figure 1).

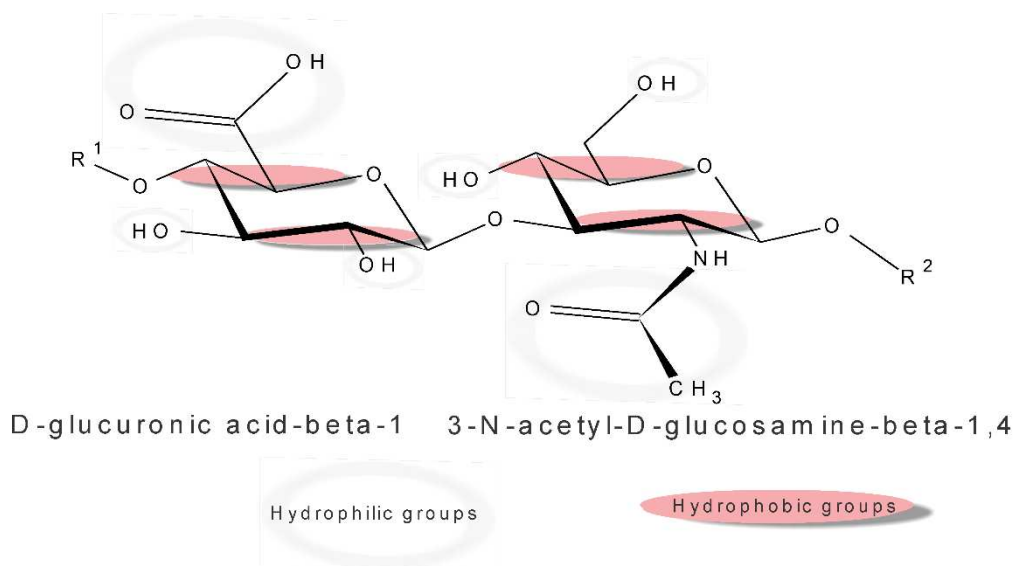


Figure 1. Molecular structure of constituent disaccharide unit of hyaluronic acid. R¹ and R² indicate the continuity of the polymer chain.

Since HA is a polyelectrolyte its spatial architecture is strongly affected by pH, concentration and molar mass mainly (Prestwich, 2001). At physiological pH, all carboxyl groups on the glucuronic acid residues are deprotonated and HA assumes the highly hydrated random coil structure as determined by crystallography (Scott, 1989). Important structural changes have been reported at pHs 2.5-4 including the helical compacted forms as rod-like (single strand) and coiled coil (double helix strands), both interpreted from molar ellipticity spectra and molecular dynamics simulations (Chakrabarti and Balazs, 1973; Haxaire et al., 2000).

The HA spatial structure is also dependent on its MM and concentration in aqueous medium (Scott et al., 1989). Studies have shown that

at physiological pH, low MM ($<10^5$ Da) and concentrations less than 1 mg/mL give rise to stiffened rod-like or coiled coil structures (Garg and Hales, 2004; La Gatta et al., 2010), while high MM ($>10^5$ Da) at concentrations from 1 mg/mL the HA chains overlap in random coil structures with progressive increase in viscosity and viscoelasticity due to physical crosslinking (Kobayashi, et al., 1994). HA degradation is critical at pH < 4 and pH > 11 leading to modifications in its rheological properties due to the structural changes as reported by Maleki and coworkers (Maleki et al., 2008).

In human body HA occurs in the skin (7-8 g, ~50% of HA body), vitreous humor of the eyes (0.1- 0.4 mg/g), connective tissues, synovial fluid of the joints (3-4 mg/mL) and other tissues in the human body (Hascall et al., 1997; Salustri and Fulop, 1998).

Exogenous HA obtained by microbial fermentation mainly (bio-HA) is structurally identical to the endogenous HA and has been widely used in osteoarthritis treatment, ophthalmology, otolaryngology, urology, dermatology (aesthetic applications and topical drug delivery), surgery and healing, cancer studies and as a carrier of DNA molecules (Falcone et al., 2006; Garg and Hales, 2004).

In vivo, amount and size of HA chains and the low pHs of environment are associated with tissue inflammation inducing the activation of genes linked to expression of pro-inflammatory cytokines, release of nitric oxide and downregulation of PI3-kinase with induction of apoptosis (Oh and Chun, 2003, Kessler et al., 2008). At physiological pH, the random coil structures of HA predominate in the ECM of tissues that exert functions of antioxidant, anti-inflammatory, shock absorber and lubricant (Figure 2).

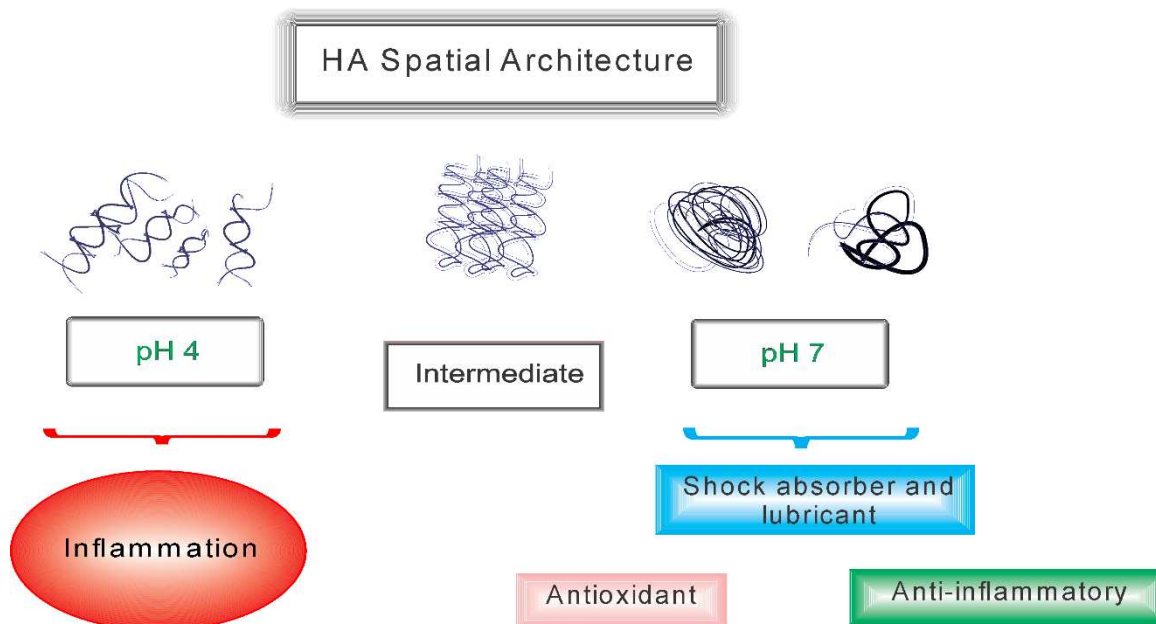


Figure 2. The structure-dependent biological functions of HA

HA performs its biological functions according to two basic mechanisms: tissue turnover and as a signaling macromolecule. Both mechanisms have been shown to be structure-dependent (Cyphert et al., 2015). Turnover of HA present in the ECM preserve its composition, organization and integrity providing adhesion and internalization of HA from signaling via CD44 and TLR4 receptors (Kresse and Glossl, 1987, Fraser et al., 1997).

Other cell surface proteins interacting with HA include: TLR2 that signaling for inflammation and angiogenesis (Powell and Horton, 2005). RHAMM (receptor for HA-mediated motility) is responsible for cell migration and proliferation (Slevin et al., 2007), ICAM-1 (intercellular adhesion) VCAM-1 (vascular cell adhesion molecule 1) facilitate migration and vascular endothelial adhesion of circulating cells of the innate immune system (Oertli et al., 1998), LYVE1 proteins (lymphatic-vessel endothelial HA receptor 1) act on the homeostasis of tissue fluids by transporting HA to lymphatic vessels (Mouta Carreira et al., 2001). HARE proteins (HA receptor for endocytosis), expressed in sinusoidal cells, act on HA turnover (Yannariello-Brown et al., 1997).

The HA structural properties and receptor interactions form the basis for the understanding of the HA behavior and functions in the gastrointestinal system which is presented in this review article. The literature search was

performed in various databases such as PubMed, Science Direct and Scopus, from February 2016 to January 2019, using the following keywords: β -glycans intestinal uptake, dysbiosis, TLR4 and orally administered hyaluronic acid.

2. Hyaluronic Acid in the Gastrointestinal System

The ingested HA is initially exposed to acidic pH of the gastric system. Studies of pH-induced degradation of dilute and semidilute solutions of HA show intramolecular cleavage of HA in dilute solutions while in the semidilute concentration regime the polymer network is disintegrated only. The degradation effect is faster and much more pronounced at pH 13 than at pH 4 (Maleki et al., 2008). Degradation also is MM-dependent. HMM-HA concentrate does not suffer appreciable degradation during its transit in the gastric system.

HA-Mucosae Interactions

Depending on the concentration, MM of HA and cell background (activation state of receptor, phase of the cell cycle and signaling pathways), the binding between HA and CD44 or TLR4 determines differentiated actions in the physiological context.

Enhanced synthesis of endogenous HA in the vasculature, in the surrounding intestinal mucosa and in the lung mucosa is found promoting intense inflammation because CD44 internalize the excess of HA, and the LMM-HA generated is received by TLR4, that has inherent phosphatase activity (de la Motte, 2011). TLR4 overexpression promotes intense trigger of pro-inflammatory cytokines, being decisive in the disruption of the epithelial barrier (Abreu, 2010).

Two possible mechanisms have been proposed to explain how the size of HA influences TLRs interactions. HMM-HA forms molecular aggregates around cell surface, thus covering TLRs surface and limiting their interactions with antigenic determinants as fragmented sizes of polymers, including LMM-HA that act as an agonist for TLR2 and TLR4, thus inducing inflammatory reactions (Cyphert et al., 2015). During inflammatory processes, uncontrolled turnover due

to pH decrease and increase in the reactive oxygen species (ROS) may lead to losses in thickness and viscosity of the HA barrier (Ebid et al., 2014, Knopf-Marques et al., 2016).

In the intestinal epithelium, TLR4 have both functions: Transepithelial uptake and signaling, while CD44 modulated the signaling (Muto et al., 2009). In other tissues, receptors exert distinct functions: CD44 modulates the turnover and TLR4 modulates the HA signaling. The failures in HA turnover culminates in a cascade of events that lead to an inflammatory process as summarized in Figure 3.

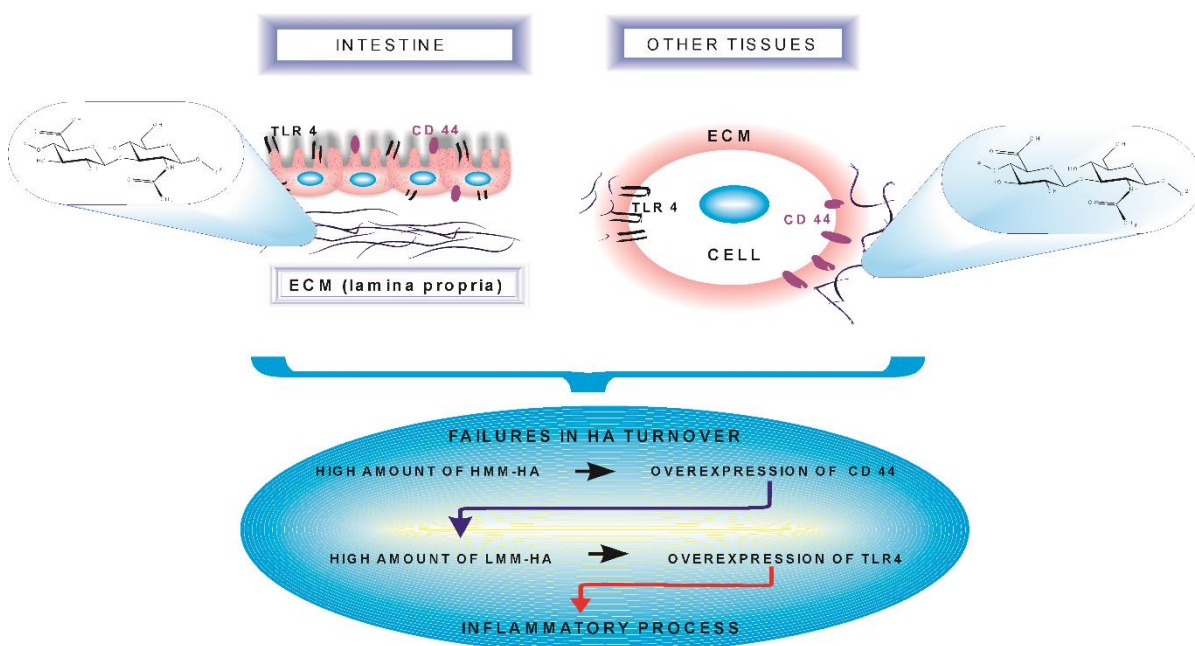


Figure 3. The cascade of events that precede the inflammatory process.

2.1. Molecular Dynamics of Intestinal Uptake

Thickness and pore size of mucus nanostructure are elements that prevent the free transit of molecules and microorganisms from luminal to basolateral side (Linden et al., 2008). Despite this, macromolecules are actively sampled and internalized.

Former studies reported the uptake of different macromolecules along the gastrointestinal tract of neonatal lambs (Smeaton and Simpson-Morgan, 1985), Charles River rats (Warshaw et al., 1974), Sprague-Dawley rats (Artursson et al., 1993) and New Zealand White rabbits (Urao et al., 1997). Despite these findings, the mechanisms involved in the intestinal uptake of macromolecules are still not clearly understood.

Particularly, there are very few studies about transepithelial uptake of HMM-HA and the conclusions are sometimes controversial. While some studies report the uptake and tissue affinity for orally administered HMM-HA in human, rats and dogs (Turley et al., 2003; Balogh et al., 2008; Laznicek et al., 2012), others studies have addressed the possibility of HMM-HA not be uptaken (Kawada et al., 2014). A convergence point in this question is the evidence based on qualitative determinations of transport of both LMM-HA and HMM-HA to the bloodstream compartment and gut associated lymphatic tissue respectively (Balogh et al., 2008; Kawada et al., 2014).

HMM-HA ingested is uptaken by epithelial cells. Endocytosis is performed by enterocytes (Neal et al., 2006), M cells (Barthe et al., 1999; Neutra et al., 1998), dendritic cells and macrophages (Corr et al., 2008). Chemical adsorption is mediated by TLR4 receptor (Oe et al., 2016).

The molecular dynamism of intestinal uptake begins with the chemical adsorption of HA on the TLR4 receptors scattered on the underlying epithelium. Afterwards, physical structuring or crosslinking of multiple TLR4 receptors stabilized by hydrogen bonds occurs into the transmembrane microdomains (Park et al., 2009; Gu et al., 1988; Triantafilou and Triantafilou, 2003). The formation of specific and non-specific interactions between the interacting surfaces is necessary for the success of the uptake (Ponchel and Irache, 1998). The specific HA binding is oriented by binding sites in the receptors and functional epitopes in the HA.

In a subsequent step, HA is internalized by the enterocytes and the M cells being differentially metabolized. The M cells deliver intact HMM-HA to the gut associated lymphatic tissue (Rubas and Grass, 1991), as represented in Fig. 4a. Interestingly, HA and others macromolecules can be also captured by

cytoplasmic projections of dendritic cells, that reach the intestinal lumen (Fig. 4a) (Chieppa et al., 2006; Rescigno et al., 2001). During uptake by enterocytes, HA undergoes lysosomal cleavage followed by presentation to memory T cells through the exteriorization of proteins from class II major histocompatibility complex (Burgdorf et al., 2007) (Fig. 4b).

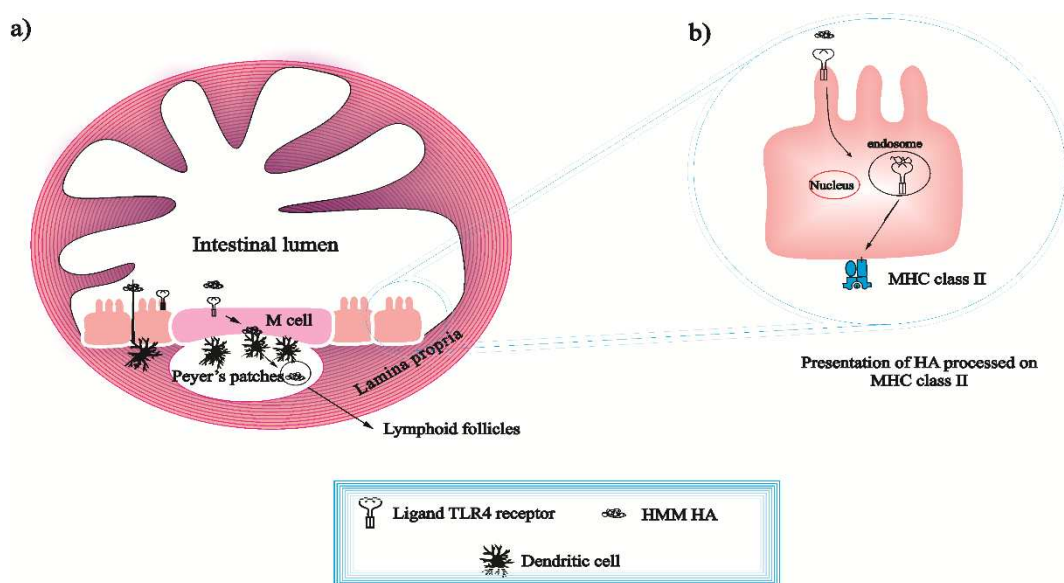


Figure 4. Illustration of the absorptive events. (a): Cross section of small gut, shows enterocytes, M cells and dendritic cells into the Peyer's patches, sampling exogenous HMM-HA from intestinal lumen. In the three different cells, internalization of HA is mediated by TLR4 receptors. (b): Enterocytes internalizing exogenous HMM-HA, followed by lysosomal cleavage and presentation to the class II major histocompatibility complex (MHC).

2.2. Crosstalk at the Intestinal and Systemic Levels

TLR receptors usually binding to microbial products in the intestinal epithelium, providing protection against pathogens through induction of IgA and anti-microbial peptides, repair of epithelium injury through induction of stem cell growth and cell migration through induction of intestinal trefoil factor 3 (Abreu,

2010). These receptors are highly expressed in cells of the intestinal epithelium and cells that identify antigenic determinants, such as enterocytes and M cells, macrophages, dendritic cells, peripheral blood leukocytes, T cells (γ/δ and α/β T cells, Th1 and Th2) and B-cell line (Medzhitov et al., 1997).

Notably, TLR4 is a constitutive receptor that has inherent phosphatase activity and is involved in the innate immunity of intestinal epithelium. Its expression and spatial location on epithelium (apical or basolateral) is dependent on ligand stimulus, as occur in human colon epithelial cells, where TLR4 changes from subcellular to apical location, allowing identification of several types of ligands (Cario et al., 2002; Hornef et al., 2003). The mechanisms of cellular control of TLR4 activity are rigorous in order to avoid autoimmunity. For instance, in order to avoid nonspecific activation by nonpathogenic microorganisms, TLR4 is compartmentalized into enterocytes and M cells (Fig. 5b). Failures in these mechanisms can lead to serious intestinal disorders, such as active inflammatory bowel disease (Cario and Podolsky, 2000).

TLR4 overexpression is commonly related to occurrence of dysbiosis (O'Neill, 2003; Macpherson and Harris, 2004). This means increased activation of the transcriptional factor NF- κ B (Takeda and Akira, 2005), responsible for the transcription of pro-inflammatory proteins, such as TNF α and interleukins 1, 2 and 6. The inflammatory response syndrome, prevents the intestinal cells from exerting their basic functions, as nutrient uptake and metabolism of xenobiotics (Round and Mazmanian, 2009). Concomitantly, nonspecific activity of protein kinase C (PKC) leads to dephosphorylation of tight junction-associated proteins and translocation of bacterial metabolites into the lamina propria becomes unavoidable as described by Li et al., 2013. Other studies have showed that release of inflammatory mediators in the intestinal epithelium is responsible by serious oxidative stress and activation of caspase-3 pathway, resulting in severe apoptosis (Tian et al., 2013).

Nowadays, various reports in the medical scientific literature relate cardiovascular diseases (Wang et al., 2011), symptomatic atherosclerosis (Karlsson et al., 2012), obesity (Ley et al., 2006; Turnbaugh et al., 2009), non-alcoholic fatty liver disease (Henao-Mejia et al., 2012), β -cell autoimmunity (Qin

et al., 2012; de Goffau et al., 2013), chronic disease of the genome (Go et al., 2005) and pulmonary inflammatory disease (Keely et al., 2012) to microbiota unbalance.

In this context, oral HA appears as a promising alternative for the preventive and incremental treatment of dysbiosis (Di Cerbo et al., 2013; Koropatkin et al., 2012; Cockburn and Koropatkin, 2016). The restoration of the relative proportion of the two main commensal phyla as well as the down-regulation of TLR4 (Fig. 5b) are functions assigned to HMM-HA. In response, the intestinal epithelium provides proliferation of stem cells, expression of growth factors, structural integrity (Riehl et al., 2012) and release of cyclooxygenase-2-derived prostaglandin E2 (Zheng et al., 2009). Figure 5 (a,b) illustrate the inflamed epithelium and its restorage mediated by the HMM-HA.

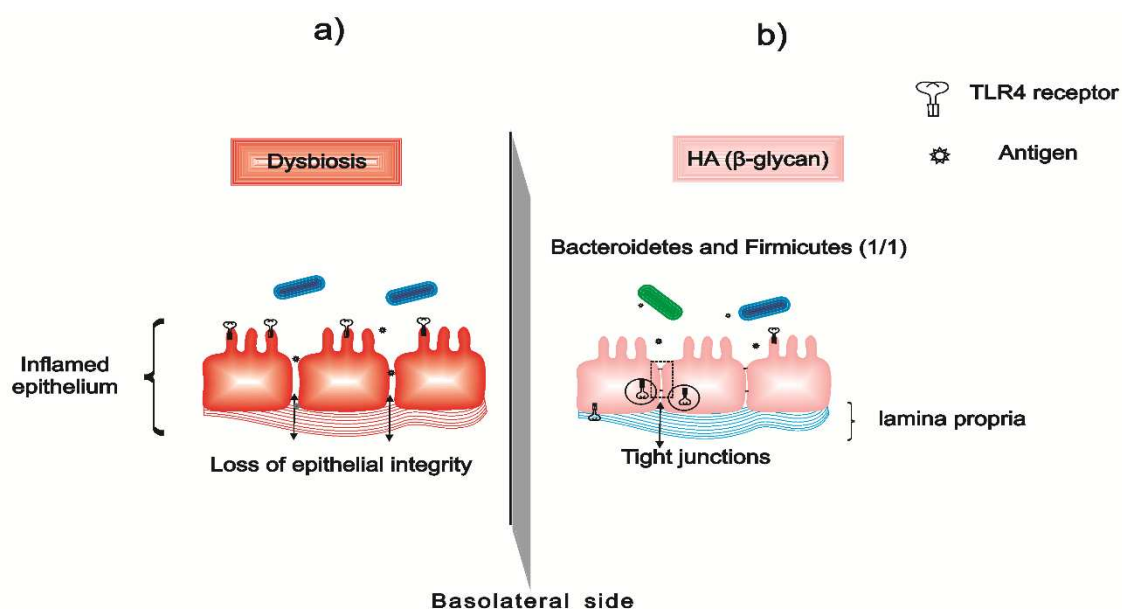


Figure 5. Representation (non-scaled) of the intestinal epithelium composed by enterocytes. Under population unbalance of microbiota, increased expression of apical TLR4 in (a) promotes the loss of structural integrity of tight junctions. After oral administration of HA, the equilibrium (1/1) between Bacteroidetes and Firmicutes species is restored, TLR4 changes for subcellular location, tight junctions are recovered and downstream effects are eliminated.

Humoral and cellular immunomodulation is mediated by a complex network of communication involving CD44 and TLR4 (Awasthi, 2014; Wagner and Cresswell, 2012). At intestinal level, occurs immunomodulation via TLR4 in

response to HA size (de la Motte and Kessler, 2015). In general, the immune response is initiated by the TLR4 and HA fragments, and involve stimulus of FoxP3⁺ CD4⁺ CD25⁺ regulatory T cells (Bollyky et al., 2009). On the other hand, HMM-HA promotes the suppressive effects of CD4⁺ CD25⁺ regulatory T cells (Bollyky et al., 2007). In other tissues, CD44 and TLR4 are responsible by the turnover and immunomodulation respectively (Fig. 6) (Campo et al., 2010).

About 70 % of the cells of the immune system are present in the lamina propria of intestinal mucosa (de Kivit et al., 2014). This means that entire organism is affected by the intestinal changes from the oral HA in a dynamic and multifactorial crosstalk. The immune-modulins and the products from the intestinal microbiota define the intestinal status that dictates the types of immune cells to be produced (Keely et al., 2012). Therefore, intestinal diseases affect systemic immunity and create a friendly environment to the installation of other diseases in consequence of the microbiota unbalance and dysfunction of the intestinal barrier (Keely et al., 2012).

Epidemiological and clinical observations have revealed intrinsic relation between abnormal pulmonary function and intestinal chronic disease (Kuzela et al., 1999).

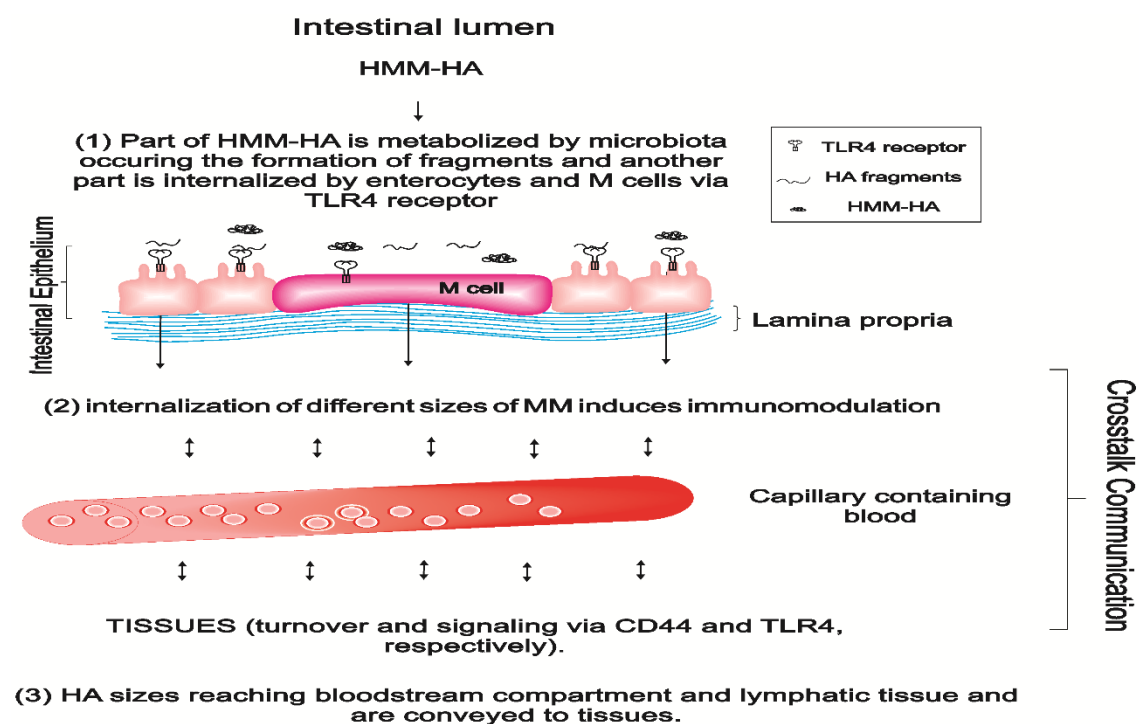


Figure 6. Flowchart shows the dynamic of intestinal uptake from hyaluronic acid (HA) ingested. (1) and (2) indicates the step of transepithelial uptake, in which a part of HMM-HA is absorbed as high molar mass (HMM) and as intermediary (IMM) and low molar mass (LMM), resulting from microbiota metabolism and pH variations. Over the intestinal epithelium, TLR4 is the key receptor in the uptake of oral HA and size-dependent signaling. In other tissues (3), CD44 is the receptor responsible by turnover of HA and TLR4 is responsible by the size-dependent signaling. Humoral and cellular immunomodulation at intestinal and systemic levels defines the crosstalk communication.

3. Oral Hyaluronic Acid in other Tissues

For a long time, the fact that HA can cross the intestinal barrier without cleavage has been debated. HA is depolymerized by hyaluronidases, forming fragments of different sizes that occurs physiologically (Cardoso et al., 2016), such as during pre-systemic and first-pass metabolism (Gustafson, 1998). Endogenous chemical degradation may occur in the presence of extreme pH, i.e., pH < 4 and pH > 11 (Maleki et al., 2008). Additionally, exposition to reactive oxygen/nitrogen species (ROS/RNS) represents an important source of physiological cleavage of HA as observed using exposition to ultraviolet (UV) light irradiation (Soltés et al., 2006).

Studies have shown that microbiota produces hyaluronidases that cleave the molecule of HA during anaerobic fermentation. Partially depolymerized HA (< 10⁵ Da) is absorbed mainly in the cecum and directed to entire organism through bloodstream compartment, whereas intact HA (> 10⁵ Da) is conveyed primarily to gut associated lymphatic tissue and then to the bloodstream compartment (Kawada et al., 2014; Kimura et al., 2016).

In contrast of that, studies using labeled-HMM-HA (10⁶ Da), showed the uptake through the bloodstream and compartmentalization in the tissues, especially connective tissues and skin. Scintigraphic imaging showed accumulation of 99mTc-HA in the joints, vertebrae and salivary glands 4 hours after oral administration. This was the first evidence of uptake of intact HMM by the gut associated lymphatic tissue and its distribution to the connective tissues (Balogh et al., 2008). In similar study, labeled-HMM-HA (10⁶ Da) of

pharmaceutical grade was orally administered in order to reach the bloodstream in its biologically active form (35 to 2000 kDa). Again, the HMM-HA was preserved during the uptake, transepithelial transit and properly transported to its destination without undergoing depolymerization. Therefore, exogenous HMM-HA was not removed or replaced by endogenous HMM (Kawada et al., 2014).

More recently, Kawada and coworkers concluded that HA of different sizes, LMM (10 kDa) and HMM (300 and 800 kDa) orally administered at dosages of 120 and 200mg/Kg/day, during six weeks in humans and rats model, provided prevention to skin dryness and skin photoageing (Kawada et al., 2015a,b). Additionally, the oral HA induced the relief of knee pain, the relief of synovial effusion or inflammation and improved the muscular knee strength (Oe et al., 2016).

Administration of exogenous LMM-HA was also related to the control of cancer metastasis, due to its properties in suppressing PI3K and Akt cell survival pathway. LMM stimulated PTEN expression (a phosphatase that degrades the PIP3, product of PI3K-action) and suppressed the cell survival pathway, leading to increased activity of the apoptotic effector, caspase-3 (Ghatak et al., 2002).

4. Effects of the Oral Hyaluronic Acid in the Intestinal Health

Two major phyla constitute the human commensal microbiota, the gram-negative Bacteroidetes and the gram-positive Firmicutes. The first one is generalist while the second is specialist to the catabolism of β -glycan (Salysers et al., 1977). Healthy individuals in Western society exhibit relative proportion of (1/1) of both phyla. It is known that the unbalance between these species impair the intestinal homeostasis (Eckburg et al., 2005).

Microbiota unbalance is accompanied by differential alteration in epithelial cell expression of TLR4 (Abreu, 2010). TLR4 overexpression is found to promote intense trigger of pro-inflammatory cytokines, being decisive in the

development of chronic inflammation disease (Wang et al., 2010; Cario and Podolsky, 2000). In consequence of that, chronic inflammatory disorders promote failures in the recognition and presentation of antigens creating a friendly environment for metabolic disorders that promote neuroendocrine system failure and non-specificity of signal transduction. The crosstalk communication developed by the inflamed organ is governed by interactive elements that regulate TLR4 activation, as intestinal environment, genetic predisposition and immune status (Cario, 2010).

In the last 20 years, orally administered β -glycans has gained special attention as preventive and complementary therapy for dysbiosis. In this scenario, HMM-HA has been exploited as element regulatory of the relative proportion of microbiota.

Orally administered HA promoted the proliferation of lactic bacteria (Di Cerbo et al., 2013), contributing to the balance of the two main phyla. In response, the information encoded by the genomes of the microbiota provide intestinal homeostasis (Koropatkin et al., 2012). Additionally, by-products of catabolism of β -glycans, such as vitamins B12 and K, short-chain fatty acids as acetate, butyrate and propionate, developed anti-inflammatory functions in the human organism and activated immune cells (Wong et al., 2006; Matsuki et al., 2013).

A more recent study has shown that short-chain fatty acids from catabolism of β -glycans inhibit histone deacetylases, and modulate the expression of genes associated with proliferation of intestinal epithelium cells (Fellows et al., 2018).

Most of the microbiota is found attached to mucin nanostructure in the ilea-distal segment and colon of human and murine (Atuma et al., 2001) (Fig. 7), obstructing the direct contact of enteric pathogens with underlying epithelium (Cameron and Sperandio, 2015). Thus, the mucin network and the microbiota represent a biophysical limitation to contact of pathogens with TLR4. Additionally, studies have shown that HA of 900 kDa founded application as natural antimicrobicide, the penetration of HA/mucin chains formed a dense network that restricted the diffusion of pathogens and antigen to epithelium and inhibited possible infection (Hansen et al., 2017).

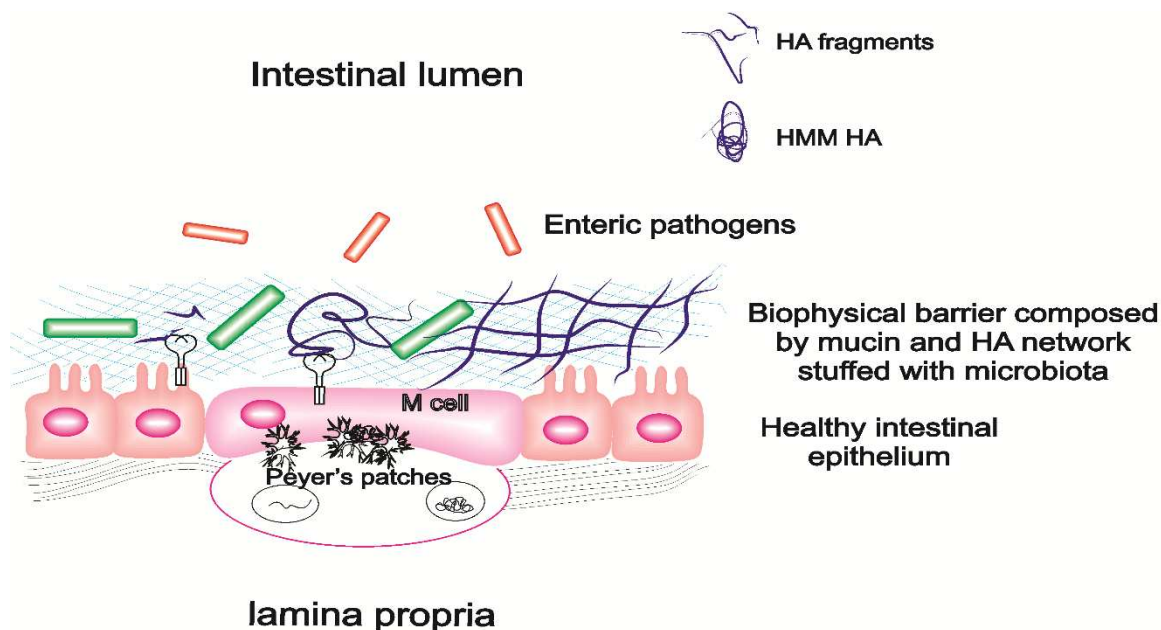


Figure 7 - Illustration (non-scaled) of the biophysical barrier composed by mucin network + HA + microbiota (in green) against free access of enteric pathogens (in red) to the healthy underlying epithelium.

Another benefit from oral HA occurs when it reaches the surface of the inflamed epithelium. The formation of larger and ordered platforms CD44/TLR4/HMM-HA cluster regulate membrane function in mammalian cells. HMM HA-induced dimerization of TLR4/TIR domains (Fig. 8a) initiates intracellular signaling directed to a cellular quiescent state (Chen and Abatangelo, 1999; Campo et al., 2010; Muto et al., 2009), promoting down-regulation of the apical expression of TLR4 receptor and down-regulation of transcription of Nuclear Factor- κ B and protein kinase C (Zheng et al., 2009; Riehl et al., 2012). The synergism of these cellular events antagonize the inflammation from dysbiosis. The positive effects from the oral HA on the intestinal epithelium reflect in the systemic health in a multifactorial crosstalk, benefiting other mucosa such as the respiratory system.

HA structures of HMM has polyvalent functional epitopes responsible by formation of cluster with TLR4 and CD44. However, LMM-HA can interrupt the normal course of cluster structuring, reducing the functional avidity of the linker complex, as showed using exogenous LMM-HA to release cluster formed by CD44 and HMM-HA in cell line of mammalian (Toole, 2004; Yang et al., 2012; Lesley et al., 2000).

Extending the liberating effect from LMM-HA to multivalent clustering formed on the intestinal epithelium between HMM-HA, TLR4 and CD44 (Fig. 8b), is expected that LMM, generated into the intestine, will reduce the uptake of HMM-HA and inhibit its anti-inflammatory properties.

Fortunately, nowadays it is known that cluster structuring is influenced by conformational flexibility of intermediate rod-to-coil structure of HA under specific size range (100–300 kDa) and diameter (~65 nm) (Weigel and Baggenstoss, 2017). Therefore, minimizing the luminal degradation of HA is an important step to optimize its uptake as well as its anti-inflammatory properties.

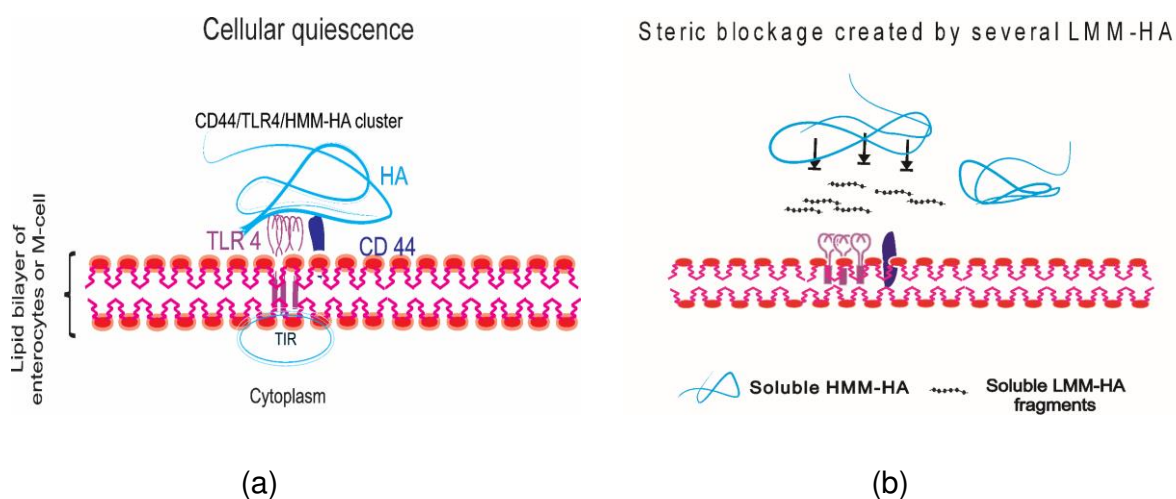


Figure 8. Schematic illustration of the formation of (a) CD44/TLR4/HMM-HA cluster on lipid bilayer of cellular membrane of enterocytes and M cells. (b) shows steric blockage of TLR4/CD44/HMM-HA engagement, precluding the structuring of clustering.

Fig. 9 summarize some of the most common benefits of oral HA.

Hyaluronic acid in oral administration

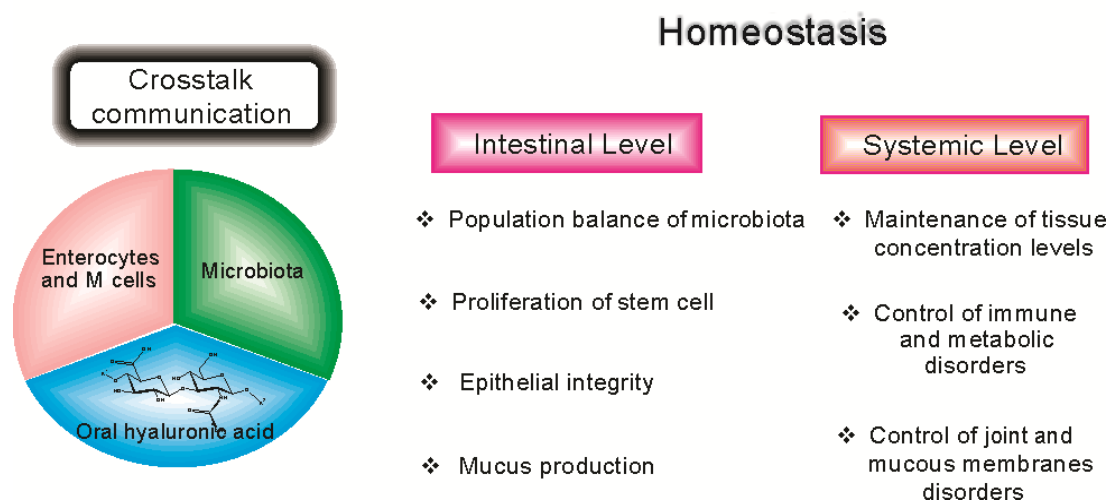


Figure 9. Flowchart shows the intestinal and systemic benefits of oral HA. A set of actions orchestrated by enterocytes, M cells and microbiota, namely crosstalk communication, is responsible by the homeostasis.

5. Nanotechnological Approach for the Oral Hyaluronic Acid

Engineered nanoparticles (NPs) are already present in many natural and processed foods in the food industry (McClements and Xiao, 2017). Most of them are nanometals (silver, iron oxide, titanium dioxide, silicon dioxide, and zinc oxide), carbon-based nanoparticles and offer potential cytotoxicity in the lung, intestinal epithelium and gut microbiota (Fröhlich and Fröhlich, 2016; Bergin and Witzmann, 2013).

Aiming to combat the damages suffered by the intestine, nanotechnology of HA needs to advance in obtaining of new oral formulations that serves the following purposes: microbial metabolism, restoration of healthy epithelium and trans-epithelial uptake in the form of HMM. For this purpose, mixed structures of HA are necessary. Random coil structures from free HA are most readily metabolized by microbiota, on the other hand, compact and stable structures from nanoparticulate cross-linked HA, if degradation resistant, is appropriate for the uptake in the form of HMM.

The mucus nanostructure provides an effective barrier against NPs uptake by the intestinal epithelium (Sinnecker et al., 2014). However, HA-NPs have targets (HA receptors) on the underlying epithelium which favor their absorption (Abreu, 2010) by process known as endocytosis. This uptake mechanism is influenced by the physicochemical properties of NPs such as size, shape and zeta potential (Salatin and Yari, 2017). Molar mass, size distribution, aggregation state, purity, chemical stability, and environment factors (pH and dielectric constant) are also parameters that influence the uptake (Abbott and Maynard, 2010). pH variance within the gastrointestinal compartments can affect aggregation status (Peters et al., 2012) and alter surface chemistry, particularly in HA-NPs where zeta potential is highly dependent on pH, affecting stability, circulation time in the bloodstream and absorption into body membranes (Honary and Zahir, 2013).

Particle size and zeta potential are critical parameters because they directly impact the stability, cellular uptake, and bio-distribution of NPs (Mora-Huertas et al., 2011). It has been showed that most cells preferentially internalize HA-NPs spherical in shape, that are smaller than 400 nm in diameter and slightly negative zeta potential, ranging from -10 to -20 mV (Xiao et al., 2015).

Based on extensive previous studies on the lifetimes and clearance of nanoparticles in the bloodstream, the stabilization of HMM HA in nanoparticles may represent a promising strategy to prevent HA depolymerization in orally administered HA.

Stabilization can be performed by chemical crosslinking or by surface modifications by attachment of polymers. (Gref et al., 1994, Storm et al., 1995, Brigger et al., 2002, Shah et al., 2015).

There are some well described and reproducible methodologies to obtain HA nanoparticles with varying degrees of stability. Extensive experimentation with different cell types has demonstrated HA nanoparticles as safety in biological systems (Campoccia et al., 1998; Pitarresi et al., 2008).

MM size of HA varying from hexasaccharide units (1,200 Da) to HMM-HA (> 2 MDa) can be cross-linked to give specific qualities, protecting its intrinsic bioadhesive properties (Prestwich et al., 1998). Nanoparticles are stabilized by

various crosslinking agents, involving specific functional groups of the polysaccharide (e.g. carboxyl, hydroxyl, N-acetyl groups) which are modified by chemical reactions such as esterification, etherification, sulphatation, reductive amidation, carbodiimide mediated reactions, acrylation, isourea coupling, periodate oxidation (Pouyani et al., 1996; Lin et al., 2011; Bicudo and Santana, 2012a,b). Changing the type of coupling reactions can make it possible to develop material surfaces with specific activity to cell adhesion and metabolic activation (Garg and Hales, 2004; Benedetti et al., 1994).

Studies have shown that interactions between targeting moieties and specific receptors at tumor sites can improve bioadhesion of NPs to specific cells and further increase the extent of endocytosis via receptor-mediated internalization (Xiao et al., 2014). The stabilized HA-NPs represent a promising technology for interactions with receptors such as TLR4 and CD44, benefiting its internalization and new partitioning to intestinal degradation and targeting to other tissues.

The presence of HA receptors has increased its use as platform for combination chemotherapy (Pradhan et al., 2015), such as in colon tumor (Xiao et al., 2015), being able to perturb oncogenic signaling (Palvai et al., 2017).

6. Conclusions and Future Perspectives

The present review addressed the oral HA as complementary therapy for inflammation of mucous membranes. The molecular mechanisms of recognition and uptake of HMM-HA were described. Considering the crosstalk intestine-tissues in the systemic expansion of inflammation, it is appropriate to think that by treating the gut, all downstream disorders will also be treated. Oral HA is a powerful tool for the reestablishment of tissue homeostasis and the response to injury.

To date, the research conducted in the molecular field has focused mostly in the interaction CD44/HA in the articular cartilage, however, interactional aspects are few studied in the intestinal epithelium between TLR4 or CD44 and

HA. Detailed study needs to be devised to determine the effect of the physicochemical properties of HA in the formation of TLR4/CD44 clusters under the influence of the intestinal environment.

Free HA takes longer time to transverse the mucin network and is more susceptible to cleavage than nanoparticles. Additionally, the disordered geometry of chains from free HA is incompatible with specific adjustment required by the binding sites in the receptors. Therefore, HA-NPs with stabilized structure combines qualities to increase therapeutic efficacy of oral formulations (Hsieh et al., 2014; Huang et al., 2007).

The question is: what is the size and structure of HA-NPs that meets the requirements needed to adjust properly on a surface filled with TLR4/CD44 receptors? Will be intermediate structure (rod-to-coil) at 65 nm of diameter, as occurs in CD44 clusters of articular cartilage?

Future investigations and technological improvements are required for more efficient oral use of HA, such as: studies on mucosal adsorptive phenomena, signage-size dependency and intestinal and systemic effects of crosslinked HA. Nanotechnology also has to be considered because represents a promising tool for preparation of stabilized and sized formulations capable of interacting with specific receptors and promoting differentiated signals.

Acknowledgment

This study was financed in part by the Coordination for the Improvement of Higher Educational Personnel (CAPES, Brazil), [grant number: 33003017034P8].

Conflicts of Interest: The authors declare no conflict of interest.

References

1. Abbott, L. C., Maynard, A. D. 2010. Exposure assessment approaches for engineered nanomaterials. *Risk Analysis*. 30(11):1634–1644.
2. Abreu, M. T. 2010. Toll-like receptor signalling in the intestinal epithelium: how bacterial recognition shapes intestinal function. *Nat. Rev. Immunol.* 10(2):131-44.
3. Artursson, P., Ungell, A. L., Löfroth, J. E. 1993. Selective paracellular permeability in two models of intestinal absorption: cultured monolayers of human intestinal epithelial cells and rat intestinal segments *Pharm. Res.* 10(8):1123-9.
4. Asari, A., Kanemitsu, T., Kurihara, H. 2010. Oral administration of high molar weight hyaluronan (900 kDa) controls immune system via Toll-like receptor 4 in the intestinal epithelium. *J. Biol. Chem.* 285:24751–8.
5. Atuma, C., Strugala, V., Allen, A., Holm, L. 2001. The adherent gastrointestinal mucus gel layer: thickness and physical state in vivo. *Am J Physiol. Gastrointest. Liver Physiol.* 280(5):G922-9.
6. Awasthi, S., 2014. Toll-like receptor-4 modulation for cancer immunotherapy. *Front. Immunol.* 5: 328.
7. Balogh, L., Polyak, A., Mathe, D., Kiraly, R., Thuroczy, J., Terez, M., Janoki, G., Ting, Y., Bucci, L. R., Schauss, A. G. 2008. Absorption, Uptake and Tissue Affinity of High-Molar-Weight Hyaluronan after Oral Administration in Rats and Dogs. *J. Agric. Food Chem.* 56, 10582–10593.
8. Barthe, L., Woodley, J., Houin, G. 1999. Gastrointestinal absorption of drugs: methods and studies. *Fundam Clin Pharmacol.* 13(2):154-68.
9. Benedetti, L., Bellini, D., Renier, D., O'Regan, M. 1994. Chemical modification of hyaluronan In: Novel biomaterials based on hyaluronic acid and its derivatives Williams DF, editor Proceedings of a Workshop held at the Annual Meeting of the European Society for Biomaterials Pisa, Italy, 1994:20-9.

10. Bergin, I. L., Witzmann, F. A. 2013. Nanoparticle toxicity by the gastrointestinal route: evidence and knowledge gaps. *Int. J. Biomed. Nanosci. Nanotechnol.* 3(1-2).
11. Bicudo, R. C., Santana, M. H. 2012a. Effects of organic solvents on hyaluronic acid nanoparticles obtained by precipitation and chemical crosslinking. *J. Nanosci. Nanotechnol.* 12(3):2849-57.
12. Bicudo, R. C., Santana, M. H. 2012b. Production of hyaluronic acid (HA) nanoparticles by a continuous process inside microchannels: Effects of non-solvents, organic phase flow rate, and HA concentration. *Chemical Engineering Science* 84 134–141.
13. Bollyky, P. L., Falk, B. A., Long, S. A., Preisinger, A., Braun, K. R., Wu, R. P., Evanko, S. P., Buckner, J. H., Wight, T. N., Nepom, G. T. 2009. CD44 costimulation promotes FoxP3⁺ regulatory T cell persistence and function via production of IL-2, IL-10, and TGF-beta. *J. Immunol.* 183(4):2232-41.
14. Bollyky, P. L., Lord, J. D., Masewicz, S. A., Evanko, S. P., Buckner, J. H., Wight, T. N., Nepom, G. T. 2007. Cutting edge: high molecular weight hyaluronan promotes the suppressive effects of CD4⁺CD25⁺ regulatory T cells. *J. Immunol.* 179(2):744-7.
15. Brigger, I., Dubernet, C., Couvreur, P. 2002. Nanoparticles in cancer therapy and diagnosis. *Adv. Drug Deliv. Rev.* 54(5):631-51.
16. Bucci, L. R., Turpin, A. A. 2004. Will the real hyaluronan please stand up?. *Journal of applied nutrition*, 54, 1.
17. Burgdorf, S., Kautz, A., Böhnert, V., Knolle, P.A., Kurts, C. 2007. Distinct pathways of antigen uptake and intracellular routing in CD4 and CD8 T cell activation. *Science.* 316(5824):612-6.
18. Cameron, E. A. Sperandio, V. 2015. Frenemies: signaling and nutritional integration in pathogen–microbiota–host interactions. *Cell Host Microbe* 18(3):275-84.
19. Campo, G. M., Avenoso, A., Campo, S., D'Ascola, A., Nastasi, G., Calatroni, A. 2010. Molar size hyaluronan differently modulates toll-like receptor-4 in LPS-induced inflammation in mouse chondrocytes. *Biochimie* 92(2):204-15.

20. Campoccia, D., Doherty, P., Radice, M., Brun, P., Abatangelo, G., Williams, D.F. 1998. Semisynthetic resorbable materials from hyaluronan esterification *Biomaterials*. 19(23):2101-27.
21. Cardoso, M. J., Caridade, S. G., Costa, R. R., Mano, J. F. 2016. Enzymatic Degradation of Polysaccharide-Based Layer-by-Layer Structures. *Biomacromolecules*. 17(4), 1347–1357.
22. Cario, E. 2010. Toll-like receptors in inflammatory bowel diseases: a decade later. *Inflamm. Bowel Dis.* 16(9):1583-97.
23. Cario, E., Brown, D., McKee, M., Lynch-Devaney, K., Gerken, G., Podolsky, D.K. 2002. Commensal-associated molecular patterns induce selective toll-like receptor-trafficking from apical membrane to cytoplasmic compartments in polarized intestinal epithelium. *Am. J. Pathol.* 160: 165 – 173.
24. Cario, E., Podolsky, D.K. 2000. Differential alteration in intestinal epithelial cell expression of toll-like receptor 3 (TLR3) and TLR4 in inflammatory bowel disease. *Infect. Immun.* 68(12):7010-7.
25. Chakrabarti, B., Balazs, E. A. 1973. Optical properties of hyaluronic acid. Ultraviolet circular dichroism and optical rotatory dispersion. *J. Mol. Biol.* 78, 135–141.
26. Chen, W.Y.J., Abatangelo, G. 1999. Functions of hyaluronan in wound repair. *Wound Repair and Regeneration*, 7, 79–89.
27. Chieppa, M., Rescigno, M., Huang, A.Y., Germain, R.N. 2006. Dynamic imaging of dendritic cell extension into the small bowel lumen in response to epithelial cell TLR engagement. *J. Exp. Med.* 203(13):2841-52.
28. Cockburn, D. W., Koropatkin, N. M. 2016. Polysaccharide Degradation by the Intestinal Microbiota and Its Influence on Human Health and Disease. *J. Mol. Biol.* pii: S0022-2836(16)30243-1.
29. Corr, S. C., Gahan, C. C., Hill, C. 2008. M-cells: origin, morphology and role in mucosal immunity and microbial pathogenesis. *FEMS Immunol. Med. Microbiol.* 52(1):2-12.
30. Cyphert, J. M., Trempus, C. S., Garantziotis, S. 2015. Size Matters: Molecular Weight Specificity of Hyaluronan Effects in Cell Biology. *Int. J. Cell Biol.* 2015:563818.

31. de Goffau, M. C., Luopajarvi, K., Knip, M., Ilonen, J., Ruohtula, T., Härkönen, T., Orivuori, L., Hakala, S., Welling, G. W., Harmsen, H.J., Vaarala, O. 2013. Fecal microbiota composition differs between children with b-cell autoimmunity and those without. *Diabetes* 62:1238–1244.
32. de Kivit, S., Tobin, M. C., Forsyth, C. B., Keshavarzian, A., Landay, A. L. 2014. Regulation of intestinal immune responses through TLR activation: implications for pro- and prebiotics. *Front. Immunol.* 5:60.
33. de la Motte, C. A. 2011. Hyaluronan in intestinal homeostasis and inflammation: implications for fibrosis. *Am. J. Physiol. Gastrointest. Liver Physiol.* 301(6):G945-9.
34. de la Motte, C. A., Kessler, S. P. 2015. The Role of Hyaluronan in Innate Defense Responses of the Intestine. *International Journal of Cell Biology*, ID 481301, 5p.
35. Di Cerbo, A., Aponte, M., Esposito, R., Bondi, M., Palmieri, B. 2013. Comparison of the effects of hyaluronidase and hyaluronic acid on probiotics growth. *BMC Microbiol.* 13: 243.
36. Ebid, R., Lichtnekert, J., Anders, H. J. 2014. Hyaluronan is not a ligand but a regulator of toll-like receptor signaling in mesangial cells: Role of extracellular matrix in innate immunity. *ISRN Nephrol.*
37. Eckburg, P. B., Bik, E. M., Bernstein, C. N., Purdom, E., Dethlefsen, L., Sargent, M., Gill, S. R., Nelson, K. E., Relman, D.A. 2005. Diversity of the human intestinal microbial flora. *Science* 308(5728):1635-8.
38. Falcone, S. J., Palmeri, D., Berg, R. A. 2006. Biomedical Applications of Hyaluronic Acid. *Polysaccharides for Drug Delivery and Pharmaceutical Applications*, 155–174.
39. Fellows, R., Denizot, J., Stellato, C., Cuomo, A., Jain, P., Stoyanova, E., Balázsi, S., Hajnády, Z., Liebert, A., Kazakevych, J., Blackburn, H., Corrêa, R. O., Fachi, J. L., Sato, F. T., Ribeiro, W. R., Ferreira, C. M., Perée, H., Spagnuolo, M., Mattiuz, R., Matolcsi, C., Guedes, J., Clark, J., Veldhoen, M., Bonaldi, T., Vinolo, M. A. R., Varga-Weisz, P. 2018. Microbiota derived short chain fatty acids promote histone crotonylation in the colon through histone deacetylases. *Nat. Commun.* 9(1):105.
40. Fraser, J. R. E., Laurent, T. C., Laurent, U. B. G. 1997. Hyaluronan: its nature, distribution, functions and turnover. *J. Intern. Med.* 242:27-33.

41. Frohlich, E. E., Frohlich, E. 2016. Cytotoxicity of nanoparticles contained in food on intestinal cells and the gut microbiota. *Int. J. Mol. Sci.* 17, 1–22.
42. Garg, H. G., Hales, C. A. 2004. *Chemistry and Biology of Hyaluronan*. Elsevier.
43. Ghatak, S., Misra, S., Toole, B. P. 2002. Hyaluronan oligosaccharides inhibit anchorage-independent growth of tumor cells by suppressing the phosphoinositide 3-kinase/Akt cell survival pathway *J Biol Chem.* 277(41):38013-20.
44. Go, V. L., Nguyen, C. T., Harris, D. M., Lee, W. N. 2005. Nutrient-gene interaction: metabolic genotype-phenotype relationship. *J. Nutr.* 135(12 Suppl):3016S-3020S.
45. Gref, R., Minamitake, Y., Peracchia, M. T., Trubetskoy, V., Torchilin, V., Langer, R. 1994. Biodegradable long-circulating polymeric nanospheres. *Science* 263 1600–1603.
46. Gu, J. M., Robinson, J. R., Leung, S. H. 1988. Binding of acrylic polymers to mucin/epithelial surfaces: structure-property relationships. *Crit. Rev. Ther. Drug Carrier Syst.* 5(1):21-67.
47. Gustafson, S. 1998. Methods of elevating amounts of hyaluronan in the human body. Patent WO1998027990 A1.
48. Hansen, I. M., Ebbesen, M. F., Kaspersen, L., Thomsen, T., Bienk, K., Cai, Y., Malle, B. M., Howard, K. A. 2017. Hyaluronic Acid Molecular Weight-Dependent Modulation of Mucin Nanostructure for Potential Mucosal Therapeutic Applications. *Mol. Pharm.* 14(7):2359-2367.
49. Hascall, V. C., Laurent, T. C., Yanagishita, M. 1997. Hyaluronan: structure and physical properties In: *Hyaluronan Today*. <http://glycoforumgrip>.
50. Haxaire, K., Braccini, I., Milas, M., Rinaudo, M., Pérez, S. 2000. Conformational behavior of hyaluronan in relation to its physical properties as probed by molecular modeling. *Glycobiology* 10(6):587-94.
51. Henao-Mejia, J., Elinav, E., Jin, C., Hao, L., Mehal, W. Z., Strowig, T., Thaiss, C.A., Kau, A. L., Eisenbarth, S. C., Jurczak, M. J., Camporez, J. P., Shulman, G. I., Gordon, J. I., Hoffman, H. M., Flavell, R. A. 2012. Inflammasome-mediated dysbiosis regulates progression of NAFLD and obesity. *Nature* 482(7384):179-85.

52. Honary, S., Zahir, F. 2013. Effect of Zeta Potential on the Properties of Nano-Drug Delivery Systems - A Review (Part 2). *Tropical Journal of Pharmaceutical Research*. 12 (2): 265-273.
53. Hornef, M. W., Normark, B. H., Vandewalle, A., Normark, S. 2003. Intracellular recognition of lipopolysaccharide by toll-like receptor 4 in intestinal epithelial cells. *J. Exp. Med.* 198: 1225 – 1235.
54. Hsieh, C. M., Huang, Y. W., Sheu, M. T., Ho, H. O. 2014. Biodistribution profiling of the chemical modified hyaluronic acid derivatives used for oral delivery system. *Int. J. Biol. Macromol.* 64:45-52.
55. Huang, S. L., Ling, P. X., Zhang, T. M. 2007. Oral absorption of hyaluronic acid and phospholipids complexes in rats. *World J. Gastroenterol.* 13(6):945-9.
56. Karlsson, F. H., Fåk, F., Nookaew, I., Tremaroli, V., Fagerberg, B., Petranovic, D., Bäckhed, F., Nielsen, J. 2012. Symptomatic atherosclerosis is associated with an altered gut metagenome. *Nat. Commun.* 3:1245.
57. Kawada, C., Kimura, M., Masuda, Y., Nomura, Y. 2015b. Oral administration of hyaluronan prevents skin dryness and epidermal thickening in ultraviolet irradiated hairless mice. *J. Photochem. Photobiol. B.* 153:215-21.
58. Kawada, C., Yoshida, T., Yoshida, H., Matsuoka, R., Sakamoto, W., Odanaka, W., Sato, T., Yamasaki, T., Kanemitsu, T., Masuda, Y., Urushibata, O. 2014. Ingested hyaluronan moisturizes dry skin. *Nutr. J.* 13:70.
59. Kawada, C., Yoshida, T., Yoshida, H., Sakamoto, W., Odanaka, W., Sato, T., Yamasaki, T., Kanemitsu, T., Masuda, Y., Urushibata, O. 2015a. Ingestion of hyaluronans (molecular weights 800 k and 300 k) improves dry skin conditions: A randomized, double blind, controlled study. *J. Clin. Biochem. Nutr.* 56, 66–73.
60. Keely, S., Talley, N. J., Hansbro, P. M. 2012. Pulmonary-intestinal cross-talk in mucosal inflammatory disease. *Mucosal Immunol.* 5(1):7-18.
61. Kessler, S., Rho, H., West, G., Fiocchi, C., Drazba, J., de la Motte, C. 2008. Hyaluronan (HA) deposition precedes and promotes leukocyte recruitment in intestinal inflammation. *Clin. Transl. Sci.* (1):57-61.

62. Kimura, M., Maeshima, T., Kubota, T., Kurihara, H., Masuda, Y., Nomura, Y. 2016. Absorption of Orally Administered Hyaluronan. *J. Med. Food.* 19(12):1172-1179.
63. Knopf-Marques, H., Pravda, M., Wolfova, L., Velebny, V., Schaaf, P., Vrana, N. E., Lavallo, P. 2016. Hyaluronic Acid and Its Derivatives in Coating and Delivery Systems: Applications in Tissue Engineering, Regenerative Medicine and Immunomodulation. *Adv. Healthc. Mater.* 5, 2841–2855.
64. Kobayashi, Y., Okamoto, A., Nishinari, K. 1994. Viscoelasticity of hyaluronic acid with different molecular weights. *Biorheology* 31, 235–244.
65. Koropatkin, N. M., Cameron, E. A., Martens, E. C. 2012. How glycan metabolism shapes the human gut microbiota. *Nat. Rev. Microbiol.* 10:323–335.
66. Kresse, H., Glossl, J. 1987. Glycosaminoglycan degradation In *Advances in Enzymology*, 60th edn (ed A Meister), pp 217-311 New York: Wiley.
67. Kuzela, L., Vavrecka, A., Prikazska, M., Drugda, B., Hronec, J., Senkova, A., Drugdova, M., Oltman, M., Novotna, T., Brezina, M., Kratky, A., Kristufek, P. 1999. Pulmonary complications in patients with inflammatory bowel disease. *Hepatogastroenterology.* 46(27):1714–1719.
68. La Gatta, A., De Rosa, M., Marzaioli, I., Busico, T., Schiraldi, C. 2010. A complete hyaluronan hydrodynamic characterization using a size exclusion chromatography-triple detector array system during in vitro enzymatic digestion. *Anal. Biochem.* 404:21–29.
69. Laznicek, M., Laznickova, A., Cozikova, D., Velebny, V. 2012. Preclinical pharmacokinetics of radiolabelled hyaluronan *Pharmacol Rep.* 64(2):428-37.
70. Lesley, J., Hascall, V.C., Tammi, M., Hyman, R. 2000. Hyaluronan binding by cell surface CD44. *J. Biol. Chem.* 275(35):26967-75.
71. Ley, R. E., Turnbaugh, P. J., Klein, S., Gordon, J. I. 2006. Microbial ecology: human gut microbes associated with obesity. *Nature.* 444(7122):1022-3.
72. Li, X., Wang, C., Nie, J., Lv, D., Wang, T., Xu, Y. 2013. Toll-like receptor 4 increases intestinal permeability through up-regulation of membrane PKC activity in alcoholic steatohepatitis. *Alcohol.* 47(6):459-65.

73. Lin, F-H., Su, W-Y., Chen, Y-C., Chen, K-H. 2011. Cross-linked oxidated hyaluronic acid for use as a vitreous substitute. Patent US8197849B2.
74. Linden, S. K., Sutton, P., Karlsson, N. G., Korolik, V., McGuckin, M. A. 2008. Mucins in the mucosal barrier to infection. *Mucosal Immunol.* 1(3):183–97.
75. Macpherson, A. J., Harris, N. L. 2004. Interactions between commensal intestinal bacteria and the immune system. *Nat. Rev. Immunol.* 4:478–85.
76. Maleki, A.; Kjønicksen, A. L.; Nystrom, B. 2008. Effect of pH on the behavior of hyaluronic acid in dilute and semidilute aqueous solutions. *Macromol. Symp.* 274, 131–140.
77. Matsuki, T., Pédrón, T., Regnault, B., Mulet, C., Hara, T., Sansonetti, P. J. 2013. Epithelial cell proliferation arrest induced by lactate and acetate from *Lactobacillus casei* and *Bifidobacterium breve*. *PLoS One.* 8(4):e63053.
78. McClements, D. J., Xiao, H. 2017. Is nano safe in foods? Establishing the factors impacting the gastrointestinal fate and toxicity of organic and inorganic food-grade nanoparticles. *npj Science of Food* 1:6.
79. Medzhitov, R., Preston-Hurlburt, P., Janeway, C. A. Jr. 1997. A human homologue of the *Drosophila* Toll protein signals activation of adaptive immunity. *Nature* 388(6640):394-7.
80. Mora-Huertas, C. E., Fessi, H., Elaissari, A. 2011. Influence of process and formulation parameters on the formation of submicron particles by solvent displacement and emulsification-diffusion methods critical comparison. *Adv. Colloid Interface Sci.* 163(2):90-122.
81. Mouta Carreira, C., Nasser, S. M., di Tomaso, E., Padera, T. P., Boucher, Y., Tomarev, S. I., Jain, R. K. 2001. LYVE-1 is not restricted to the lymph vessels: expression in normal liver blood sinusoids and down-regulation in human liver cancer and cirrhosis. *Cancer Res.* 61, 8079–8084.
82. Muto, J., Yamasaki, K., Taylor, K. R., Gallo, R. L. 2009. Engagement of CD44 by hyaluronan suppresses TLR4 signaling and the septic response to LPS. *Mol. Immunol.* 47(2-3):449-56.
83. Neal, M. D., Leaphart, C., Levy, R., Prince, J., Billiar, T. R., Watkins, S., Li, J, Cetin, S., Ford, H., Schreiber, A., Hackam, P. J. 2006. Enterocyte TLR4 mediates phagocytosis and transcytosis of bacteria across the intestinal barrier, *J. Immunol.* 176 3070–3079.

84. Necas, J., Bartosikova, L., Brauner, P., Kolar, J. 2008. Hyaluronic acid (hyaluronan): a review. *Veterinarni Medicina*, 53, (8): 397–411.
85. Neutra, M. R. 1998. Current concepts in mucosal immunity. V Role of M cells in transepithelial transport of antigens and pathogens to the mucosal immune system. *Am. J. Physiol.* 274(5 Pt 1):G785-91.
86. Oe, M., Mitsugi, K., Odanaka, W., Yoshida, H., Matsuoka, R., Seino, S., Kanemitsu, T., Masuda, Y. 2014. Dietary hyaluronic acid migrates into the skin of rats. *Scientific World Journal*. 2014:378024.
87. Oe, M., Tashiro, T., Yoshida, H., Nishiyama, H., Masuda, Y., Maruyama, K., Koikeda, T., Maruya, R., Fukui, N., 2016. Oral hyaluronan relieves knee pain: a Review. *Nutrition Journal*, 15:11.
88. Oertli, B., Beck-Schimmer, B., Fan, X., Wüthrich, R. P. 1998. Mechanisms of hyaluronan-induced up-regulation of ICAM-1 and VCAM-1 expression by murine kidney tubular epithelial cells: hyaluronan triggers cell adhesion molecule expression through a mechanism involving activation of nuclear factor-kappa B and activating protein-1. *J. Immunol.* 161(7):3431-7.
89. Oh, C-D., Chun, J-S. 2003. Signaling Mechanisms Leading to the Regulation of Differentiation and Apoptosis of Articular Chondrocytes by Insulin-like Growth Factor-1. *J. Biol. Chem.* 278, 36563-36571.
90. O'Neill, L.A. 2003. Therapeutic targeting of Toll-like receptors for inflammatory and infectious diseases. *Curr Opin Pharmacol.* 3(4):396-403.
91. Palvai, S., Kuman, M.M., Sengupta, P., Basu, S. 2017. Hyaluronic Acid Layered Chimeric Nanoparticles: Targeting MAPK-PI3K Signaling Hub in Colon Cancer Cells. *ACS Omega.* 2(11): 7868–7880.
92. Park, B. S., Song, D. H., Kim, H. M., Choi, B. S., Lee, H., Lee, J. O. 2009. The structural basis of lipopolysaccharide recognition by the TLR4-MD-2 complex. *Nature* 458, 1191–1195.
93. Pitarresi, G., Palumbo, F. S., Calabrese, R., Craparo, E. F., Giammona, G. 2008. Crosslinked hyaluronan with a protein-like polymer: novel bioresorbable tablets for biomedical applications *J Biomed Mater Res A.* 84(2):413-24.
94. Ponchel, G., Irache, J. 1998. Specific and non-specific bioadhesive particulate systems for oral delivery to the gastrointestinal tract. *Adv. Drug Deliv. Rev.* (2-3):191-219.

95. Pouyani, T., Brook, S., Prestwich, G. D., James, St. 1996. Functionalized derivatives of hyaluronic acid. Patent US005616568 A.
96. Powell, J. D., Horton, M. R. 2005. Threat matrix: low-molecular-weight hyaluronan (HA) as a danger signal. *Immunol. Res.* 31: 207–218.
97. Pradhan, R., Ramasamy, T., Choi, J. Y., Kim, J. H., Poudel, B. K., Tak, J. W., Nukolova, N., Choi, H. G., Yong, C. S., Kim, J. O. 2015. Hyaluronic acid-decorated poly(lactic-co-glycolic acid) nanoparticles for combined delivery of docetaxel and tanespimycin. *Carbohydr. Polym.* 123:313-23.
98. Prestwich, G. D. 2001. Biomaterials from chemically-modified hyaluronan. In: *Hyaluronan Today* <http://www.glycoforum.grjp>.
99. Prestwich, G. D., Marecak, D. M., Mareck, J. F., Vercruysee, K. P., Ziebell, M. R. 1998. Controlled chemical modification of hyaluronic acid: synthesis, applications, and biodegradation of hydrazide derivatives. *J. Control Release*, 53, 93-103.
100. Qin, J., Li, Y., Cai, Z., Li, S., Zhu, J., Zhang, F., Liang, S., Zhang, W., Guan, Y., Shen, D., Peng, Y., Zhang, D., Jie, Z., Wu, W., Qin, Y., Xue, W., Li, J., Han, L., Lu, D., Wu, P., Dai, Y., Sun, X., Li, Z., Tang, A., Zhong, S., Li, X., Chen, W., Xu, R., Wang, M., Feng, Q., Gong, M., Yu, J., Zhang, Y., Zhang, M., Hansen, T., Sanchez, G., Raes, J., Falony, G., Okuda, S., Almeida, M., LeChatelier, E., Renault, P., Pons, N., Batto, J.M., Zhang, Z., Chen, H., Yang, R., Zheng, W., Li, S., Yang, H., Wang, J., Ehrlich, S.D., Nielsen, R., Pedersen, O., Kristiansen, K., Wang, J. 2012. A metagenome-wide association study of gut microbiota in type 2 diabetes. *Nature*. 490(7418):55-60.
101. Rescigno, M., Di Sabatino, A. 2001. Dendritic cells in intestinal homeostasis and disease. *Journal of Clinical Investigation* 119 2441–2450.
102. Riehl, T.E., Ee, X., Stenson, W.F. 2012. Hyaluronic acid regulates normal intestinal and colonic growth in mice. *Am J Physiol Gastrointest Liver Physiol.* 303(3): G377–G388.
103. Round, J. L., Mazmanian, S. K. 2009. The gut microbiota shapes intestinal immune responses during health and disease. *Nat. Rev. Immunol.* 9(5):313-23.

104. Rubas, W., Grass, G. M. 1991. Gastrointestinal lymphatic absorption of peptides and proteins. *Advanced Drug Delivery Reviews* 7 15-69.
105. Salatin, S., Yari, K. A. 2017. Overviews on the cellular uptake mechanism of polysaccharide colloidal nanoparticles. *J. Cell. Mol. Med.* 21(9):1668-1686.
106. Salustri, A., Fulop, C. 1998. Role of Hyaluronan during Ovulation and Fertilization. In: *Hyaluronan Today* <http://wwwglycoforumgrjp>.
107. Salyers, A. A.; Vercellotti, J. R.; West, S. E.; Wilkins, T. D. 1977. Fermentation of mucin and plant polysaccharides by strains of *Bacteroides* from the human colon, *Appl. Environ. Microbiol.* 33 319–322.
108. Scott, J. E. 1989. Secondary structures in hyaluronan solutions: chemical and biological implications, in: *The Biology of Hyaluronan*, Ciba Foundation, J. Wiley and Sons, Ltd, Chichester, UK, pp 6–20.
109. Seed, S. M., Dunican, K. C., Lynch, A. M. 2011. Treatment options for osteoarthritis: considerations for older adults. *Hosp. Pract.* 39(1):62-73.
110. Shah, K., Crowder, D., Overmeyer, J., Maltese, W., Yun, Y. 2015. Hyaluronan drug delivery systems are promising for cancer therapy because of their selective attachment, enhanced uptake, and superior efficacy. *Biomed Eng. Lett.* 5:109-123.
111. Sinnecker, H., Krause, T., Koelling, S., Lautenschläger, I., Frey, A. 2014. The gut wall provides an effective barrier against nanoparticle uptake. *Beilstein. J. Nanotechnol.* 5:2092-101.
112. Slevin, M., Krupinski, J., Gaffney, J., Matou, S., West, D., Delisser, H., Savani, R. C., Kumar, S. 2007. Hyaluronan-mediated angiogenesis in vascular disease: uncovering RHAMM and CD44 receptor signaling pathways. *Matrix Biol* 26: 58–68.
113. Smeaton, T.C., Simpson-Morgan, M.W., 1985. Epithelial cell renewal and antibody transfer in the intestine of the foetal and neonatal lamb. *Aust. J. Exp. Biol. Med. Sci.* 63 (Pt 1):41-51.
114. Soltés, L., Mendichi, R., Kogan, G., Schiller, J., Stankovska, M., Arnhold, J. 2006. Degradative action of reactive oxygen species on hyaluronan. *Biomacromolecules* 7(3):659-68.

115. Storm, G., Belliot, S. O., Daemen, T., Lasic, D. D. 1995. Surface modification of nanoparticles to oppose uptake by the mononuclear phagocyte system. *Adv. Drug Deliv. Rev.* 17 31–48.
116. Takeda, K., Akira, S. 2005. Toll-like receptors in innate immunity. *Int. Immunol.* 17(1):1-14.
117. Tian, R., Tan, J. T., Wang, R. L., Xie, H., Qian, Y. B., Yu, K. L. 2013. The role of intestinal mucosa oxidative stress in gut barrier dysfunction of severe acute pancreatitis. *Eur. Rev. Med. Pharmacol. Sci.* (3):349-55.
118. Toole, B. P. 2004. Hyaluronan: from extracellular glue to pericellular cue. *Nat. Rev. Cancer.* 4(7):528-39.
119. Triantafilou, M., Triantafilou, K. 2003. Receptor cluster formation during activation by bacterial products. *J. Endotoxin Res.* 9 331–335.
120. Turley, E. A., Asculai, S. S. 2003. Oral administration of effective amounts of forms of hyaluronic acid. US6537978 B1.
121. Turnbaugh, P. J., Hamady, M., Yatsunencko, T., Cantarel, B. L., Duncan, A., Ley, R. E., Sogin, M. L., Jones, W. J., Roe, B. A., Affourtit, J. P., Egholm, M., Henrissat, B., Heath, A. C., Knight, R., Gordon, J. I. 2009. A core gut microbiome in obese and lean twins. *Nature.* 457(7228):480-4.
122. Urao, M., Okuyama, H., Drongowski, R. A., Teitelbaum, D. H., Coran, A. G. 1997. Intestinal permeability to small- and large-molecular-weight substances in the newborn rabbit. *J. Pediatr. Surg.* 32(10):1424-8.
123. Wagner, C. S., Cresswell, P. 2012. TLR and nucleotide-binding oligomerization domain-like receptor signals differentially regulate exogenous antigen presentation. *J. Immunol.* 188(2):686–93.
124. Wang, Y., Devkota, S., Musch, M. W., Jabri, B., Nagler, C., Antonopoulos, D. A., Chervonsky, A., Chang, E. B., 2010. Regional mucosa-associated microbiota determines physiological expression of TLR2 and TLR4 in murine colon. *PLoS One.* 5(10):e13607.
125. Wang, Z., Klipfell, E., Bennett, B.J., Koeth, R., Levison, B. S., Dugar, B., Feldstein, A. E., Britt, E. B., Fu, X., Chung, Y. M., Wu, Y., Schauer, P., Smith, J. D., Allayee, H., Tang, W. H., DiDonato, J. A., Lusis, A. J., Hazen, S. L. 2011. Gut flora metabolism of phosphatidylcholine promotes cardiovascular disease. *Nature.* 472(7341):57-63.

126. Warshaw, A. L., Walker, W. A., Isselbacher, K. J. 1974. Protein uptake by the intestine: evidence for absorption of intact macromolecules. *Gastroenterology* 66(5):987-92.
127. Weigel, P. H., Baggenstoss, B. A. 2017. What is special about 200 kDa hyaluronan that activates hyaluronan receptor signaling? *Glycobiology*. 27(9):868-877.
128. Wong, J. M., de Souza, R., Kendall, C. W., Emam, A., Jenkins, D. J. 2006. Colonic health: fermentation and shortchain fatty acids, *J. Clin. Gastroenterol.* 40 235–243.
129. Xiao, B., Han, M. K., Viennois. E., Wang, L., Zhang, M., Si, X., Merlin, D. 2015. Hyaluronic acid-functionalized polymeric nanoparticles for colon cancer-targeted combination chemotherapy. *Nanoscale*. 7(42):17745-55.
130. Xiao, B., Yang, Y., Viennois, E., Zhang, Y., Ayyadurai, S., Baker, M., Laroui, H., Merlin, D. 2014. Glycoprotein CD98 as a receptor for colitis-targeted delivery of nanoparticle. *J. Mater. Chem. B*. 2(11):1499-1508.
131. Yang, C., Cao, M., Liu, H., He, Y., Xu, J., Du, Y., Liu, Y., Wang, W., Cui, L., Hu, J., Gao, F. 2012. The high and low molar weight forms of hyaluronan have distinct effects on CD44 clustering. *J. Biol. Chem.* 287(51):43094-107.
132. Yannariello-Brown, J., Zhou, B., Weigel, P. H. 1997. Identification of a 175 kDa protein as the ligand-binding subunit of the rat liver sinusoidal endothelial cell hyaluronan receptor. *Glycobiology*. 7, 15–21.
133. Zheng, L., Riehl, T., Stenson, W. F. 2009. Regulation of Colonic Epithelial Repair in Mice by Toll-like Receptors and Hyaluronic Acid. *Gastroenterology*. 137(6): 2041–2051.

**CAPÍTULO 3:
METODOLOGIA,
RESULTADOS E DISCUSSÃO**

3 RESULTADOS E DISCUSSÃO

Esta seção é composta pelos artigos experimentais: (1) “*Penetration of free and nanoparticle hyaluronic acid in mucin tablets and in rat intestinal mucosa*”. Este artigo investigou o comportamento mucoadesivo de formulações de AH nas formas livres e nanoestruturadas em mucina de estômago de porco e em mucosa intestinal de ratos. (2) “*Intestinal uptake assessment of the oral hyaluronic acid in rats*”. Este artigo investigou a permeação intestinal e a absorção de formulações de AH pré-selecionadas no estudo de adesão.

3.1 Penetration of free and nanoparticle hyaluronic acid in mucin tablets and in rat intestinal mucosa

Penetration of free and nanoparticle hyaluronic acid in mucin tablets and in rat intestinal mucosa

Alexandro Barbosa de Souza¹, Marco Vinicius Chaud², Thais Francine Ribeiro Alves²,
Juliana Ferreira de Souza² & Maria Helena Andrade Santana^{1*}

¹Department of Materials and Bioprocesses Engineering, School of Chemical Engineering, University of Campinas, P.O. Box 6066, 13083-852, Campinas, SP, Brazil and ²Laboratory of Biomaterials and Nanotechnology, University of Sorocaba, 18300-000, Sorocaba, SP, Brazil.

*Correspondence should be addressed to mariahelena.santana@gmail.com

ABSTRACT

Advances in knowledge of the effects of orally administered hyaluronic acid (HA) have shown that besides treating dysbiosis and promoting immunomodulation, it can also target other tissues by means of molecular signalization. Therefore, the HA-mucus penetration controls HA uptake in the intestinal epithelium as well as the extent of its functions. Although various HA interpenetrating systems has been reported in the literature, the HA-mucus system has been poorly explored. In this work we investigate the influence of the three dimensional HA structure on its penetration in mucin tablets and in rat intestinal mucosa. Mucoadhesive tensile assays were carried out for penetration evaluation. Formulations of free HA presenting fractions of highest molar mass (MM) $>10^5$ Da (H-MM), intermediate MM $\leq 10^5$ Da (I-MM), and low MM $\leq 10^4$ Da (L-MM) as well as a formulation of HA nanoparticles with 485.3 ± 87.61 nm mean diameter and a mixture of I-MM with 25 % or 50 % (wt.) of nanoparticles were previously prepared and characterized. According to the peak detachment force (F_{adh}) and the work of adhesion (W_{adh}), the 2.5 g/L nanoparticles ($F_{adh} 1.06 \pm 0.08$; $W_{adh} 0.04 \pm 0.01$), the 25 wt. % mixed HA ($F_{adh} 1.05 \pm 0.04$; $W_{adh} 0.05 \pm 0.01$) and 10 g/L I-MM ($F_{adh} 0.74 \pm 0.14$; $W_{adh} 0.14 \pm 0.03$) formulations were the most promising for penetration in the mucus network. A qualitative model was proposed for explain the results for HA penetration. As far as we know, there is no studies in literature on intestinal penetration of free and nanostructured HA. These results are relevant for selecting HA structures with improved penetration properties for further *in vivo* assays and also for oral administration.

Keywords: Oral hyaluronic acid; Polymer penetration; Nanoparticles.

1. Introduction

Hyaluronic acid (HA) is a natural polymer found in human at specific sites of connective, neural and epithelial tissues (Kogan et al, 2007). HA is composed of disaccharide units of D-glucuronic acid and N-D-acetylglucosamine, coupled via alternating β (1'-4) and β (1-3') glycosidic bonds, yielding chains with average molar mass from 10^3 to 10^6 Da (Garg and Hales, 2004).

HA performs biological functions throughout its range of molar mass. At the intestinal mucosa, intermediate and high molar mass (MM) HA presents antioxidant and anti-microbial properties (Hansen et al, 2017; Fukuda et al., 1997; Balazs and Band, 2008). Additionally, complementary structures bind HA on the surface of the epithelium stimulating the endocytosis and inhibiting the release of inflammatory mediators as reported by Jiang et al, 2002.

The transposition of the mucus network is determinant for the HA functions on the intestinal epithelium, as well as for its transit to the bloodstream compartment and different tissues. Therefore, exogenous oral HA may have beneficial effects in dysbiosis treatment, in the articular and skin homeostasis, and as an auxiliary in osteoarthritis treatment (Di Cerbo et al., 2013; Kawada et al., 2014; Balogh et al., 2008; Falcone et al., 2006).

Besides HA turnover, which preserves the integrity of intestinal membrane, the uptake of exogenous HA is performed by signalization via CD44 and TLR4 receptors (Fraser et al., 1997; Kresse and Glossl, 1987). In the intestinal epithelium, TLR4 modulate the transepithelial uptake and signaling, while CD44 modulate the signaling (Muto et al., 2009).

The molecular dynamism of intestinal uptake begins with the chemical adsorption of HA on the TLR4 receptors scattered on the underlying epithelium. In a subsequent step, HA is internalized by the enterocytes, one part being metabolized while the M cells deliver intact HA polymer to the gut associated lymphatic tissue (Rubas and Grass, 1991), Therefore, considering homeostasis conditions for the intestinal membrane the depth of HA penetration plays an important role in its functions. In addition, the transport events, the signaling and interaction with cells depend on the structuring of HA.

The lining of the intestinal mucosa consists of a hydrated network of mucus, composed of 99% of glycoproteic mucin secretion (Feldstein and Moscalets, 2016). Particularly, the mucus network offers many opportunities for penetration and diffusion of free HA in the mucin matrix (Salehi Dashtebayaz and Nourbakhsh, 2018). As both polymers (HA and glycoproteic mucin) contains hydrophobic and hydrophilic domains, entanglements of chains from van der Waals interactions and hydrogen bonds, or some combination of chemical and physical interactions may occur (Ponchel and Irache, 1998; Peppas and Buri, 1985). Adsorptive events can be affected by the properties of the HA structure related to hydration, structural stability and surface charge (Teubl, 2013; Serra et al., 2009). Thus, the adhesion phenomenon is a consequence of a broad set of interactions.

Mucoadhesion is defined as binding between two interacting surfaces where one is at least mucus layer (Robinson, 1990; Jones et al, 1996 a,b). The tensile assay of adhesion is an in vitro method used to analyze the mucoadhesion of formulations based in two responses: Peak force (F_{adh}) defined as the maximum force to separate two adherent surface and work of adhesion (W_{adh}), the adhesion energy equivalent to area under a force-distance curve (Bassi da Silva et al., 2017; Cook and Khutoryanskiy, 2015; Nair et al., 2013). Setting parameters such as contact force, contact time and the speed of probe withdrawal can be previously standardized. Optimal parameters were obtained by Wong and collaborators from buccal adhesion studies (Wong et al, 1999). Mucin gel has been used as a model of the intestinal mucoadhesive environment in in vitro assays (Jones et al., 1997; Georgiades et al., 2014).

In this study, the influence of HA structuring on its penetration into type III mucin of porcine stomach and also into rat intestinal mucosa were studied using free, nanoparticles and mixed formulations. The free HA formulations had the same average MM (10^5 Da) but different size distributions: rich in fractions $>10^5$ (H-MM) and rich in fractions $\leq 10^5$ Da (I-MM). In addition, low MM (average MM 10^4 Da) and rich in fractions $\leq 10^4$ Da (L-MM) also was used. Therefore, particle sizes in free HA colloidal dispersion correspond to the globules formed from folding of the chains. The HA nanoparticles were crosslinked adipic

dihydrazide, and had 485.3 ± 87.61 nm average particle size and polydispersity was 0.28 ± 0.04 at semi-diluted regime. A mixed formulation was composed of 25 % or 50 % (wt.) of HA nanoparticles dispersed in free I-MM.

The results highlighted the importance of the HA structuring on mucoadhesion as well as allowed to select promising formulations with improved penetration properties for HA oral administration or for mechanism investigation in pre-clinical assays.

2. Material and Methods

2.1. Polymers and Chemicals

Hyaluronic acid sodium salt at 1 % (w/v) were purchased from Mapric Pharmaceutical Products Ltd., (Sao Paulo, Brazil) and Euflexxa (São Paulo, Brazil). The HA from Mapric was used in the synthesis of HA nanoparticles. Water-soluble adipic acid dihydrazide (ADH) and N,N-dimethylaminopropyl carbodiimide (EDCI) used for nanoparticles crosslinking were purchased from Sigma (St. Louis, USA). Ethanol and all other analytical grade chemicals were purchased from Merck (Darmstadt, Germany).

Type III mucin partially purified powder from porcine stomach was purchased from Sigma-Aldrich Ltd., (São Paulo, Brazil) for using in the mucoadhesion assays.

2.2. Pre-treatments and characterization of the HA types

The HA Euflexxa distributed by the manufacturer into sterile syringes for medical use, was used without any complementary pretreatment. The HA Mapric with major distribution for cosmetic use, was previously precipitated with ethanol for purification before to be used in the formulations. The precipitated Mapric HA was also later hydrolyzed to be used in formulation containing HA of

low average MM. The three free HA types were characterized in terms of purity, average MM and distribution before its use in formulations.

2.2.1. Pre-Treatments

Precipitation was carried out with ethanol at pH 7.0 and in the presence of NaCl (2 M), according to protocol described by Cavalcanti et al., 2018. The precipitate was separated by centrifugation at 1318 ×g by 20 min., and suspended in NaCl 0.15 M for stabilization. The purity relative to proteins was calculated measuring HA and proteins concentration using cetyltrimethylammonium bromide (CTAB) (Chen and Wang, 2009) and bicinchoninic acid (BCA) (Smith et. al, 1985) methods, respectively.

The purity (P) was calculated by Eq. 1:

$$P (\%) = \frac{C_{HA}}{(C_{HA} + C_{SP})} \times 100 \quad \text{Eq. (1)}$$

in which C_{HA} and C_{SP} mean the concentration of the HA and soluble protein respectively.

The HA hydrolysis was carried out resuspending the precipitated HA in a 0.1M phosphate buffer at pH 12. The obtained solution (5 g/L) was left at 60 °C during 24 h in a reciprocal shaker bath with 500 rpm stirring (Lab-Line Instruments Inc., Melrose Park, ILL, USA). After that, the hydrolyzed HA was freeze-dried for storage.

2.2.2. HA Characterization

HA Concentration

The HA concentration was quantified by CTAB method (Chen and Wang, 2009). Briefly, HA solutions and CTAB were mixed at 0.5/1 (v/v). The mixture was maintained during 10 min at room temperature, after that the optical

density was measured at 400 nm wavelength. Spectrophotometer was calibrated using control solution prepared from 0.15 M NaCl and CTAB at same ratio. Analytical grade sodium hyaluronate (Hylumed™) from Genzyme Corporation (Cambridge, MA, USA) was used as a standard for calibration curve.

Protein Concentration

The protein content was quantified according to the methodology proposed by Smith et. al, (1985). Briefly, precipitate and BCA protein assay kit (Sigma-Aldrich, St. Louis, MO, USA) were mixed in the 1/20 (v/v) ratio. Then, incubated in water bath at 37°C by 30 min. Bovine serum albumin (BSA) was used as the standard. After reacting, the optical density was measured at 562 nm wavelength.

Average Molar Mass Distribution

Molar mass (MM) distribution of free HA was determined through size exclusion chromatography using a gel filtration column (Polysep-GFC-P6000, 7.8 mm x 300 mm; Phenomenex, Torrance, CA, USA) coupled to a Shimadzu RID-6A refractive index detector (Shimadzu Corporation, Kyoto, Japan). Briefly, 20 µL of free HA at 0.01g/L and pH 7.4, was injected using 0.1M NaNO₃ as a mobile phase at 1.0 mL min⁻¹ at 25° C. HA analytical standards (Hyalose, Oklahoma, OK, USA) with MM ranging from 50 to 1000 kDa was correlated with retention time using Eq. 2.

$$\log MM = 10.9 - (0.62 \times \text{retention time}) \quad \text{Eq. (2)}$$

2.3. Preparation of HA formulations

2.3.1. Free HA

The formulations of free HA were classified according to the average MM and distribution of MM used in it, and named: High MM (H-MM) prepared from Euflexxa HA (average MM 10^5 Da and distribution richer in the highest fractions $>10^5$ Da), Intermediate MM (I-MM) prepared from the precipitated Mapric HA (average MM 10^5 Da and distribution richer in the intermediate fractions $\leq 10^5$ Da), and low MM containing the hydrolyzed I-MM (L-MM) (average 10^4 Da and distribution rich in low fractions $\leq 10^4$ Da).

The H-MM formulation were prepared by diluting HA in phosphate buffer, pH 7.4, to obtain a dispersion of 0.5, 5 and 10 g/L HA. For I-MM formulation, the previously precipitated HA was resuspended in phosphate buffer, pH 7.4, to obtain a dispersion of 0.5, 5 and 10 g/L HA. The L-MM formulation was prepared solubilizing the freeze-dried hydrolyzed HA in phosphate buffer, pH 7.4, to obtain a dispersion of 10 g/L HA.

2.3.2. HA Nanoparticles

Crosslinked HA nanoparticles were prepared from free I-MM described in 2.3.1 item. The synthesis and crosslinking were according to protocol described by Hu et al. (2006) with modifications introduced by Bicudo and Santana (2012). Nanoparticles were formed by HA precipitation due to its local dehydration. Briefly, the process was carried out in a jacket glass reactor (400mL) under controlled temperature 21°C and gentle mechanical stirring. Ethanol (Merck, Darmstadt, Germany) was dropped at a flow rate 7 mL/min into a 0.1% (w/v) solution of sodium hyaluronate with average molar mass 10^5 Da (Mapric Pharmaceutical Products Ltd.). Initially, an ethanol volume (100mL approx.) was added and the reacting system maintained under stirring for 2h. Next, 40 mg/mL EDCI and a 20 mg/mL ADH both in aqueous solution were added to the reactor for crosslinking under more 24h stirring. The reaction was ended by addition of more 100mL ethanol and stirring for another 20h. Nanoparticles were recovered from the dispersion by ultrafiltration in a Ultracel® cell, containing a 10 kDa ultrafiltration disc and a 44.5 mm diameter filter (EMD Millipore Co.,

Billerica, MA, USA), while was operated at 0.5 psi inlet nitrogen pressure. The recovery yield (Y) was evaluated using Eq. 3:

$$Y (\%) = \frac{(T_m - F_m)}{T_m} \times 100 \quad \text{Eq. (3)}$$

The total mass (T_m) corresponded to the sum of the masses in the filtrate (F_m) and retentate (R_m).

The crosslinked HA nanoparticles was characterized by mean diameter, polydispersity and also by zeta potential.

2.3.3. HA Mixed Formulation

Freeze-dried powder from I-MM described in 2.3.1 item was mixed with 25 % or 50 % (wt.) nanoparticles to obtain a 10 g/L buffered 7.4 aqueous dispersion. Compositions were stirred overnight at 37 °C to ensure dispersion homogeneity.

2.4. Characterization of the formulations

2.4.1. Particle Size Distribution

Formulations of free HA (I-MM and H-MM) were hydrated at 0.01 g/L and 0.2 g/L, HA nanoparticles were hydrated at 0.2 g/L and 0.5 g/L and mixed HA 25 % and 50 % (wt.) were hydrated at 10 g/L, all with a viscosity of about 1 mPa.s. Particle size distribution, zeta potential (ZP) and polydispersity index (Pdl) were measured by dynamic light scattering (DLS) and the data analyzed by photon correlation spectroscopy (PCS). The measurements were performed with a 4mW HeNe Laser (633 nm), in a Autosizer 4700, Zetasizer Nano Series (Malvern, Malvern, U.K.), at a fixed angle of 173° and 25 °C.

The spectra were analyzed in terms of the intensity of scattering (I-distribution $\propto d^6$) for the various size classes and number of particles (N-distribution $\propto d$) to obtain the predominant particle sizes.

2.4.2. Rheological characterization

The rheological behavior of the prepared formulations was characterized using an Anton Paar MCR-102 Modular Compact Rheometer. Tests were conducted using a cone-plate geometry (CP50-1) with a 50 mm diameter, a cone angle of 0.9815° and a truncation of $0.97 \mu\text{m}$. Rheological measurements were performed at 37°C . Steady-state shear and oscillatory measurements were performed at shear rates from 0.01 to 1000 s^{-1} and angular frequency from 0.1 to 600 rad.s^{-1} respectively, both with the plate at 37°C .

2.5. Preparation of Biological Substrates

The mucoadhesion assays were carried out with two model of biological substrate: Type III mucin of porcine stomach and freshly tissue of rat intestinal mucosa.

Type III mucin of porcine stomach is a partially purified powder, containing $0.5 - 1.5 \%$ of sialic acid bound to glycoprotein polymer. Mucin tablets were manufactured by the compression of mucin powder in a compressing machine for tablets (LM-D-8, Lemaq. São Paulo. Brazil). Briefly, the mucin was pulverized, and the compression chamber of machine calibrated to obtain tablets in the dry form with plane and smooth surface, absence of edges, a weight of 120 mg , a diameter of 8 mm and a thickness of $2.2 \pm 0.12 \text{ mm}$, according to the principles described in the Brazilian Pharmacopoeia reference standards. The friability and hardness of the mucin tablets were respectively $2.9 \pm 0.4 \%$ and $37.5 \pm 3.8 \text{ N}$. Loss of mass by friability and hardness were $0.3 \pm 0.08 \%$ and $8 \pm 0.11 \text{ Kg}$ respectively.

The intestinal mucosa of rats was extracted of male Wistar rat (*Mus norvegicus albinis*) which were sourced from a local supplier (Anilab, Paulínia, Brazil). Approval for the animal study was given by the Animal Ethics Committee of the University of Sorocaba, São Paulo, Brazil (application number 091/2016).

Adult male of the same age and weighing 260-280g were fasted for 10h and water *ad libitum*. The operative procedure began with intraperitoneal anesthesia using thiopental sodium (0.05mg/100g weight body). The small intestine was exposed after longitudinal scission of the abdomen. Non-traumatic hemostatic tweezer was used to facilitate the scission and occlusion of the duodenum proximal (0.5 cm below the pylorus) and duodenum distal (8.5 cm below the pylorus). Then, the mesentery over 8 cm length duodenum was carefully removed. Freshly tissue sections (duodenum, jejunum and ileum) were cut off in approximately 10 cm² piece. Each segment was opened lengthwise, everted with the aid of a flexible rod (2.5 mm in diameter) with an end covered by fine silk fabric and gently washed with 0.9% NaCl solution at 37 °C. All mucosa was visualized for integrity and viability.

2.6. Mucoadhesion Assays

The mucodhesive properties of the HA formulations were investigated using a TA-XTplus texture analyzer (Stable Micro Systems, Surrey, UK) (Otero-Espinar et al., 1998). Mucin tablets were preconditioning and pre-swelling with purified water at 37 °C during 15 min (Ponchel et al., 1987) and freshly intestinal mucosa were used after washed with 0.9% NaCl solution at 37 °C. Mucin tablets and tissue sections were horizontally attached on to the lower end of analytical P/10 probe using double side adhesive tape and suture thread respectively.

HA formulations were placed inside of a compartment at fixed volume and conditioned in a water bath at 37°C. In texture profile analysis (TPA) mode, the analytical probe descended onto the surface of each formulation at a constant speed of 0.2 mm/s, penetrated 10 mm inside the formulation and a downward tensile force (F) of 0.49 N was applied during 3 min (Fig. 1a). In sequence, biological substrate returned vertically to surface of formulation at a constant speed of 5.0 mm/s (Fig. 1b). After every cycle, HA formulation and biological substrate were replaced. The force versus distance profiles provided the peak force, the maximum force of detachment (F_{adh}) and the work of adhesion (W_{adh}) or adhesion energy as the integral of the resulting force-distance profile (Fig. 1c).

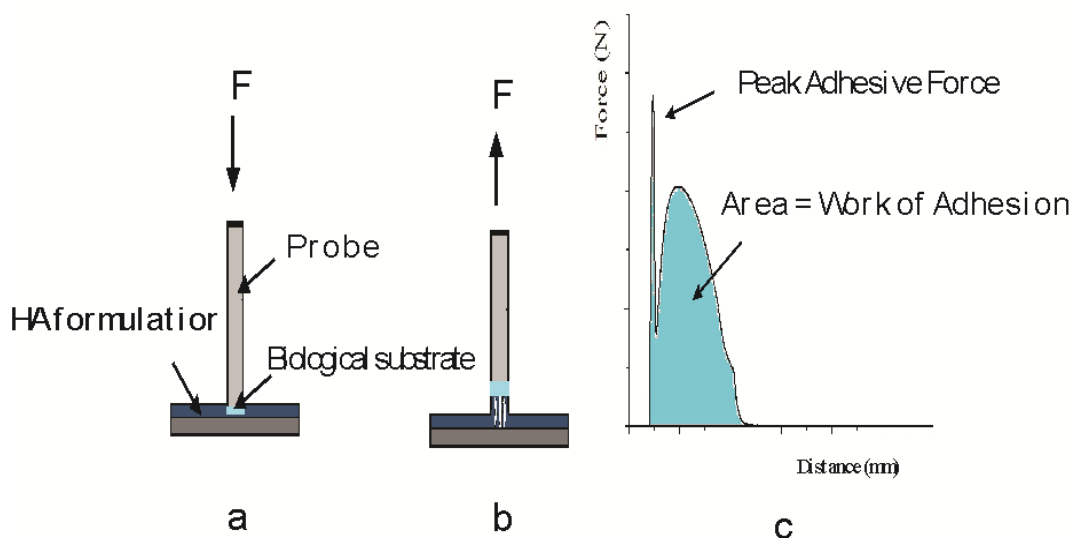


Figure 1. Schematic representation of a typical adhesion measurement apparatus during (a) contact and (b) separation steps. (c) A typical force vs. distance curve obtained from an adhesion measurement.

2.7. Statistical Data Analysis

The responses of adhesion were compared using a one-way analysis of variance (ANOVA) with post-hoc Tukey. A level of $p < 0.05$ was set for significant. Values were expressed as mean (\pm S.D.) of at least: three replicates in mucin tablets and six replicates in freshly tissue sections.

3. Results and Discussion

3.1. Viscosity of the HA formulations

The viscosity of the HA formulations is a variable that affects the mucoadhesion and must be taken into account during the interpretation of the results of the tensile assays. Viscosities were more responsive to high fractions of 10^6 Da from H-MM, followed by predominant fractions of 10^5 Da from I-MM. On the other hand, nanoparticles presented low viscosity, reducing significantly

the viscosity of mixture. Table 1 shows the viscosities of the formulations used in the mucoadhesion.

Table 1. Viscosities of HA formulations as function of the concentration.

Formulation		Free			Nanoparticles	Mixture	
		H-MM	I-MM	L-MM		25 wt. %	50 wt. %
Viscosity at 25°C (mPa. s)							
Concentration (g/L)	0.5	49.6	13.7	---	1.1	---	---
	2.5	---	---	---	1.8	---	---
	5	86.9	37.6	---	4.9	---	---
	10	390	349	7.8	---	1.5	0.7

H-MM: high MM distribution; I-MM: intermediate MM distribution; L-MM: low MM distribution; Nanoparticles: crosslinked adipic dihydrazide HA; Mixture: I-MM with 25 % or 50 % (wt.) of nanoparticles.

--- concentrations not investigated.

3.2. Molar Mass and Size Distributions of the Free HA Formulations

MM distribution in the classes of 10^6 , 10^5 and 10^4 Da are shown for the free HA formulations that also were characterized by its zeta potential (ZP) and purity. Values are depicted in Table 2 at diluted (0.01 g/L) and semi-diluted (0.2 g/L) regimes. Table 2 shows the characterization of free HA for percentage distribution of MM in Da and purity in (%) HA/protein. ZP varied according to the concentration in the formulations due to structuring and entanglement of the HA chains. Therefore, the variations of ZP reflect the changes in the HA spatial architecture.

Table 2. Distributions of molar mass (MM) obtained by size exclusion chromatography for H-MM and I-MM formulations, both at 0.01 g/L and 0.2 g/L, buffered 7.4 aqueous dispersions.

Formulation	Concentration (g/L)	MM distribution Da (%)			ZP (mV)	Purity (%)
		10 ⁶	10 ⁵	10 ⁴		
H-MM	0.01	34.0	50.0 ±	16.0 ±	-8.3 ± 8.7	100
	0.2	± 0.4	0.7	0.0	-4.9 ± 1.7	
I-MM	0.01	16.0	74.0 ±	10.0 ±	-6.5 ± 1.1	90
	0.2	± 0.1	0.8	0.0	-40.0 ± 6.1	
L-MM	0.2	0	6 ± 0.0	94.0 ± 1.9	-24.0 ± 5.7	

L-MM: refers to hydrolyzed of I-MM.

The effects of MM distributions on size of the HA structures at 0.01 g/L are depicted in terms of Intensity (I) and Number (N) distributions for H-MM (Figures 2 a,b) and I-MM (Figures 2c,d).

Buffered HA aqueous dispersions form stable structures which in diluted regime are small and dense. In consequence of that, they are less responsive to the size of HA chains. This is the reason why the sizes of the structures were around 100 nm, with mean diameter (Z-average) and polydispersity index (PDI): narrower distributions to H-MM (114.0 ± 14.51 ; 0.59 ± 0.04) and (538.3 ± 186.5 ; 0.66 ± 0.12) to I-MM, due to its larger MM polydispersity compared to H-MM.

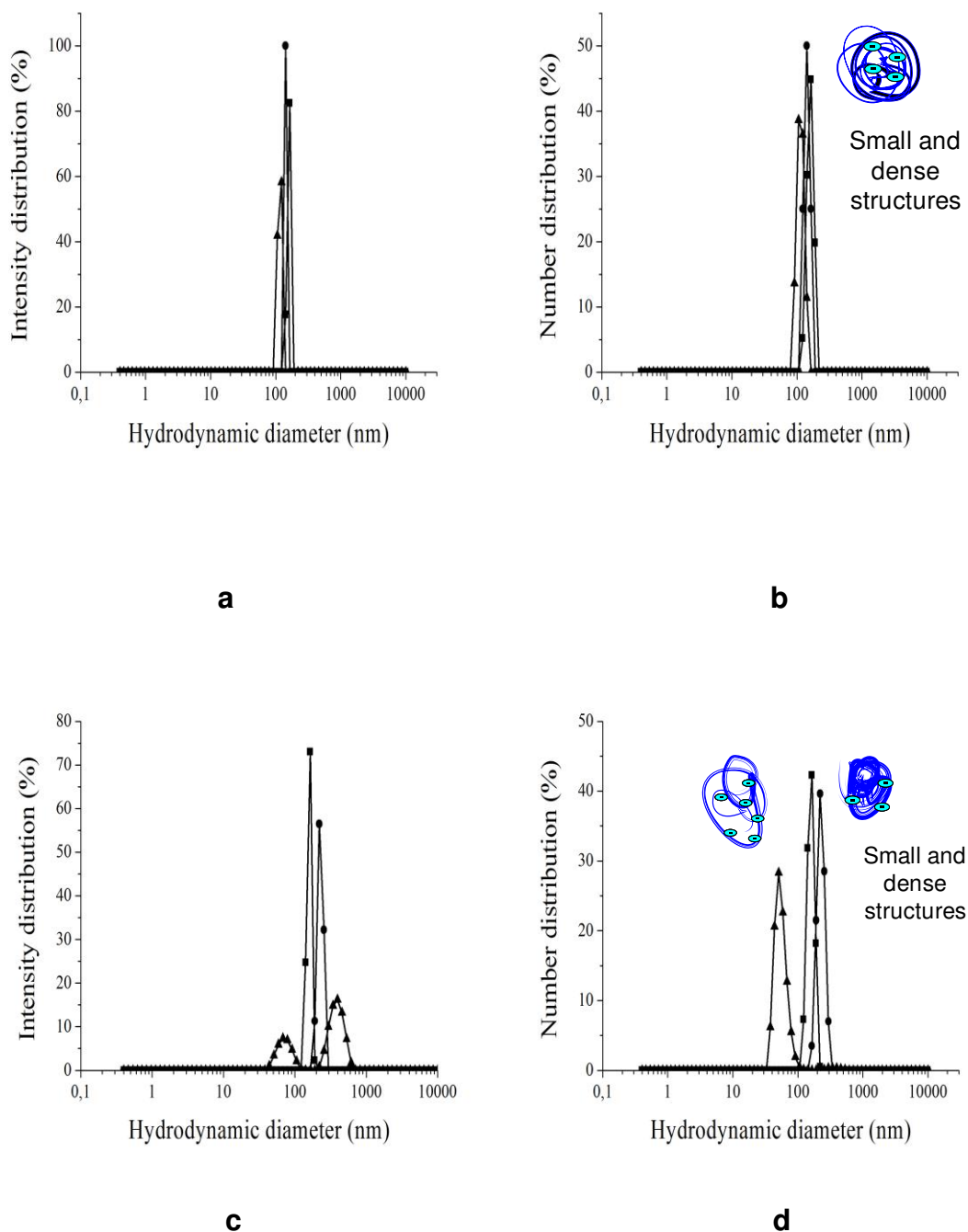
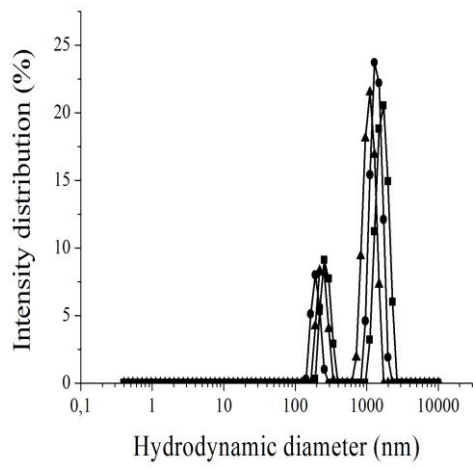
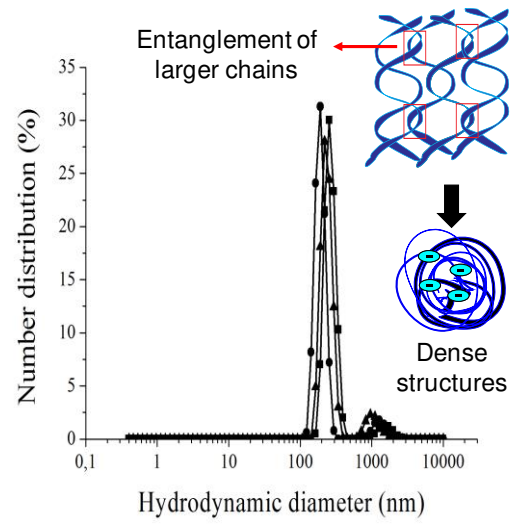
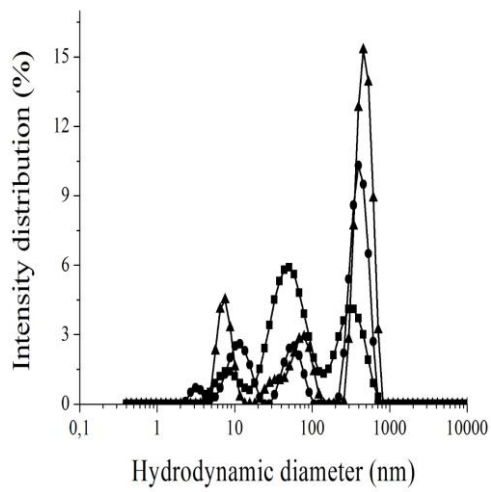
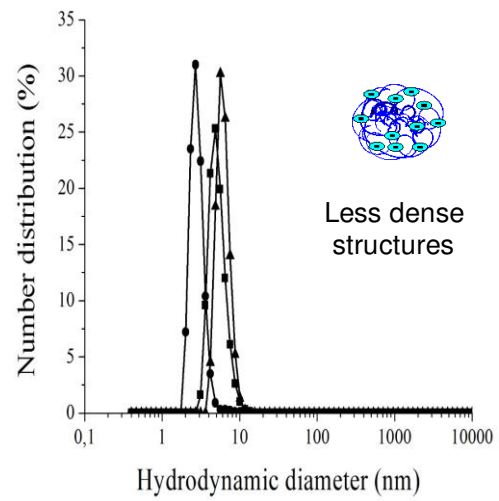


Figure 2. Size distribution spectra for formulations of free HA at 0.01 g/L. (2a,b) H-MM, (2c,d) I-MM. The samples were buffered 7.4 aqueous dispersions. The measurements of Intensity and Number of distributions were done in three independent samples.

The effects of MM distributions on size of the HA structures at 0.2 g/L are depicted in terms of Intensity (I) and Number (N) distributions for H-MM (Figures 3a,b), I-MM (Figures 3c,d) and L-MM (Figures 3e,f).

**a****b****c****d**

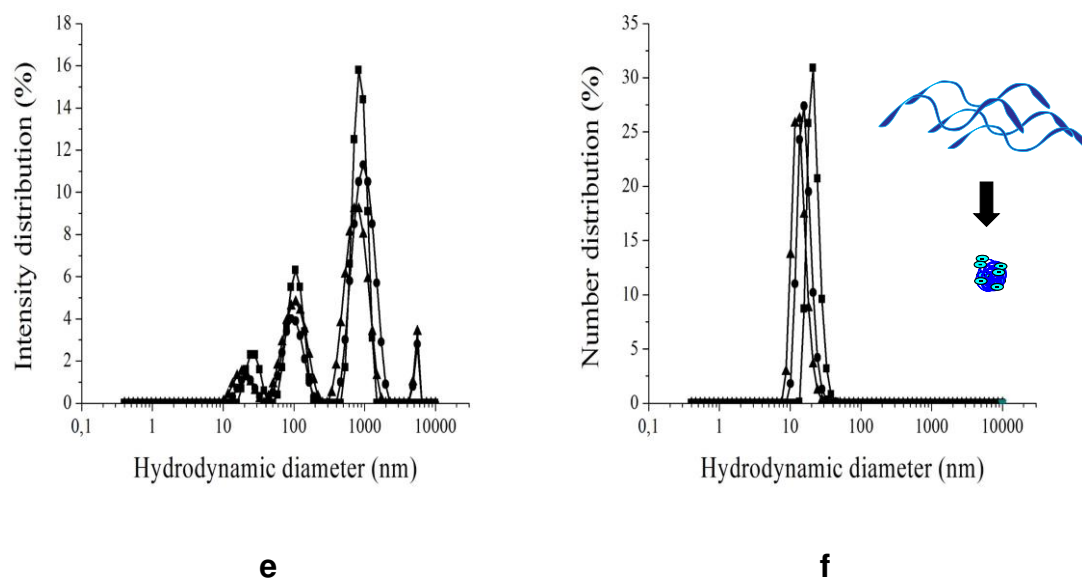


Figure 3. Size distribution spectra of the formulations of free HA at 0.2 g/L: (3a,b) H-MM, (3c,d) I-MM, and (3e,f) L-MM. The samples were buffered 7.4 aqueous dispersions. The measurements were done in three independent samples. Mean diameter (Z-average); polydispersity index (PDI) were: H-MM (1386 ± 27.58 ; 0.89 ± 0.11); I-MM (964.2 ± 125.8 ; 0.80 ± 0.00) and L-MM (345.7 ± 105.3 ; 0.75 ± 0.22).

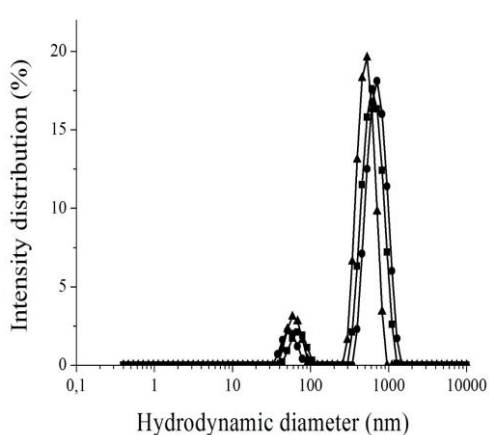
The spectra for H-MM at the semi-diluted regime show size peaks at 200 nm and 1000 nm approximately in (I) distribution (Figure 3a), while the predominant size peaked around 200 nm, corresponding to the dense networks formed by entanglement of the larger chains (MM 10^5 , 10^6 Da) (Figure 3b).

At semi-dilute regimes, polymer networks are formed due to the entanglement of the chains, resulting in large structures which are much more responsive to MM distribution. Therefore, to more polydisperse MM as for I-MM, the structures are less dense due to the lower entanglement of the chains thus providing a greater volume of hydration. Despite this, the hydrodynamic radius is lower because, as is known, the scattering of light is proportional to the density of the structure (Stanley-Wood and Lines, 1992). Therefore, a broad range of sizes was obtained in (I) distribution, due to the signal amplification to diameter raised to the sixth power ($I \propto d^6$) (Figure 3c). However, in (N) distribution ($N \propto d$) the light scattering corresponds to the predominant network size, which was equivalent to that of a solid particle of 10 nm radius, due to the hydration degree (Figure 3d).

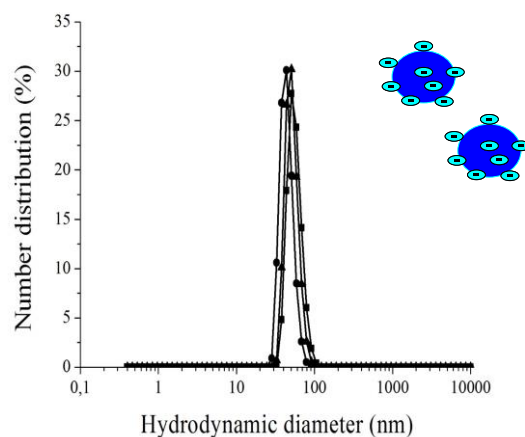
Figures 3 (e,f) show the size spectra obtained for hydrolyzed of I-MM (L-MM). (I) distribution was similar to non-hydrolyzed I-MM (similar polydispersity index). However, the (N) distribution has a predominant peak in 50 nm, which is coherent with dense structures formed by entanglement of 10^5 Da chains mainly.

3.3. Size Distributions of the Nanoparticles HA formulation

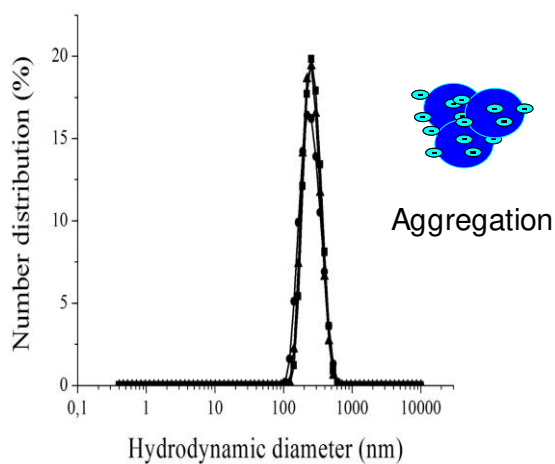
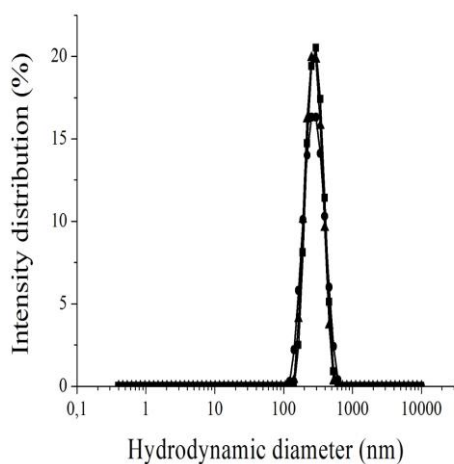
About 31.2 ± 1.1 % of HA nanoparticles were recovered in the aqueous dispersion. Compositions at semi-dilute regimes were characterized by its distributions of size. Particle size is depicted concerning (I) and (N) distributions, Figures (4a,b) at 0.2 g/L and Figures (4c,d) at 0.5 g/L.



a



b



c

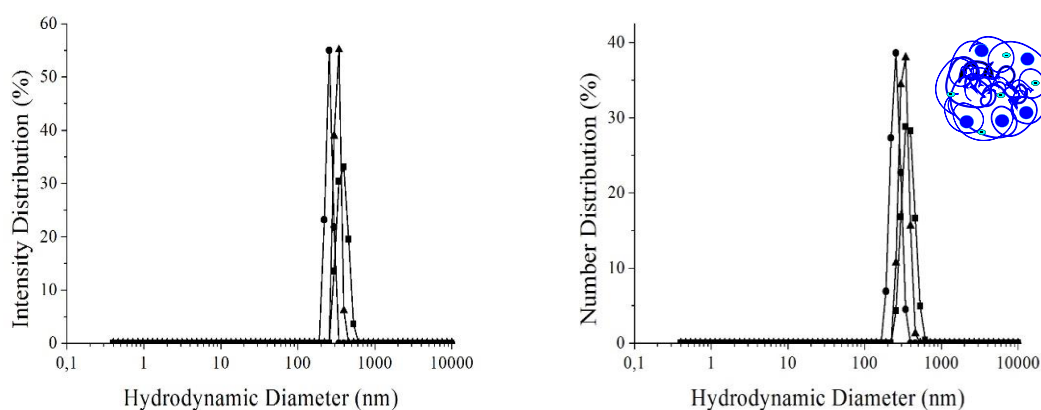
d

Figure 4. Size distribution spectra from HA nanoparticles formulation at 0.2 g/L (4a,b) and 0.5 g/L (4c,d). The samples were buffered 7.4 aqueous dispersions. The measurements were done in three independent samples. Mean diameter (Z-average); polydispersity index (PDI) were: $(268.7 \pm 3.57; 0.56 \pm 0.11)$ for 0.2 g/L and $(485.3 \pm 87.61; 0.28 \pm 0.04)$ for 0.5 g/L.

Spectra in Figure 4(a,b) show that particles of low (50 nm) and intermediate (500 nm) sizes are present in the compositions of HA nanoparticles at the diluted regimes. Primary particles tend to associate into larger structures due to aggregation at the semi-diluted regimes and corresponds to increases in the (N) distribution (Fig 4c,d), with a population of intermediate zeta potential (ZP) (from -20.0 ± 0.14 to -16.6 ± 0.58 mV), as ZP value is between + 30 mV and – 30 mV (Kerker, 1969).

3.4. Size Distributions of the Mixed HA Formulation

Formulation of free I-MM HA was mixed with 25 % and 50 % (wt.) of nanoparticles to obtain a mixed formulation. Both compositions were prepared at concentrated dosage form (10g/L) and were characterized by its new distribution of particle sizes and are depicted in terms of Intensity (I) and Number (N) distributions in the Figures (5a,b) and (5c,d).



a

b

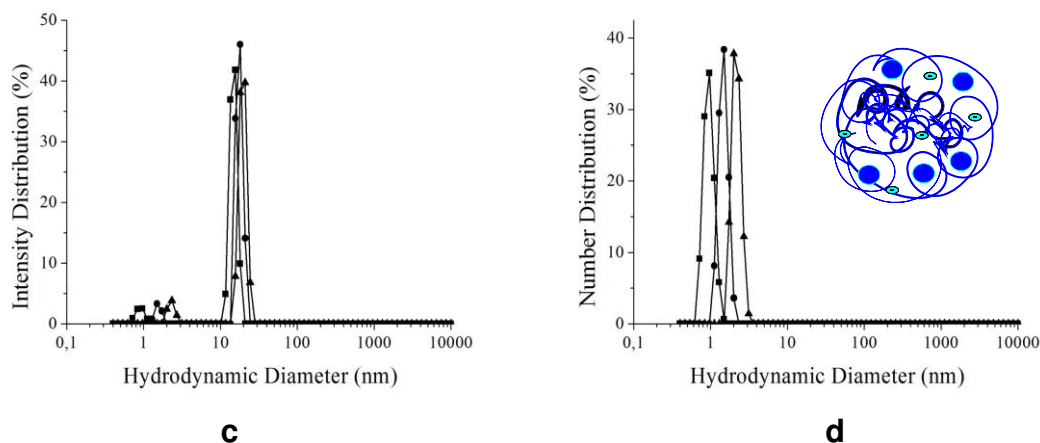


Figure 5. Size distribution spectra of the I-MM at 10 g/L with 25 wt. % (a,b) and 50 wt. % (c,d) of nanoparticles. The samples were buffered 7.4 aqueous dispersions. The measurements were done in three independent samples. Mean diameter (Z-average); polydispersity index (PDI) were: (928.8 ± 170.9 ; 0.73 ± 0.07) and (2652 ± 222.1 ; 0.88 ± 0.13) respectively.

At lower composition (25 wt. %), nanoparticles of intermediate ZP (around -20 mV) and mean diameter (50-500 nm) diffuse into the hydrodynamic domains of the globules from free I-MM HA, forming dense structures (predominant sizes at 342 nm) compared to I-MM (predominant sizes at 10 nm) (Figure 5a,b). When nanoparticles composition was increased from 25 % to 50 % (wt.), an opposite effect was observed, and predominant particle size spectrum was similar to I-MM (Figure 3d). Probably, nanoparticles diffuse into the domains of free HA globules which are now in lower concentration and electrostatic repulsion of HA structures changed the interaction between the globules and the neighborhoods, promoting an changed in the ZP, varying from -7.41 ± 0.0 mV (25 wt. %) to -11.60 ± 0.70 mV (50 wt. %) with significant increase in the mean diameter (from 928.8 ± 170.9 to 2652 ± 222.1 nm) (Figure 5c,d).

3.5. Adhesion Studies

3.5.1. Assays with Type III Mucin

Table 3 shows the F_{adh} (N) and W_{adh} (N.mm) as function of concentration of HA formulations. An intra- and interassay statistical analysis was conducted according to one-way ANOVA test with post-hoc Tukey's multiple

comparisons test ($p < 0.05$). (b) peak force intra-assay and (K) work of adhesion interassay were statistically significant.

Table 3. Peak force (N) and work of adhesion (N.mm) as function of concentration.

Formulations		Free		Nanoparticles	Mixture	
		H-MM	I-MM		25 wt. %	50 wt. %
Mean \pm S.D.		F _{adh} ; W _{adh}	F _{adh} ; W _{adh}	F _{adh} ; W _{adh}	F _{adh} ; W _{adh}	F _{adh} ; W _{adh}
Concentration (g/L)	0.5	(a)2.38 \pm 0.28; (G)0.74 \pm 0.04	(b)2.80 \pm 0.06; (H)0.97 \pm 0.08	(e)2.42 \pm 0.27; (J)0.88 \pm 0.09	---	---
	2.5	---	---	(e)2.00 \pm 0.14; (J)0.93 \pm 0.14	---	---
	5	(a)2.85 \pm 0.10; (G)1.57 \pm 0.42;	(c)2.20 \pm 0.21; (H)1.00 \pm 0.05	(e)2.47 \pm 0.12; (J)0.74 \pm 0.02	---	---
	10	(a)2.66 \pm 0.06; (G)0.86 \pm 0.05	(c)2.06 \pm 0.06; (H)0.82 \pm 0.00	---	(f)2.59 \pm 0.17; (K)2.55 \pm 0.83	(f)2.77 \pm 0.16; (K)2.53 \pm 0.76

Mucoadhesion from HA formulations are presented as mean \pm (S.D.) (n=3). Letters at lower case indicates statistical analysis of Peak Force (F_{adh}) and bigger case indicates statistical analysis of Work of Adhesion (W_{adh}).

--- concentrations not investigated.

Intrassay statistical difference was identified at more diluted composition (0.5 g/L) for I-MM formulation. Particle size spectrum showed the presence of less dense structures with a high zeta potential (-40.0 ± 6.1 mV). The hydrated structures were provided by hydrogen bond forming groups (carboxylic and the hydroxyl groups). Probably, interpenetrating chains of HA and mucin network occurred as a result of osmotic forces as the HA was drawn by the water into the pores (Smart, 1999; 2005; Hansen et al., 2017).

In one independent tensile test, preformed mixture HA-mucin containing 20 wt. % of free I-MM was prepared by mild sonication during 1 h at 37°C and tested in tensile deformation. Maximum F_{adh} measured was 2.40 ± 0.04 N and the corresponding W_{adh} was 0.98 ± 0.02 N.mm. This result shows that more than 20% of the I-MM interpenetrated with the mucin network in the composition at 0.5 g/L.

Another statistical difference occurred when formulations containing free I-MM were mixed with crosslinked structures. Under the tensile force, the W_{adh} stands out due to synergism created by mixed structures on the elasticity and plasticity of adhesion

Force-distance profiles allowed to achieve important concerns about the mucoadhesive behavior of the formulations. Typical force vs. distance curves are shown in Figure 6, to: I-MM (a), H-MM (b), Nanoparticles HA (c) and Mixed HA (d), respectively.

The areas under the curves of force vs. distance refers to W_{adh} of formulations on the mucin tablets and vice-versa. The profiles in the Figure 6a-d, show that adhesion energy varied as function of the formulation and composition. The profiles in blue refers to the compositions that showed highlighted adhesion with mucin.

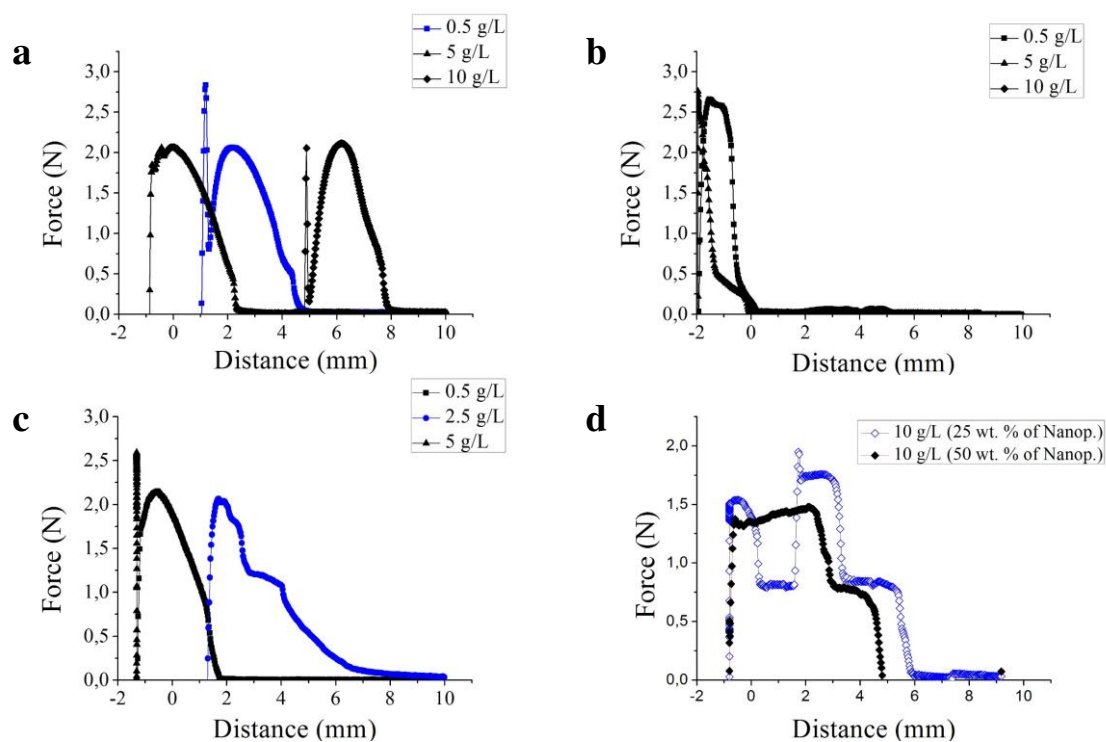


Figure 6. Variations of the force necessary for detachment of the HA formulation from the probe (porcine stomach type III mucin surface) as a function of distance for the formulations I-MM (a), H-MM (b), Nanoparticles HA (c) and Mixed HA (d), at increased compositions: 0.5 g/L (\blacksquare), 2.5 g/L (\bullet), 5 g/L (\blacktriangle) and 10 g/L (\blacklozenge , \circ).

Formulation I-MM at 10 g/L showed the following behavior (Figure 6a): mucin penetrated 10 mm inside the formulation and shifted 2 units (10mm to 8mm) during the upward movement without resistance. At 8 mm depth, the viscosity of formulation offers resistance to movement of probe and a positive force of adhesion was recorded until reaching approximately 5 mm under the surface when occurred the detachment. In the 5 g/L composition, the W_{adh} was also to remove the probe from the viscous medium. Because there was not uniform trend about viscosity and the distance of detachment for the compositional range studied, the differentiated behavior of composition at 0.5 g/L was an indicative that the less dense and therefore more hydrated structures of I-MM penetrated well in the mucin tablets, and interpenetrating force provided the higher resistance to detachment (high F_{adh}).

In Figure 6b, physical stabilization among hydrophobic patches of 10^6 Da sizes chains created self-cohesive forces inside the H-MM HA formulation. In this configuration, chains form a patch on the surface of the mucin tablets and

the polymers interpenetrate at low depths, thus, the deformation and the failure occurred outside the formulation (negative distance values) in the compositional range studied.

Nanoparticles penetrates into the porous nanostructure of mucin in a different mechanism compared to the free HA structures. The incorporation occurs due to size compatibility with the mucin cut-off pores (from 20 to 200 nm) (Round et al, 2012). Therefore, composition at 2.5 g/L of low viscosity performed a W_{adh} at the beginning of the upward movement of the probe, at 8 mm depth, meaning that this composition reaching an enhanced depth in the mucin network compared to other compositions studied. On the other hand, the F_{adh} and W_{adh} occurred above the surface of the formulation at 0.5 g/L and 5 g/L with formation of overlapping peaks. In the first one, the reduced concentration and in the second one the incompatibility of size of primary aggregates with the mucin cut-off pores justify the low adhesion (Figure 6c).

Mixed formulation (Figure 6d) at single concentration (10 g/L) and two compositions of nanoparticles 25 % and 50 % (wt.) provided a combination of viscosity and viscoelasticity that created a synergism of adhesion. The variations in adhesive responses were due to differences in depth of incorporation of nanoparticles or interpenetration of free HA. There were 2 stages of detachment because adherence corresponded to the sum of the events provided by the qualities from individual HA structures. In the 1st stage (from 6mm to 2 mm of depth) a heterogeneous distribution of force occurred due to the different sizes of the nanoparticles, whereas in the 2nd stage (above 2 mm up to negative distance values) the effect of free chain interpenetration was imperative.

The adhesion on mucin tablets presented the following rank order of F_{adh} and W_{adh} based on the joint interpretation of the mean values and profiles of force-distance. F_{adh} : I-MM > H-MM = Mixed HA = Nanoparticles HA and W_{adh} : Mixed HA > I-MM = Nanoparticle HA = H-MM.

The figure 7 shows the mucin tablets composed by layers. When in contact with formulation, the force of detachment (F) varies as functions of depth achieved by HA structures inside mucin layers. The mucin network layers are

differentially filled with HA structures. Deeper layers in the mucin are filled by the lower HA particles (10^4 Da of free HA or 10 nm sized of nanoparticles or both for mixed formulation), while fractions of larger MM and particle size become more superficially or forming patches on the mucin surface.

Figure 7a shows that concentrated dispersion of free HA form superficial patches on the mucin surface and F_{adh} tend to be lower. On the other hand, at diluted/semi-diluted dispersions, the MM penetrate at different depths depending on the size MM (high, intermediate and low) and flexibility of the chain. In Figure 7b, concentrated dispersion of nanoparticles form gradient on the tablets that penetrated at deeper layers, thus, F_{adh} tend to be high than semi-diluted/diluted dispersions. In Figure 7c, concentrated dispersion of mixed HA structures presents a heterogeneous distribution of F_{adh} and W_{adh} that positively benefits the mucoadhesion due to detachment in stages.

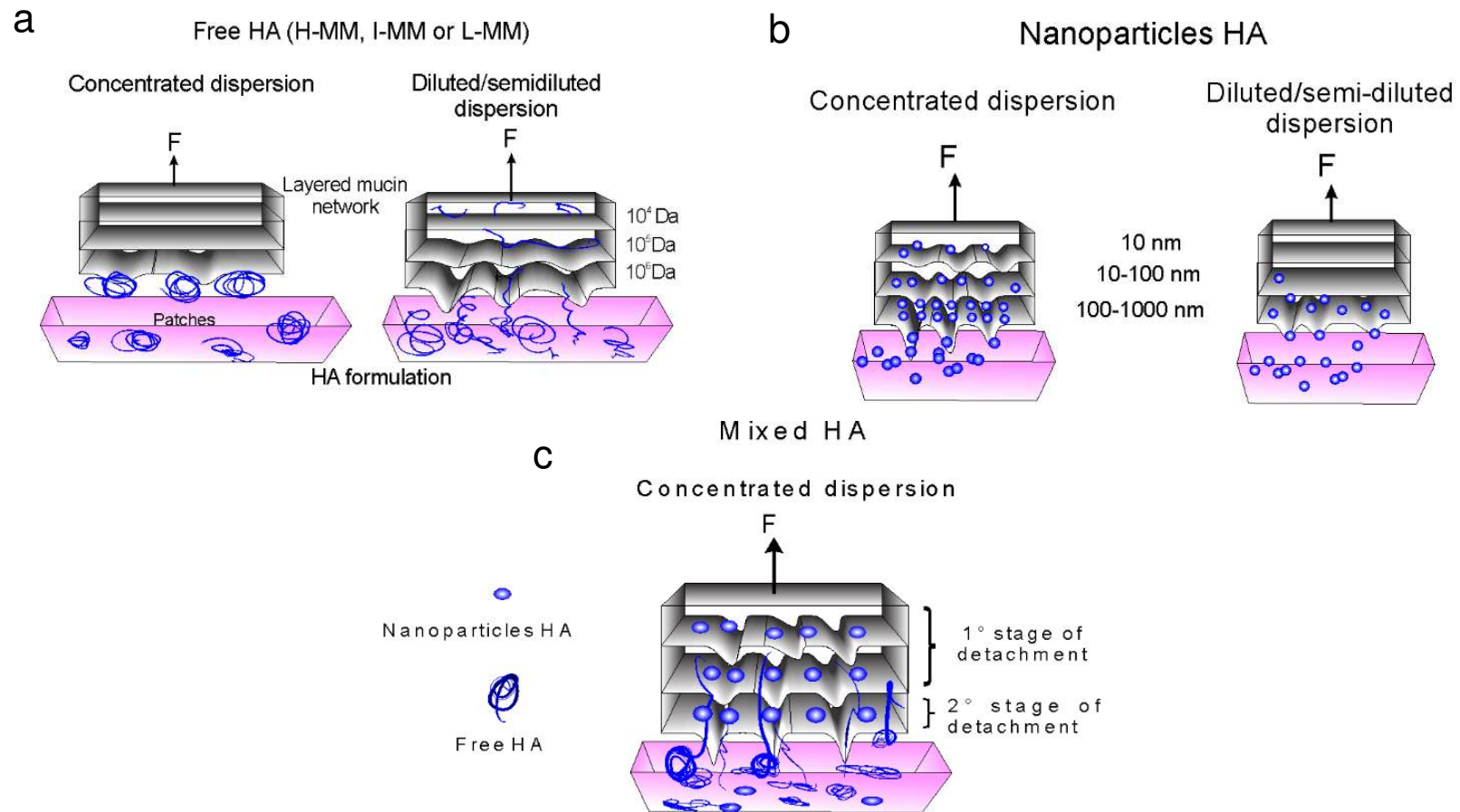


Figure 7. Schematic illustration of the possible configurations of HA-mucin interaction according predominant HA structures. (a) Free HA penetrates into the mucin depending on concentration and its MM, (b) HA nanoparticles penetrates depending on concentration and its particles sizes and (c) Incorporation of mixed HA is a combination of events from individual free and nanoparticles structures that form the detachment stages. (F = tensile force).

3.5.2. Assays with Rat Intestinal Mucosa

The magnitude of the values of mucoadhesion presented in this topic was reduced on *ex vivo* intestinal mucosa of rats because its mucus thickness can be up to 150 times thinner than thickness of mucin tablets (2.2 ± 0.12 mm). Intestinal mucus reaches a maximum thickness of $480 \mu\text{m}$ in the ileum segment (Atuma et al, 2001), as showed in Figure 8.

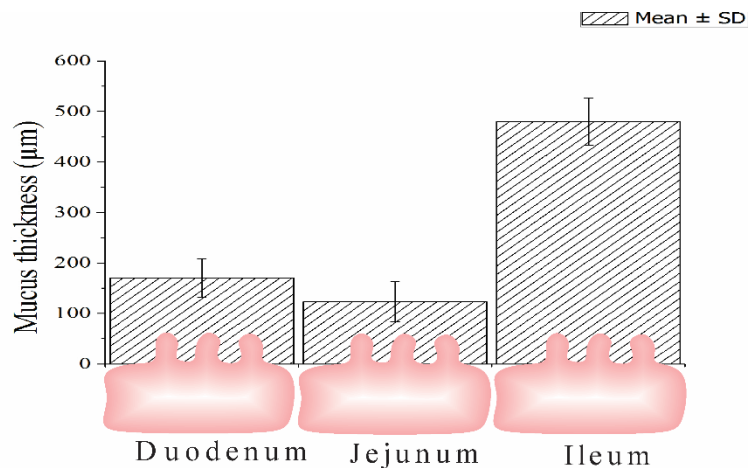


Figure 8. Variations in mucus-layer thickness in intestinal mucosa of rats is shown as mean \pm (S.D.).

(a) Formulations of the Free Hyaluronic Acid

Values of F_{adh} and W_{adh} were determined in the three intestinal segments: duodenum, jejunum and ileum. Values are summarized as mean \pm S.D in Figure 9 (a,b) and (c,d) for the I-MM and H-MM respectively.

Numbers on the X-axis corresponds to concentration range 0.5 g/L (I-MM1), 5 g/L (I-MM2), 10 g/L (I-MM3) and hydrolyzed of I-MM3 (L-MM) respectively.

From profiles 9a,b, F_{adh} from I-MM3 and L-MM compositions presented intra- and interassay variability, according one-way ANOVA with post-hoc Tukey's multiple comparisons test ($p < 0.05$). (*) refers to statistical difference between mean from duodenum and jejunum for I-MM3. (**) refers to statistical

difference between duodenum segment from L-MM and other compositions. (***) refers to interassay statistical difference in the W_{adh} from I-MM3.

From profiles 9c,d, no significance was identified in the F_{adh} of any concentration evaluated. However, W_{adh} was significant in the ileum segment from H-MM3 (****). The absence of (*) indicate no statistical difference intra- or inter-assay.

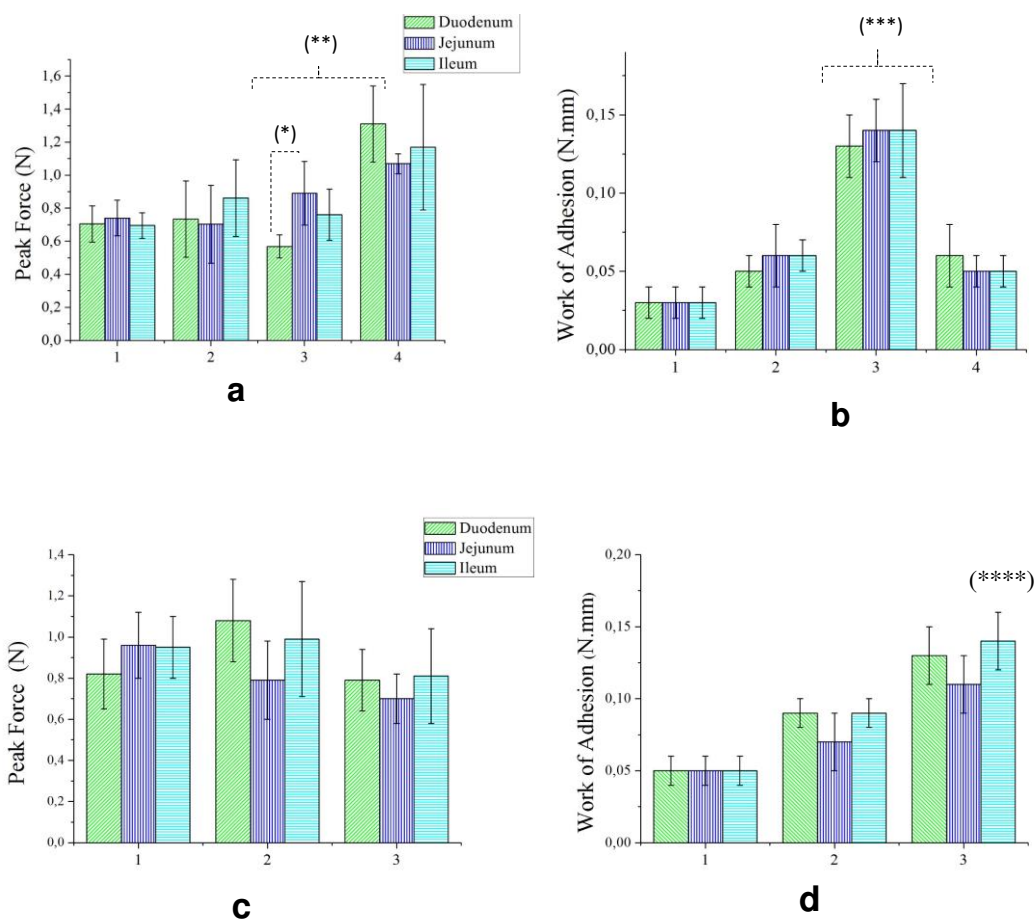


Figure 9. Detachment force and work of adhesion of the free I-MM (a,b) and H-MM (c,d), of the intestinal segments: duodenum (green hatched), jejunum (blue hatched) and ileum (cyan hatched) using rat intestinal mucosa. (1) 0.5 g/L, (2) 5 g/L, (3) 10 g/L and (4) hydrolyzed at 10 g/L. Error bar = \pm S.D. (n=6). (*), (**), (***), (****) Mean statistically different at p-value < 0.05, denoting significance, according to one-way ANOVA test with post-hoc Tukey.

Figure 10 shows the force vs. distance curves in the intestinal segments that presented statistical difference in the F_{adh} and W_{adh} means from I-

MM (10a) and W_{adh} mean from H-MM (10b). Area under force vs. distance curves refers to the adhesion energy.

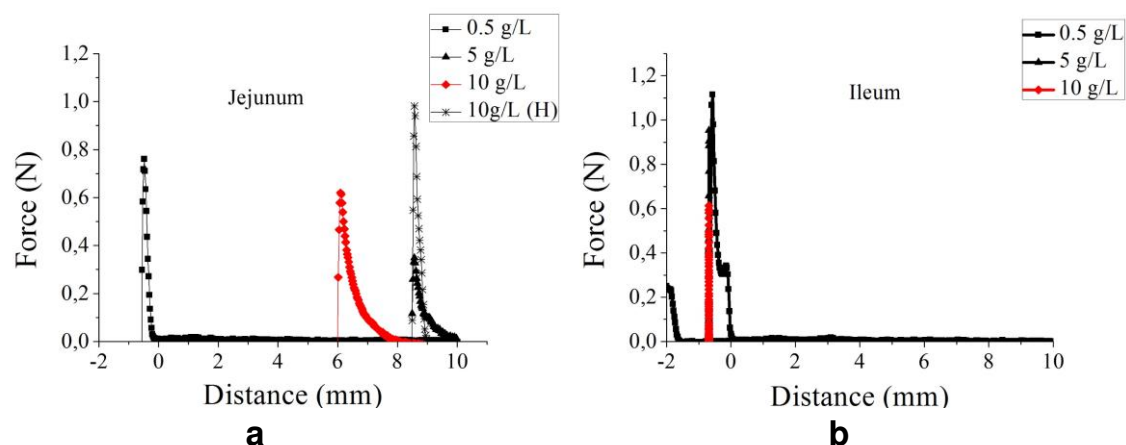


Figure 10. Variations of the force necessary for detachment of the free HA formulation adhered to rat intestinal mucosa. Force was a function of probe upward distance for I-MM and L-MM in (a) and H-MM in (b), to increased compositions: 0.5 g/L (\blacksquare), 5 g/L (\blacktriangle), 10 g/L (\blacklozenge) and hydrolyzed at 10 g/L (\ast).

In Figure 9a, F_{adh} of the I-MM3 and L-MM compositions were responsive to mucus thickness in the jejunum segment and size fragments in the duodenum segment, respectively. The profile of W_{adh} from I-MM3 (Figure 10b) was compatible with the larger area under distance-force curve in the Figure 11A, meaning a detachment gradual over time. It is known that intestinal mucosa is a highly hydrated system and concentrated dosage form acts to dehydrate the mucosa and strengthen the adherent layer. Reported studies have shown that a low water content in composition of hydrophilic polymers was essential for the establishment of adhesion in a different mucosa (Andrews et al., 2009; Laffleur, 2018). Therefore, the behavior in rat intestinal mucosa was contrary to observed in the mucin tablets system, in which, diluted composition of I-MM (0.5 g/L) promoted the most intimate contact between interacting surfaces.

Values of F_{adh} were statistically similar for the compositions I-MM1 and I-MM2 and reached the highest value using L-MM (Figure 9a) in which reduced chain size (low MM) reaches depth into the mucin. According to variations of force in Figure 10a, compositions I-MM2 and L-MM were the first to perform W_{adh} ,

however, the detachment was fast (not gradual), meaning low interpenetration and entanglements of chains. The L-MM was used in the intestinal mucosa in order to evaluate the additional detachment force from the TLR4-HA binding affinity (Underhill et al, 1983). However, a faster detachment may mean that interactions with the receptor do not provide measurable force variation, probably because of the low polyvalence of the L-MM-TLR4 interaction.

In Figure 9c, the F_{adh} of free H-MM was not responsive at compositional range studied, while the W_{adh} was statistically significant in the ileum using 10 g/L composition. However, variations of force in Figure 10b show absence of positive W_{adh} , which seems to be a deviation created by the cohesive forces. Indeed, cohesive forces overcome the mucoadhesion into the formulation as a consequence of the dense structures arising from the self-entanglements of large chains of 10^6 Da. When probe leaves the formulation a new equilibrium of forces makes the W_{adh} measurable.

(b) Formulation of the Nanoparticles Hyaluronic Acid

Are summarized in Figure 11 (a,b) as mean \pm S.D the profiles of F_{adh} and W_{adh} for nanoparticles HA formulation. Values on the X-axis corresponds to concentrations 0.5 g/L (1), 2.5 g/L (2) and 5 g/L (3) respectively. F_{adh} and W_{adh} were determined in the three intestinal segments: duodenum, jejunum and ileum. No statistical difference intra- and interassay was identified according one-way ANOVA with post-hoc Tukey's multiple comparisons test ($p < 0.05$).

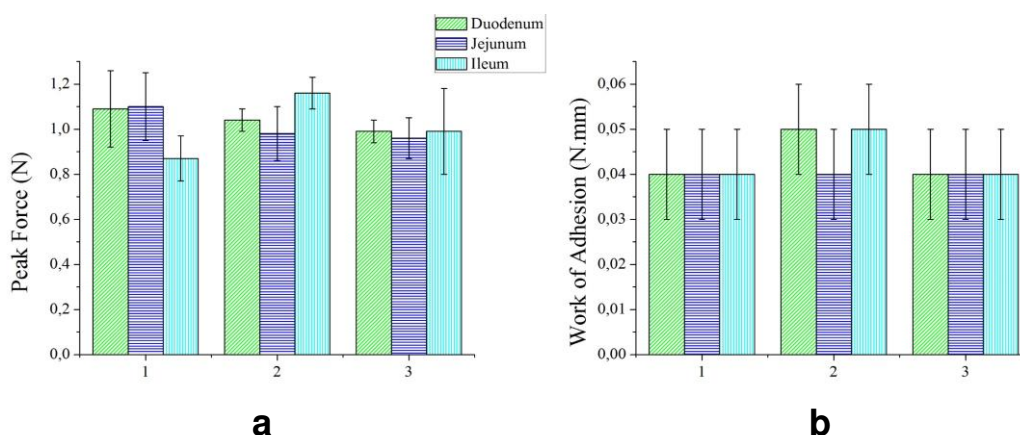


Figure 11. Detachment force and work of adhesion of the nanoparticles HA formulation in the intestinal segments: duodenum (▨), jejunum (▩) and ileum (▧). Compositions (1), (2) and (3) correspond to at 0.5 g/L, 2.5 g/L and 5 g/L respectively. Error bar = \pm S.D. (n=6).

Figure 12 shows force vs. distance curves on the jejunum, the intestinal segment of lesser thickness, in which is expected that cytoadhesive performance is easier to occur due to the proximity of the epithelium to the intestinal lumen. Area under force vs. distance curves refers to W_{adh} of the range compositional of nanoparticles HA. Profiles from 0.5 g/L and 5 g/L were overlapped.

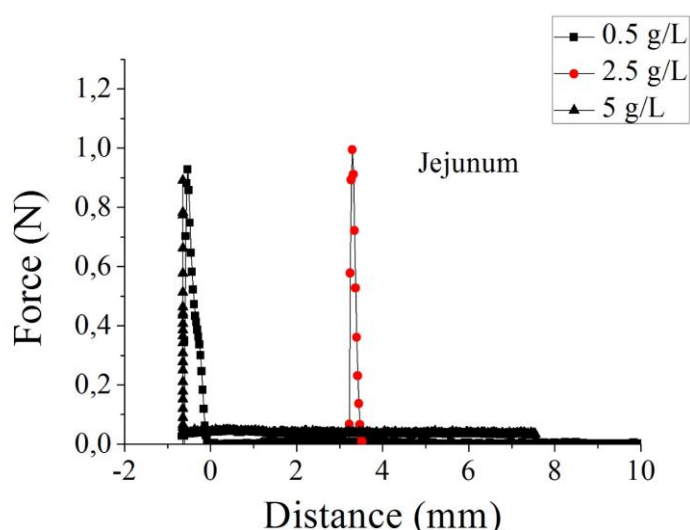


Figure 12. Variations of the force for the detachment of the nanoparticles HA adhered to rat intestinal mucosa. Force was a function of probe upward distance for the compositions: 0.5 g/L (▣), 2.5 g/L (●), and 5 g/L (▲).

Structural stability associated with accessibility into the thin layer of mucus in intestinal mucosa confer the HA nanoparticles a low sensitivity to concentration variations, therefore, no statistical difference was found among the mean values of F_{adh} and W_{adh} into compositional range studied (Figure 11a,b). However, according force vs. distance curves the structures present at 2.5 g/L must have the greatest mucoadhesiveness because a W_{adh} inside a low viscosity formulation indicates that HA structures have reached depth into the mucin network (Figure 12). The order of resistance to detachment was: 2.5 g/L > 0.5 g/L = 5 g/L.

(c) Mixed Formulation of the Hyaluronic Acid

Profiles of F_{adh} and W_{adh} from mixed formulation of HA of are summarized in Figure 13 (a,b) as mean \pm S.D. Values on the X-axis corresponds to compositions: (1) 25 wt. % and (2) 50 wt. %. F_{adh} and W_{adh} were determined in the three intestinal segments: duodenum, jejunum an ileum.

Statistical difference at p-value < 0.05 , according one-way ANOVA with post-hoc Tukey's multiple comparisons test. The absence of (*) indicate no statistical difference intra- or interassay.

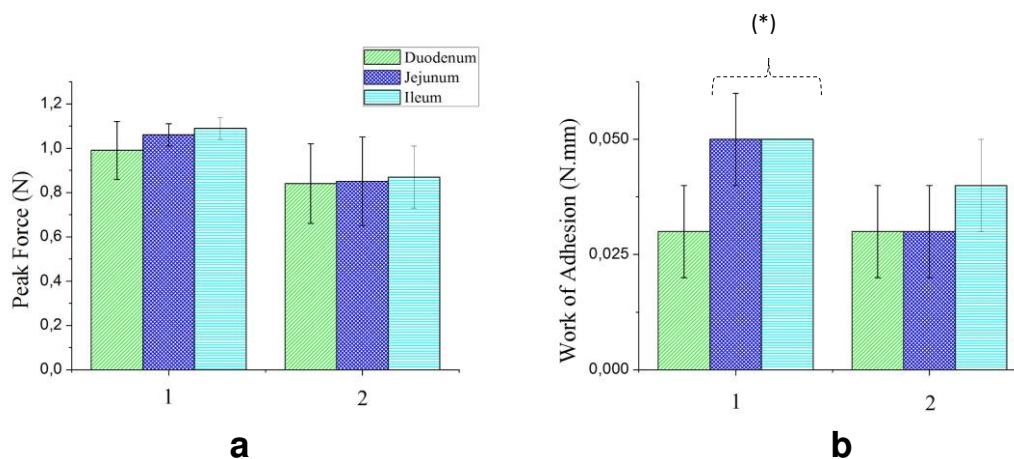


Figure 13. Detachment force and work of adhesion of the preformed mixture (Mixed HA) in the intestinal segments: (green) duodenum, (blue) jejunum and (cyan) ileum. Compositions correspond to (1) 25 wt. % and (2) 50 wt. %. Error bar = \pm S.D. (n=6).

Figure 14 shows force vs. distance curves from 25 wt. % composition with statistical significance.

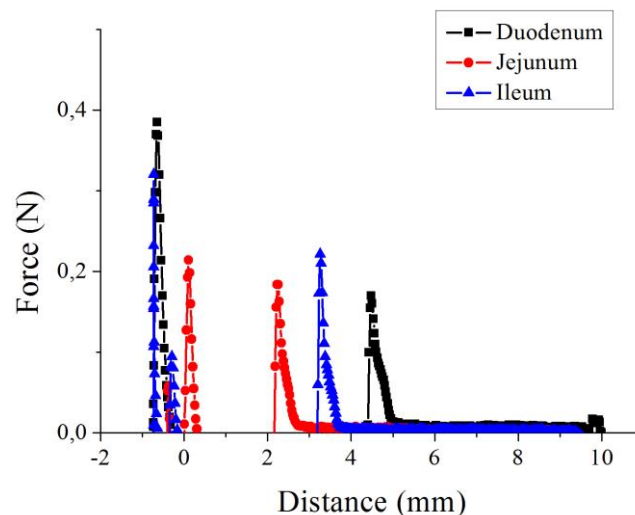


Figure 14. Variations of the force necessary for detachment of the mixed HA structures from 25 wt. % composition adhered to rat intestinal mucosa. Force was a function of probe upward distance was obtained in the duodenum (-■-), jejunum (-●-) and ileum (-▲-).

According to force vs. distance curves, no defined tendency was observed for the W_{adh} on three intestinal segments, however the existence of multiple peaks of force from jejunum segment indicates resistance to rupture at different depths inside the formulation. Although the jejunum is more resistant to detachment, a synergism occurred in all segments in the attempt to avoid a single rupture (Figure 14).

Results of adhesion on the intestinal mucosa showed that F_{adh} was a quantity that directly responded to the depth of incorporation, presented higher values using nanoparticles than free HA. However, nanoparticles have poor resistance to detachment, as observed by the reduced area (Figure 14), suggesting that HA uses chain size, hydration and structural flexibility to establish interaction with mucin. Thus, the W_{adh} was high for free I-MM because the viscosity and interpenetration of chains acted simultaneously on the mucoadhesion.

Using rat intestinal mucosa as a biological substrate gave a different rank-order according to joint interpretation of mean and profile force vs. distance. F_{adh} : Nanoparticles > Mixed > I-MM > H-MM and W_{adh} : I-MM > H-MM > Nanoparticles = Mixed.

3.6. Mechanism of Mucoadhesion of HA Structures

Figure 15 is a schematic illustration of the proposed mechanism of adhesion between HA structures and mucin network: In (a) is presented HA structures. (b) refers to initial configuration of system. In (c) Free HA chains match their active adhesive sites with the mucin to form a physical bond. In (d) Nanoparticles swell and retain their structure with adhesion dependent of depth achieved into the mucin network.

Due to the preswelling of the contact surface of the mucin tablets, the interfacial layers were in the quasi-equilibrium-swollen state and mucoadhesion was assumed to be a summation of capillary attraction and osmotic forces drawing HA structures into the deeper layers of mucin network. In this process, mucin network or HA act to dehydrate the more hydrated component, strengthening the adherent layer, occurring the three-dimensional expansion of the network, mainly with the interpenetration of the 10^5 Da free HA.

In both mechanisms of penetration of HA structures (Figure 15c,d), zeta potential (ZP) influences electrostatic repulsion of chains polymeric, as mucin is also polyelectrolyte. Therefore, the ZP modulus modulates the HA-mucin interaction. Additionally, a reported study has shown that critical chain length of at least 10^5 Da (Chen and Cyr, 1970) modulates the penetration and molecular entanglement.

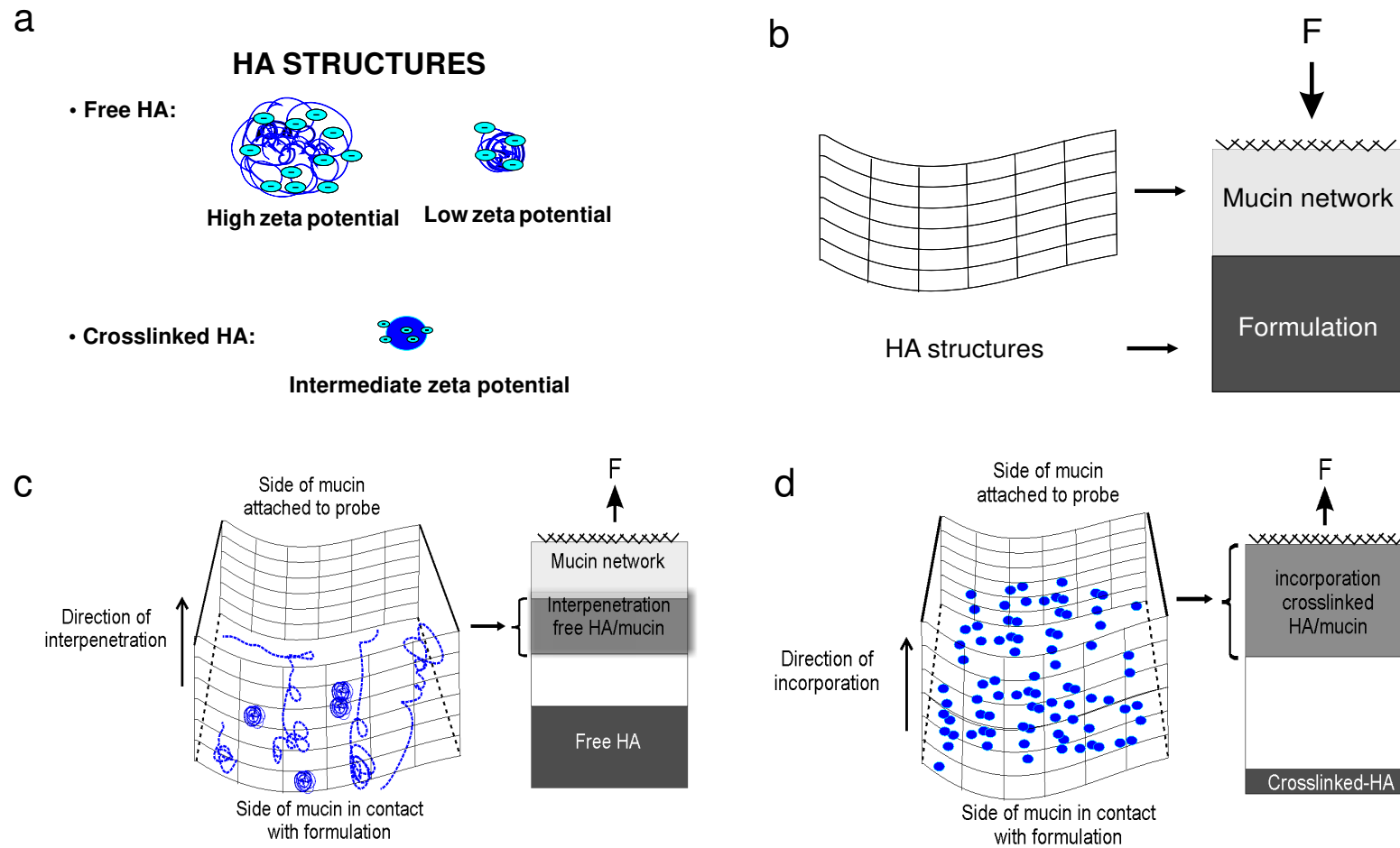


Figure 15. Schematic representation of the mechanisms of interaction of HA with mucin network. In (a) spatial architecture of HA structures. (b) shows pre-contact step. (c,d) show mechanism of interaction structure-dependent.

3.7. Rheology of the HA formulations

As previously discussed, the flow resistance from tensile force was modulated by the viscosity of free HA structures with fraction of larger chains in the order of 10^5 Da and 10^6 Da. H-MM and I-MM presented the highest viscosity in contrast to nanoparticles. As expected, mixed HA had an intermediate viscosity (Figure 16a).

Transition (cross-over point) from a liquid-like dominated domain ($G'' > G'$) to a solid-like dominated domain ($G' > G''$) was a consequence of different distributions of MM. H-MM had a high relaxation time ($\omega_x = 1 \text{ rad.s}^{-1}$) due to the higher fraction of 10^6 Da, while I-MM had an intermediate relaxation time ($\omega_x = 38.4 \text{ rad.s}^{-1}$) due to the higher fraction of 10^5 Da (Figure 16b).

Nanoparticles and mixed HA has an elastic gel behavior, with $G' > G''$ and constant in the frequency range evaluated due to high structural stability of nanoparticles composing both formulations (Figure 16c,d).

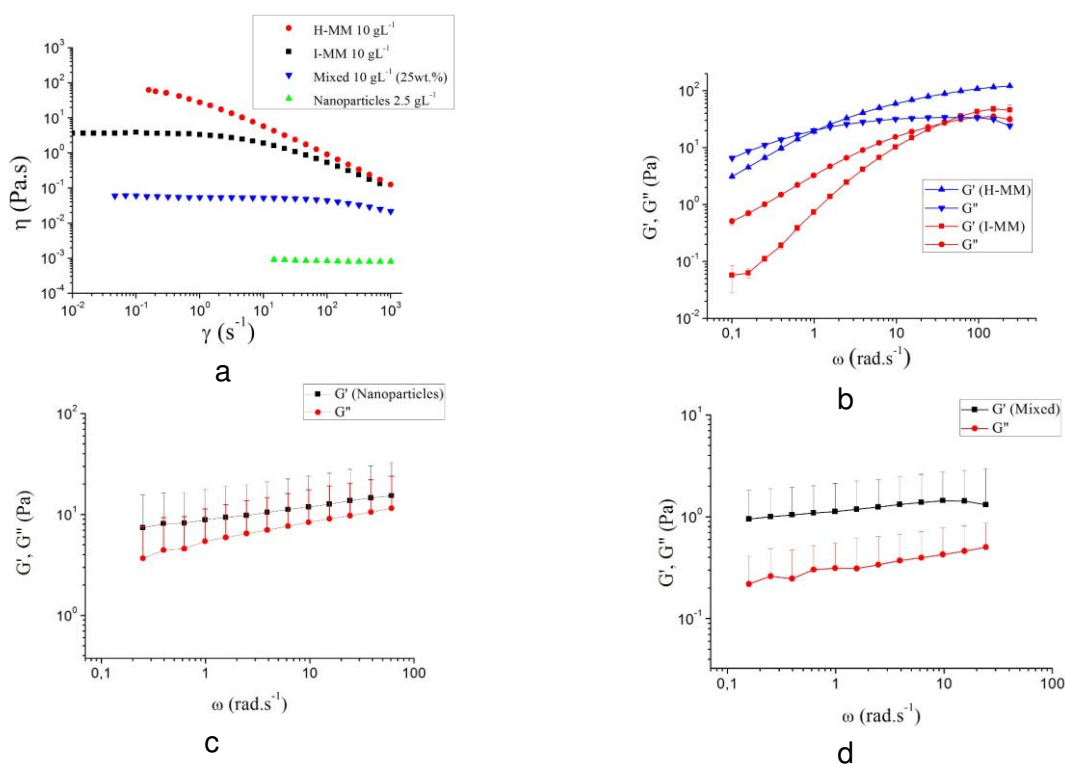


Figure 16. Rheological behavior of HA formulations shows (a) viscosity η as a function of the shear rate $\dot{\gamma}$. (b, c, and d) show the loss modulus (G'') and storage modulus (G') as a function of angular frequency ω . Values are expressed as mean \pm S.D.

3.8. Interplay Between Adhesive Response and Structures of Hyaluronic Acid

The variable concentration, purity and distribution of MM modulated the physical structuring of free HA. Additionally, chemical crosslinking provided increased structural stabilization, providing size and slightly negative zeta potential with a range of values appropriate for cellular uptake and bio-distribution as reported by Xiao et al., 2015. The combination of the cited variables affected particle mobility and surface chemistry of the interacting surfaces, modulating mucoadhesion.

Additionally, cellular viability (Levine et al, 1970) and functionality of the TLR4 receptors from the freshly excised mucosae raising interesting questions. Stabilization of binding from polyvalent HA structure provides synergistic effects on the TLR4 (Underhill et al, 1983).

Spatial architecture of the free HA structures modulated the one-way mass transport from the outside to inside the mucin network. Dense structures of free HA were formed at higher concentration as consequence of cohesive forces in bulk, thus competing by the mucoadhesion with mucin. I-MM at semi-diluted regime provided less dense structures whose adhesion was successful in mucin tablets. In the intestinal mucosa, however, structures from concentrated dosage forms were more successful for adhesion. Diffusion and capillarity of water from a more diluted component (mucosa) to the more concentrated one (HA formulation) strengthens the intimate contact of the interacting surfaces.

Molar mass (MM) and particle size influenced the adhesive response as follows:

(a) Free HA H-MM penetrated only superficially while structures from I-MM penetrated to intermediate depths inside the mucin network due to lowest fraction of 10^6 Da ($16 \pm 1\%$) or highest fraction of 10^5 Da ($74.0 \pm 0.8\%$).

Consequently, I-MM and mucin formed interpenetrating chains and entanglements as supported by the high F_{adh} and slowly detachment. By analogy, interpenetration of chains also occurred with intestinal mucosa, however, in a lower magnitude due to the reduced thickness of mucus.

(b) Nanoscaled structures from 50 to 500 nm of cross-linked HA was appropriate choice for to transpose the mucin network (20-200 nm cut-off pores). It is known that HA structures nanoscaled (roughly 65 nm) and specific size range (100–300 kDa) positively influenced the structuring of multiple HA receptors into the transmembrane assembly, essential to stabilization of binding (Weigel et al., 2017). Indeed, the contact time HA-mucosa used in this study was 3 min., presumably sufficient to exploit the cytoadhesive behavior (Hsieh et al., 2014).

(c) Combined structures from mixed formulation have brought greater mucoadhesion, due to the synergism of the adhesion mechanisms inherent to each HA structure.

This study revealed that formulations containing cross-linked structures at 2.5 g/L, mixed structures at 25 wt. % and I-MM at 10 g/L, were the most promising adhesive formulations in intestinal mucosa.

Based on our findings, we believe that formulations of 90 % (HA/proteins) purity, high fractions of 105 Da and low particle size (< 200 nm) represent a consistent choice to optimize the oral bioavailability because they showed the best adhesion responses in the intestinal mucosa of rats.

4. Conclusions

Oral HA has emerged as a supplement to prevent or to treat diseases caused by decreasing of its levels in the tissues, as well as a complementary therapy for mucosal disorders. Despite this, the exact mechanisms involved in the mucoadhesion of HA in biological membranes are poorly investigated. Thereby, the present study was undertaken in the attempt to investigate the mucoadhesive performance of the different HA structures.

The purity, concentration, molar mass and chemical stabilization modulated the structural architecture of HA and the physicochemistry of interacting surfaces. Structural qualities such as particle size, zeta potential, flexibility and hydration were decisive in the improving mucoadhesion.

In the intestinal mucosa, HA structures from concentrated dosage form conditioned greater W_{adh} because the mucosa was a richly hydrated environment. On the other hand, nanoparticles had a higher F_{adh} due to its ease of incorporation by the mucus nanostructure.

Acknowledgements

This study was financed in part by the Coordination for the Improvement of Higher Educational Personnel (CAPES, Brazil), [grant number: 33003017034P8].

References

1. Andrews, G. P., Lavery, T. P., Jones, D. S. Mucoadhesive polymeric platforms for controlled drug delivery. *Eur J Pharm Biopharm.* 2009, 71(3):505-18.
2. Atuma, C., Strugala, V., Allen, A., Holm, L. The adherent gastrointestinal mucus gel layer: thickness and physical state in vivo. *Am J Physiol Gastrointest Liver Physiol.* 2001, 280(5): G922-9.
3. Balazs, E. A., Band, P. A. Therapeutic Use of Hyaluronan-Based Products. *Carbohydrate Chemistry, Biology and Medical Applications.* 2008. 311- 332..
4. Balogh, L., Polyak, A., Mathe, D., Kiraly, R., Thuroczy, J., Terez, M., Janoki, G., Ting, Y., Bucci, L.R., Schauss, A.G. Absorption, uptake and tissue affinity of high-molar-weight hyaluronan after oral administration in rats and dogs *J Agric Food Chem.* 2008, 56, 10582–10593.
5. Bassi da Silva, J., de Souza Ferreira, S.B., de Freitas, O., Bruschi, M.L. A critical review about methodologies for the analysis of mucoadhesive properties of drug delivery systems. *Drug Dev. Ind. Pharm.* 2017, 9045, 1–67.
6. Bicudo, R.C., Santana, M.H. Effects of Organic Solvents on Hyaluronic Acid Nanoparticles Obtained by Precipitation and Chemical Crosslinking. *J Nanosci Nanotechnol.* 2012 Mar;12(3):2849-57.
7. Cavalcanti, A. D. D., Melo, B. A. G., Oliveira, R. C., Santana, M. H. A. Recovery and purity of high molar mass bio-hyaluronic acid via precipitation strategies modulated by pH and sodium chloride. *Applied Biochemistry and Biotechnology.* 2018, 1-13. doi: 10.1007/s12010-018-02935-6.
8. Chen, J. L., Cyr, G. N. Compositions producing adhesion through hydration, in: R.S. Manly (Ed.), *Adhesion in Biological Systems*, Academic Press, New York, NY, 1970, p. 163
9. Chen, Y. H., Wang, Q. Establishment of CTAB Turbidimetric method to determine hyaluronic acid content in fermentation broth. *Carbohydr. Polym., Elsevier Ltd.* 2009, 78, 178–181.

10. Cook, M.T., Khutoryanskiy, V.V. Mucoadhesion and mucosa-mimetic materials - A mini-review. *Int. J. Pharm.* 2015, 495, 991–998.
11. Di Cerbo, A., Aponte, M., Esposito, R., Bondi, M., Palmieri, B. Comparison of the effects of hyaluronidase and hyaluronic acid on probiotics growth. *BMC Microbiol.* 2013, 13: 243.
12. Falcone, S. J., Palmeri, D., Berg, R. A. Biomedical Applications of Hyaluronic Acid. *Polysaccharides for Drug Delivery and Pharmaceutical Applications*, 2006, 155–174.
13. Feldstein, M.M., Moscalets, A.P. *Innovations in Pressure-Sensitive Adhesive Products*. Smithers Rapra Technology, 2016, 148 p.
14. Fraser, J. R. E., Laurent, T. C., Laurent, U. B. G. Hyaluronan: its nature, distribution, functions and turnover. *J. Intern. Med.* 1997, 242:27-33.
15. Fukuda, K., Takayama, M., Ueno, M., Oh, M., Asada, S., Kumano, F., Tanaka, S. Hyaluronic acid inhibits interleukin-1-induced superoxide anion in bovine chondrocytes. *Inflamm. Res.* 1997, 46(3):114-7.
16. Garg, H.G., Hales, C.A. *Chemistry and Biology of Hyaluronan*. Elsevier. 2004.
17. Georgiades, P., Pudney, P.D., Thornton, D.J., Waigh, T.A. Particle tracking microrheology of purified gastrointestinal mucins. *Biopolymers.* 2014, 101 (4) 366–377.
18. Hansen, I.M., Ebbesen, M.F., Kaspersen, L., Thomsen, T., Bienk, K., Cai, Y., Malle, B.M., Howard, K.A. Hyaluronic Acid Molar Weight-Dependent Modulation of Mucin Nanostructure for Potential Mucosal Therapeutic Applications. *Mol Pharm.* 2017, 14(7):2359-2367.
19. Hsieh, C.M., Huang, Y.W., Sheu, M.T., Ho, H.O. Biodistribution profiling of the chemical modified hyaluronic acid derivatives used for oral delivery system. *Int. J. Biol. Macromol.* 2014, 64:45-52.
20. Hu, Z., Xia, X., Tang, L., 2006. Process for Synthesizing Oil and Surfactant-Free Hyaluronic Acid Nanoparticles and Microparticles. US Patent 20060040892A1. Available at

<<http://www.freepatentsonline.com/20060040892.pdf>> (Accessed 09 November 2018).

21. Jiang, H., Peterson, R.S., Wang, W., Bartnik, E., Knudson, C.B., Knudson, W. A requirement for the CD44 cytoplasmic domain for hyaluronan binding, pericellular matrix assembly and receptor mediated endocytosis in COS-7 cells *J Biol Chem.* 2002, 277, 10531-10538.

22. Jones, D.S., Woolfson, A.D., Brown, A.F. Textural, viscoelastic and mucoadhesive properties of pharmaceutical gels composed of cellulose polymers. *International Journal of Pharmaceutics.* 1997, 151(2):223-233.

23. Jones, D.S., Woolfson, A.D., Djokic, J. Texture profile analysis of bioadhesive polymeric semisolids: mechanical characterisation and investigation of interactions between formulation components. *J. Appl. Poly. Sci.* 1996b, 61 2229–2234.

24. Jones, D.S., Woolfson, A.D., Djokic, J., Coulter, W.A. Development and mechanical characterisation of bioadhesive semi-solid polymeric systems containing tetracycline for the treatment of periodontal diseases. *Pharm. Res.* 1996a, 13 1732–1736.

25. Kawada, C., Yoshida, T., Yoshida, H., Matsuoka, R., Sakamoto, W., Odanaka, W., Sato, T., Yamasaki, T., Kanemitsu, T., Masuda, Y., Urushibata, O. Ingested hyaluronan moisturizes dry skin *Nutr J.* 2014, 13:70.

26. Kerker, M. The scattering of light and other electromagnetic radiation. Volume 16 in *Physical Chemistry: A Series of Monographs*. Chapter 7 - Analysis of Particle Size. 1969, pages 311-413.

27. Kogan, G., Soltés, L., Stern, R., Mendichi, R. Hyaluronic acid: a biopolymer with versatile physico-chemical and biological properties, in: R. A. Pethrich, B. Antonio, G.E. Zaikov (Eds.), *Handbook of Polymer Research: Monomers, Oligomers, Polymers and Composites*, Nova Science Publishers Inc., New York. 2007, pp. 393-439.

28. Kresse, H., Glossl, J. Glycosaminoglycan degradation In *Advances in Enzymology*, 60th edn (ed A Meister). 1987, pp 217-311 New York: Wiley.

29. Laffleur, F. Comparative mucoadhesive study of hyaluronic acid-based conjugates on different mucosae. *J. Appl. Polym. Sci.* 2018, 135 (14), 46071.
30. Levine, R.R., McNary, W.F., Kornintestinalh, P.J., LeBlanc, R. Histological reevaluation of everted intestinal technique for studying intestinal absorption. *Eur J Pharmacol.* 1970, 9(2):211-9.
31. Muto, J., Yamasaki, K., Taylor, K. R., Gallo, R. L. Engagement of CD44 by hyaluronan suppresses TLR4 signaling and the septic responseto LPS. *Mol. Immunol.* 2009, 47(2-3):449-56.
32. Nair, A.B., Kumria, R., Harsha, S., Attimarad, M., Al-Dhubiab, B.E., Alhaider, I.A. In vitro techniques to evaluate buccal tablets. *J. Control. Release.* 2013, 166, 10–21.
33. Otero-Espinar, F.J., Delgado-Charro, B., Anguiano-Igea, S., Blanco-Mendez, J. Use of tensile test in the study of the bioadhesive and swelling properties of polymers. In *Data Adquisition and Measurement Techniques*; Muñoz-Ruiz, A., Vromans, H., Eds.; Interpharm Press Inc.: Buffalo Grove, IL, USA. 1998, pp. 295–342.
34. Peppas, N. A., Buri, P. A. Surface, interfacial and molecular aspects of polymer bioadhesion on soft tissue, *J. Controlled Release*, 2, 1985, 257-275.
35. Ponchel, G., Irache, J. Specific and non-specific bioadhesive particulate systems for oral delivery to the gastrointestinal tract *Adv Drug Deliv Rev.* 1998, 34(2-3):191-219.
36. Ponchel, G., Touchard, F., Duchene, D., Peppas, N. A. Bioadhesive analysis of controlled-release systems. I. Fracture and interpenetration analysis in poly(acrylic acid)-containing systems. *J. Controlled Release*, 1987, 5: 129-141.
37. Robinson, J. R. Rationale of bioadhesion/ mucoadhesion, In: Gurny R. and Junginger HE. (Eds.), *Bioadhesion Possibilities and Future Trends*, Wissenschaftliche Verlagsgesellschaft, Stuttgart, 1990, pp.13-15.
38. Round A.N., Rigby N.M., Garcia de la Torre A., Macierzanka A., Mills E.M.C., Mackie A.R. Lamellar structures of MUC2-rich mucin: a potential role in

governing the barrier and lubricating functions of intestinal mucus. *Biomacromolecules*, 2012, 13:3253.

39. Rubas, W., Grass, G. M. Gastrointestinal lymphatic absorption of peptides and proteins. *Advanced Drug Delivery Reviews*. 1991, 7 15-69.

40. Salehi Dashtebayaz, M. S., Nourbakhsh, M. S. Interpenetrating networks hydrogels based on hyaluronic acid for drug delivery and tissue engineering. *International Journal of Polymeric Materials and Polymeric Biomaterials*. 2018, 1–10.

41. Serra, L., Doménech, J., Peppas, N. Engineering Design and Molecular Dynamics of Mucoadhesive Drug Delivery Systems as Targeting Agents. *European journal of pharmaceutics and biopharmaceutics*, 2009, 71(3):519-528.

42. Smart, J.D. The basics and underlying mechanisms of mucoadhesion. In: *Advanced Drug Delivery Reviews*. 2005, 57, pp. 1556 – 1568.

43. Smart, J.D. The role of water movement and polymer hydration in mucoadhesion, in *Bioadhesive Drug Delivery Systems: Fundamentals, Novel Approaches and Development*, Mathiowitz E, Chickering D E and Lehr C M Eds, Marcel Decker, New York. 1999, pp. 11-23.

44. Smith, P. K., Krohn, R. I., Hermanson, G. T., Mallia, A. K., Gartner, F. H., Provenzano, M. D., Fujimoto, E. K., Goeke, N. M., Olson, B. J. Klenk, D. C. Measurement of protein using bicinchoninic acid. *Anal. Biochem*. 1985,150, 76–85.

45. Stanley-Wood, N.G., Lines, R.W. 1992. *Particle Size Analysis*. The Royal Society of Chemistry, Cambridge.

46. Teubl, B. J., Meindl, C., Eitzlmayr, A., Zimmer, A., Fröhlich, E., Roblegg, E. In-vitro permeability of neutral polystyrene particles via buccal mucosa. *Small*. 2013, 457-466.

47. Underhill, C.B., Chi-Rosso, G., Toole, B.P. Effects of detergent solubilization on the hyaluronate-binding protein from membranes of simian virus 40-transformed 3T3 cells *J Biol Chem*. 1983, 258(13):8086-91.

48. Weigel, P.H., Baggenstoss, B.A. What is special about 200 kDa hyaluronan that activates hyaluronan receptor signaling? *Glycobiology*. 2017, 27(9):868-877.
49. Wong, C., Yuen, K., Peh, K. An in-vitro method for buccal adhesion studies: importance of instrument variables, *Int. J. Pharm.* 1999, 180 47–57.
50. Xiao, B., Han, M. K., Viennois, E., Wang, L., Zhang, M., Si, X., Merlin, D. Hyaluronic acid-functionalized polymeric nanoparticles for colon cancer-targeted combination chemotherapy. *Nanoscale*. 2015, 7(42):17745-55.

3.2 Intestinal uptake assessment of the oral hyaluronic acid in rats

Intestinal uptake assessment of the oral hyaluronic acid in rats

Alexandro Barbosa de Souza¹, Marco Vinicius Chaud², Thais Francine Ribeiro Alves²,
Juliana Ferreira de Souza² & Maria Helena Andrade Santana^{1*}

¹Department of Materials and Bioprocesses Engineering, School of Chemical Engineering, University of Campinas, Box 6066, 13083 852, Campinas, SP, Brazil and ²Laboratory of Biomaterials and Nanotechnology, University of Sorocaba, 18300 000, Sorocaba, SP, Brazil.

*Correspondence should be addressed to mariahelena.santana@gmail.com

ABSTRACT

Hyaluronic acid (HA) is an endogenous polymer found in different tissues of mammals performing structural, lubricant, antioxidant and anti-inflammatory functions. Nowadays, formulations for oral administration containing exogenous HA has gained attention as a supplement to prevent or to treat diseases caused by decreasing of its concentration in the tissues, as well as a complementary therapy for dysbiosis. As known, the HA structuring plays an important role on its intestinal uptake as well as on its distribution to other tissues. However, studies focusing these aspects are still scarce. Formulations of free HA (f-HA) (average molar mass 10^5 Da), HA structured in nanoparticles (n-HA) with 475.3 ± 75.8 nm mean diameter as well as a mixed formulation (mix-HA) containing 25 wt. % nanoparticles dispersed in the f-HA were previously prepared and characterized. An improved single-pass intestinal perfusion (SPIP) method which consider the whole small intestine was used to assesses the intestinal effective permeability (P_{eff}) of the formulations. The results showed that f-HA and mix-HA had the slower intestinal transit ($P_{\text{eff}} = 0.96 \cdot 10^{-5}$ mm/min and $P_{\text{eff}} = 1.05 \cdot 10^{-5}$ mm/min respectively) compared with the n-HA ($2.62 \cdot 10^{-5}$ mm/min). In addition, the blood clearance was 1h (f-HA), 0.5h (n-HA) and 1.5h (mix-HA). The permeated concentrations were $21 \pm 3\%$ (f-HA), $80 \pm 5\%$ (n-HA) and $45 \pm 4\%$ (mix-HA) related the inlet concentration. Therefore, the HA structuring modulate the dynamic of its intestinal uptake, with consequences on its metabolization and distribution to the other tissues.

Keywords: Hyaluronic acid. HA structuring. Permeation. Absorption.

1. Introduction

Hyaluronic acid (HA) is a glycosaminoglycan that acts as a scaffold surrounds cells in various tissues and fluids as well as it binds to specific cell surface receptors (Necas et al., 2008). Structural, lubricant and antioxidant functions are dependent on its concentration, molar mass (MM) and size distribution of its chains (Fukuda et al, 1997; de la Motte, 2011; Toole, 2004; Bowers, 1983) structured in different spatial architectures. While the integrity of polymeric HA structures regulates tissue homeostasis, the decreasing of its endogenous production or cleavage of its chains is linked with various diseases related to age mainly. Nowadays, the exogenous HA from fermentation (bio-HA) has been widely used to restore the endogenous HA properties that have been lost. (Kawada et al, 2014; Martinez-Puig et al, 2013).

The methods of HA administration may vary, being the topical or injectable the most common applications (Berenbaum, 2013). The orally administered HA has gained attention for prevention or complementary dosage to traditional therapies (Sardi, 2004).

Due to the passage through the aggressive conditions of the gastric system, during the last four decades has been postulated that a low and incomplete fraction dose of ingested HA is absorbed as high molar mass ($MM \geq 10^5$ Da) (Oe et al., 2016; Kawada et al., 2014; Schultz et al., 1989). However, the reported studies are generally qualitative, based on fluorescent methods for identification of HA in the tissues. Therefore, the knowledge about the intestinal uptake of HA needs to be advanced in terms of the kinetic aspects as well as to those related to HA structuring.

Various studies have shown a high correlation ($r^2 = 0.8-0.95$) between intestinal permeability in rats and in the human jejunum for a variety of drugs (Zakeri-Milani et al., 2007). Additionally, the whole small intestine of rats can be used to assess human correlations, which is difficult to be performed in humans (Lennernäs, 2014; Lozoya-Agullo et al., 2015).

The methods used for intestinal perfusion studies in rats are approved by FDA and emerge as the simplest, accurate and cost effective option. (CDER/FDA, 2015).

The single-pass intestinal perfusion (SPIP) is a physiologically relevant method that investigates the disappearance of a biologically active compound from an analyzed segment as a measure for its intestinal permeation. This method assures the necessary elements for an accurate uptake such as intact blood and nerve supply to the intestinal tract, local endocrine conditions, and membrane integrity (Li et al., 2011). In addition, blood sampling enables more sensitive pharmacokinetic assessment of the absorption (Haserodt et al., 2011). Nowadays, the improved SPIP represents an evolution of the technique, by using the whole small intestine of rats for more accurate determinations (Rabba et al., 2011; Han et al., 2016, Kim et al., 2018), due to regional variability the Peyer's patches and variable thickness of the mucus layer along the intestine (Abe and Ito, 1978; Atuma et al., 2001).

In this study, improved SPIP was used to assess the effects of HA structuring on its effective intestinal permeability by using formulations of free HA (f-HA) (average molar mass 10^5 Da), HA structured in nanoparticles (n-HA) with 475.3 ± 75.8 mean diameter as well as a mixed formulation (mix-HA) containing 25 wt. % nanoparticles dispersed in the f-HA. HA in the ingoing and outgoing perfusate formulations were characterized by its molar mass (MM), particle size and distribution and zeta potential.

Figure 1 shows schematically the fluxes involved in the continuous intestinal perfusion of the formulations. Initially HA is tangentially fed across the intestinal lumen. The microvilli retain the structures that permeate the membrane by paracellular transport which is regulated by tight junctions while the carrier-mediated transcellular transport is activated by the receptors and the interacting structures (Lennernäs et al., 2007).

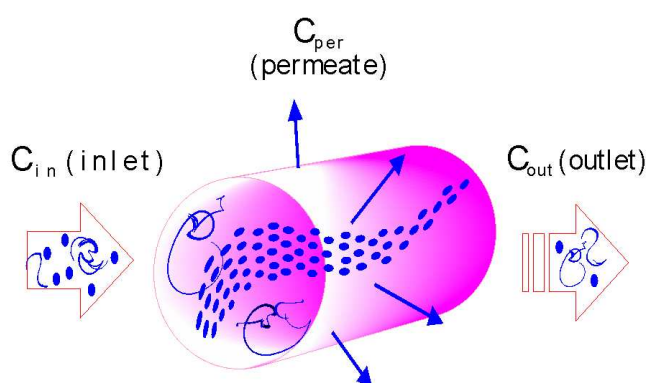


Figure 1. Schematic representation of the fluxes involved in the continuous intestinal perfusion of free, nanoparticulate and mixed HA formulations.

The results were analyzed in terms of HA concentration in the perfusate (ingoing and outgoing) and blood for determination of the performance of permeation and absorption.

Surface properties and rheological behavior of macerated of small intestine perfused, also were determined for interpretation of data and evaluation of interpenetration of f-HA and mucin or incorporation of n-HA into the mucin network.

2. Material and Methods

2.1. Polymers and Chemicals

Hyaluronic acid sodium salt at 1 % (w/v) was purchased from Mapric Pharmaceutical Products Ltd., (Sao Paulo, Brazil). Nanoparticulate HA was synthesized from Mapric HA. ELISA-like assay Kit was purchased from FineTest (Wuhan Fine Biotech Co., Ltd.), catalog #EU2556, lot #U2556C069 and used for concentration measurements of HA in the blood serum. Water-soluble adipic acid dihydrazide (ADH) and N,N-dimethylaminopropyl carbodiimide (EDCI) were purchased from Sigma (St. Louis, USA) and used for nanoparticle crosslinking. Tanohalo (halotano 100%) 1mL/mL was purchased from Sanofi-Aventis Pharmaceutical Ltd (Brazil) and thiopental sodium was purchased from Cristália Pharmaceutical and Chemical Products Ltd (Brazil), both used for induction and maintenance of general anesthesia. The other agents were all analytical grade.

2.2. Synthesis of HA-ADH Crosslinked Nanoparticles

Nanoparticulate HA was synthesized by chemical crosslinking using ADH and EDCI, according to the protocol described by Hu et al. (2006) with modifications described by Bicudo and Santana (2012). Nanoparticles were formed by HA precipitation due to its local dehydration. Briefly, the process was carried out in a jacket

glass reactor (400mL) under controlled temperature 21°C and gentle mechanical stirring. Ethanol (Merck, Darmstadt, Germany) was dropped at a flow rate 7 mL/min into a 0.1% (w/v) solution of sodium hyaluronate with average molar mass 10^5 Da (Mapric Pharmaceutical Products Ltd.). Initially, an ethanol volume (100mL approx.) was added and the reacting system maintained under stirring for 2h. Next, 40 mg/mL EDCI and a 20 mg/mL ADH both in aqueous solution were added to the reactor for crosslinking under more 24h stirring. The reaction was ended by addition of more 100mL ethanol and stirring for another 20h. Nanoparticle recovery was ensured using an Ultracel® cell, containing a 10 kDa ultrafiltration disc and a 44.5 mm diameter filter (EMD Millipore Co., Billerica, MA, USA), while was operated at 0.5 psi inlet nitrogen pressure.

The recovery yield was calculated by Eq. 1:

$$Y (\%) = \frac{(T_m - F_m)}{T_m} \times 100 \quad \text{Eq. (1)}$$

Where the total mass (T_m) corresponded to the sum of the masses in the filtrate (F_m) and retentate (R_m).

2.3. Perfusate Preparations

Three HA formulations were used in the perfusion experiments: (I). Free-HA (f-HA) 10 g/L prepared from a 1 % (w/v) sodium hyaluronate solution. (II) HA nanoparticles (n-HA) 2.5 g/L. (III) Mix-HA, composed by a mixture of f-HA and 25 wt. % n-HA to a final concentration of 10 g/L. NaCl 0.9 wt. % was used as a control in the perfusion assays.

2.4. HA Concentration

Measure in the Perfusate

The cetyltrimethylammonium bromide (CTAB) method (Chen and Wang, 2009) was used to ingoing (C_{in}) and outgoing (C_{out}) HA concentration. Briefly, HA aqueous dispersion and CTAB were mixed at 0.5/1 (v/v). After 10 min., the optical density was measured at 400 nm wavelength and recorded. Spectrophotometer was calibrated using blank solution prepared from 0.15 M NaCl and CTAB at same ratio. Analytical grade sodium hyaluronate (HylumedTM) from Genzyme Corporation (Cambridge, MA, USA) was used as a standard.

Measure in the Permeated

The blood of rats was drawn from brachiocephalic vein after a variety of time points and then was centrifuged after the serum separation. Afterwards, HA ELISA-like assay was used to quantify the amount of HA from the serum. The detection range varied from 1.56 - 100 ng/ml and presented sensitivity < 0.94 ng/ml.

For the measurements, samples of serum were initially allowed to clot for 2h at room temperature, then centrifuged for 20 min. at approximately 1000×g. The serum pool was collected and immediately frozen and stored at -20 °C awaiting analysis. Samples of serum and standards were incubated with biotinylated detection antibody in a 96-well microplate that has fixed amount of HA immobilized on the bottom of each well for 45 min. at 37°C. During the reaction, HA in the samples or in the standard competes with a fixed amount of HA on the solid phase supporter for sites on the biotinylated detection antibody specific to HA. Antibodies and sample/standard were washed from the plate, and streptavidin conjugated to horseradish peroxidase (HRP) was added to each microplate well and incubated for 30 min. at 37°C. After wash steps, a HRP substrates tetramethylbenzidine (TMB) was added to each well and incubated for 15 min. at 37°C. The enzyme-substrate reaction was terminated by the addition of a sulphuric acid solution and the absorbance of the samples color was measured at 450 nm wavelength. A standard curve relating absorbance and HA concentration was previously constructed and adjusted to a graphed using a linear regression. A blank containing only the diluent was used to correct for background.

2.5. Molar Mass Distribution

Molar mass (MM) distribution of HA in the ingoing and outgoing perfusate was determined through size exclusion chromatography using a gel filtration column (Polysep-GFC-P6000, 7.8 mm x 300 mm; Phenomenex, Torrance, CA, USA) coupled to a Shimadzu RID-6A refractive index detector (Shimadzu Corporation, Kyoto, Japan). Briefly, 20 μ L of buffered 7.4 aqueous dispersion of HA, was injected using 0.1M NaNO₃ as a mobile phase at 1.0 mL min⁻¹ at 25° C. HA analytical standards (Hyalose, Oklahoma, OK, USA) with MM ranging from 50 to 1000 kDa was correlated with retention time through following equation:

$$\log \text{MM} = 10.9 - (0.62 \times \text{retention time}) \quad \text{Eq. (2)}$$

2.6. Particle Size Distribution

Particle size distribution, zeta potential (ZP) and polydispersity index (Pdl) in the ingoing and outgoing perfusate were measured by dynamic light scattering (DLS) and the data analyzed by photon correlation spectroscopy (PCS). The measurements were performed with a 4mW HeNe Laser (633 nm), in a Autosizer 4700, Zetasizer Nano Series (Malvern, Malvern, U.K.), at a fixed angle of 173° and 25 °C.

The spectra were analyzed in terms of the intensity of scattering (I-distribution $\propto d^6$) for the various size classes and number of particles (N-distribution $\propto d$) to obtain the predominant particle sizes.

2.7. Rheological Characterization

Rheological measurements of macerated of small intestine was carry out at 37°C using an Anton Paar MCR-102 Modular Compact Rheometer. Tests were conducted using a cone-plate geometry (CP50-1) with a 50 mm diameter, a cone angle of 0.9815° and a truncation of 0.97 μ m. Steady-state shear and oscillatory

measurements were performed at shear rates from 0.01 to 1000 s⁻¹ and angular frequency from 0.1 to 600 rad.s⁻¹ respectively, both with the plate at 37°C.

2.8. Animals and Study Design

Anesthesia, surgical and perfusion procedures were justified in detail and were approved by the Animal Ethics Committee of the University of Sorocaba, São Paulo, Brazil (application number 091/2016) following the guidelines described in the Brazilian national laws governing the use of animals in research. *Mus norvegicus albinis* rats (male, 260-280g in weight, aged 8-10 weeks) were kept in a 12h light/dark cycle, at 25 °C, and 50% relative humidity. They come from the same local supplier (Anilab, Paulínia, Brazil), and had the same diet and housing conditions.

Twelve healthy rats were divided into 4 groups randomly with 3 rats in each group. The 4 groups were: (1) a normal saline (NS) control group; (2) a free HA group; (3) a mixed HA group and (4) a nanoparticulate HA group.

Improved In Situ Single-Pass Intestinal Permeability

The improved *in situ* perfusion study was performed using established method (Li et al., 2011), with minor modifications. The rats were fasted overnight (10 h) and water *ad libitum* in pre-operative. Then, rats were previously anesthetized with an intra-peritoneal injection of thiopental sodium (0.05 mg/100g weight body), placed on a table and maintained at 37 °C. The abdomen was opened by a 3–5 cm longitudinal incision along the midline, and the intestines were exposed.

Proximal and distal ends of the small intestines were identified, incised and cannulated using silicone tubing (O.D. 4 mm, I.D. 2 mm) for inlet and outlet perfusion respectively. The entire length of small intestine ranging from 88 cm to 96 cm was used. The intestine was carefully placed back into the peritoneal cavity, and the abdomen was covered with parafilm to prevent peritoneal dehydration and cotton wool

pads to prevent heat loss, leaving the inlet and outlet tubing accessible from the outside. This set up ensures the isolation of the small intestine, and HA aqueous dispersion can be introduced and sampled with the aid of the peristaltic pump and stopcock valves.

Inlet tubing was attached to peristaltic pump (Petro Gas Ausrüstungen, Berlin, Germany). Normal saline solution (37°C) was gently pumped through the inlet tubing until filling the whole intestine, to remove adherent and non-adherent particulates present inside the intestinal lumen. The procedure time was 15 min. until the outlet is clear. Then, at the starting point of each experiment a 17.6-19.2 mL of 37 °C perfusate formulation was infused (5 mL/min) to fill the entire segment. The small intestine was feed at steady state regime with a flow rate varying with the used formulation depending on its viscosity. Free HA have high viscosity (349 mPa. s) and was pumped at a flow rate of 0.5 mL/min. The other two formulations (mixed and nanoparticulate HA) of low viscosity (1.5 and 1.8 mPa. s, respectively) were pumped at a flow rate of 0.2 mL/min.

Collection of blood was done following a pre-established schedule of 6, 30, 60, 90 and 120 min., in continuous perfusion. The samples of blood were manipulated according description in item 2.4.

Net water flux (NWF) was quantified by weight and volume measurements. NWF is the ratio of the volume of perfusion solution in the outgoing perfusate to the volume of perfusion solution in the ingoing perfusate (Li et al, 2011). Achievement of steady state levels of HA in the perfusate volumes was obtained after 60 - 90 min.

At the endpoint of the experiment the intestine was emptied with the air pressure and the rats were euthanized by a single lethal intracardiac dose of anesthetic (thiopental sodium). The length of the intestinal segment was measured and then macerated using digital disperser Ultraturrax (T-25 – IKA Works GmbH & Co. KG) for further rheological measurements. Figure 2 summarize the perfusion procedure used in this study.

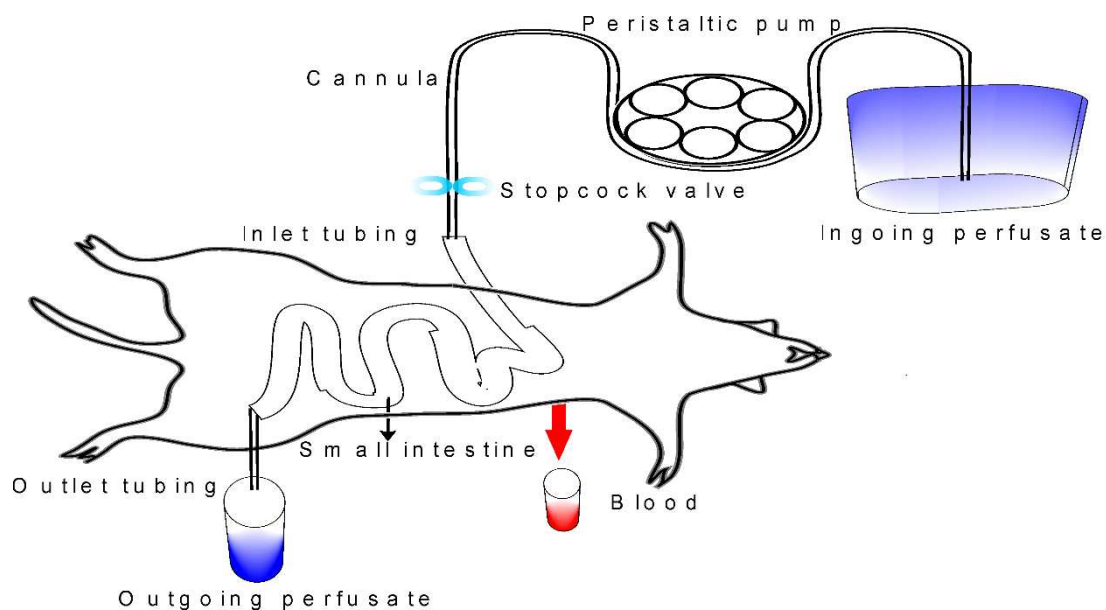


Figure 2. Schematic illustration of improved *in situ* single pass intestinal perfusion (SPIP) method that uses the whole length of the animal intestine.

2.9. Data Analysis and Statistics

Effective permeability coefficient (P_{eff}) of HA structures was calculated using the parallel-tube model (Ahmad et al, 1983), from the steady-state concentrations in the perfusate collected, after correction for NWF.

Permeability values (mm/min) were calculated by Eq. 3:

$$P_{eff} = Q_{in} \times \left[-\ln \frac{(C_{out}/C_{in})}{A} \right] \quad \text{Eq. (3)}$$

Where Q_{in} is the flow rate, C_{in} is the inlet concentration and C_{out} is the outlet concentration of HA, and $A = 2\pi rL$ is the area of the exposed intestinal segment described as a smooth cylinder with a radius r (set to 0.2 cm) (Zakeri-Milani et al, 2005), and a length L , measured after completion of the experiment.

All animal experiments were replicated with $n=3$. The data are expressed as means \pm standard deviation (S.D). Student's T-test was performed between experimental groups and a value of $P < 0.05$ was termed significant.

3. Results and Discussion

3.1. Physicochemical Characterization of Perfusate HA Formulations

Molar Mass Distribution

Table 1 shows molar mass (MM) distribution of f-HA in the classes of 10^6 , 10^5 and 10^4 Da. It could be observed that there were changes in the ingoing and outgoing perfusate as consequence of the permeation of the MM classes. The values indicate 10^5 Da was the best class of permeated MM ($40 \pm 4\%$), followed by 10^4 Da ($20 \pm 1\%$) and 10^6 Da ($6 \pm 0\%$).

Table 1. Molar mass distribution of f-HA formulation

MM class (Da)	Free HA Perfusate		Permeate (%)
	Ingoing (%)	Outgoing (%)	
10^6	16.0 ± 0.0	15 ± 0.0	6 ± 0
10^5	74.0 ± 0.8	46 ± 0.0	40 ± 4
10^4	10.0 ± 0.0	8.1 ± 0.0	20 ± 1

*Permeate (%): calculated by difference between the ingoing and outgoing MM classes.

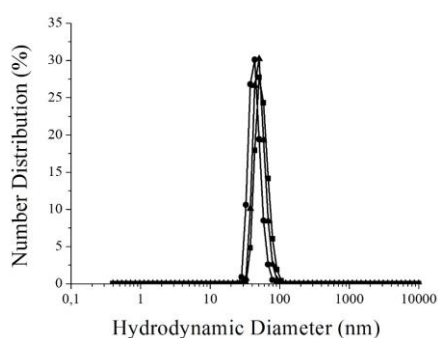
Recovery of HA-ADH Crosslinked Nanoparticles

About $33.6 \pm 2.2 \%$ of HA nanoparticles were recovered in the aqueous dispersion from synthesis of nanoparticulate cross-linked HA (n-HA).

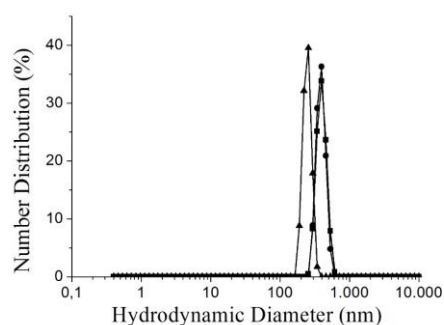
Particle Size Distribution

The size distribution spectra of initial ingoing (left) and outgoing at 2h perfusion time (right) were measured at semi-diluted regime, with the samples diluted

- Crosslinked HA-ADH Nanoparticles

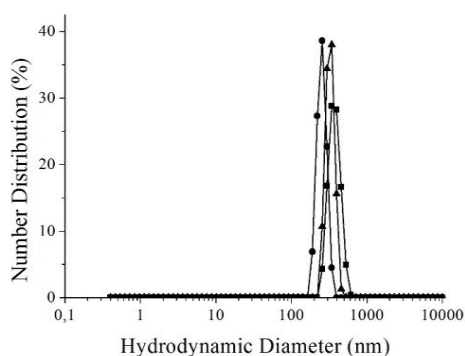


c

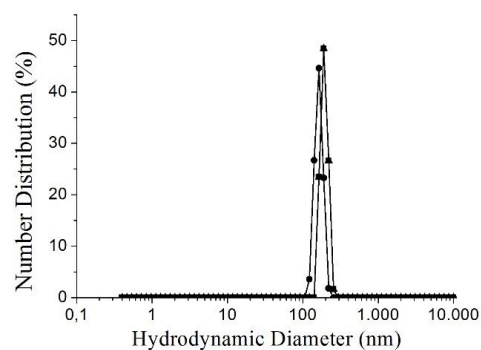


d

- Mix 25 wt.% n-HA



e



f

Figure 3. N- distribution spectra from the ingoing perfusate (left) and outgoing perfusate (right). The measurements of number of distributions were done in three independent samples.

Figure 4 shows variations of (a) zeta potential (ZP) and (b) polydispersity in the ingoing perfusate at zero time and in outgoing perfusate at endpoint time (2h) of perfusion.

Higher ZP (-40.0 ± 6.1 mV) and intermediate ZP (-20.0 ± 0.14 mV) were obtained from initial f-HA and n-HA formulations. Therefore, the HA structuring in nanoparticles reduced zeta potential. At endpoint time, ZP decreased in both formulations confirming the aggregations previously observed in the size distribution spectra (Honary and Zahir, 2013). The polydispersity index (PDI) also was reduced in

outgoing perfusate, in consequence of aggregations. The mix-HA formulation presented little change of ZP (around -5.35 ± 0.92 mV) and Pdl (around 0.80 ± 0.09) after perfusion, indicating that the n-HA filled the voids in the structures of coil coiled globules of f-HA.

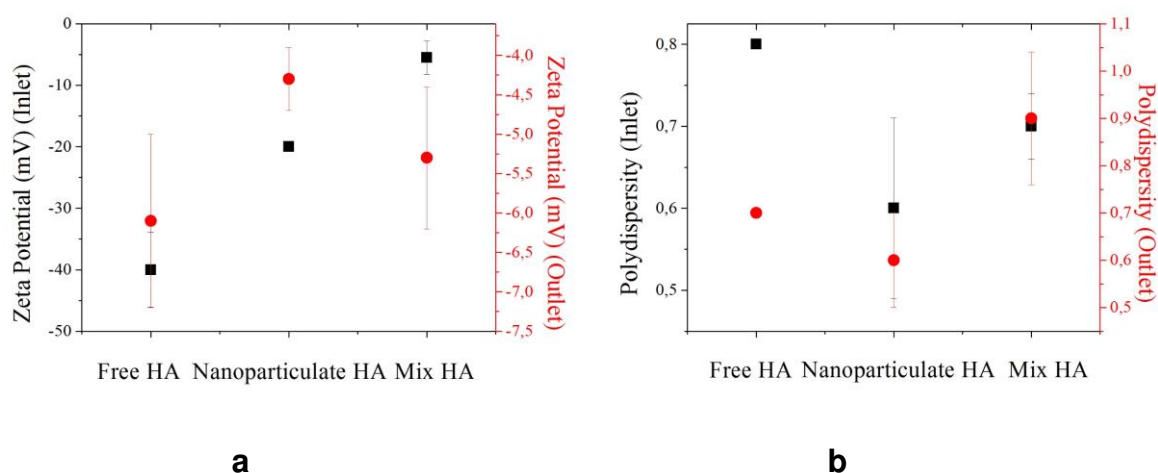


Figure 4. Profiles of (a) zeta potential and (b) polydispersity in the ingoing (■) and outgoing (●) perfusates. Error bars represent the S.D. of $n=3$.

Rheology of Membrane Macerate

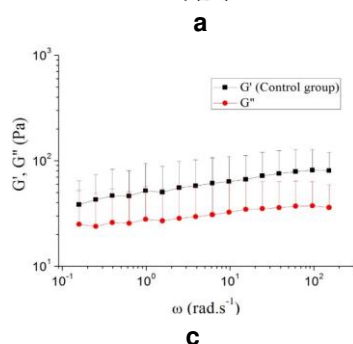
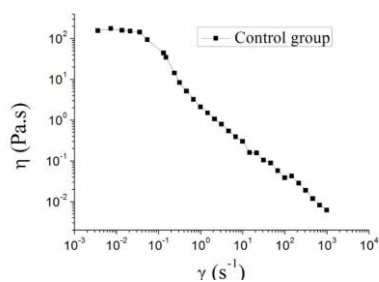
The permeated HA may be retained into the mucus network depending on its structuring and physicochemical properties, such as MM distribution, particle size, zeta potential mainly. Thus, changes in viscosity and in mechanical behavior of the intestinal mucosa macerate indicate the ability of HA formulation to transpose the mucus layer.

Figure 5 (a-d) shows the shear viscosity profiles as well as the viscous and viscoelastic modulus of macerated of small intestine of rats emptied after perfusion. The control group corresponds to the intestine that was perfused with normal saline.

Figure 5a shows the pseudoplastic behavior, shear thinning (shear viscosity decreasing with shear rate), of the intestinal membrane macerate. This macerate also has an elastic gel behavior, com $G' > G''$ and constant in the frequency range studied

(Figure 5c). The profiles of membrane macerate of the small intestine of rats perfused with the HA formulations are shown in Figures 5 (b,d). The presence of HA in the intestinal membrane did not change the pseudoplastic behavior of the shear viscosity at higher shear rates mainly (Figure 5b). The viscoelastic gel behavior was observed for mix-HA, and the highest G' modulus for n-HA. However, the gel behavior of the intestinal membrane was lost with the retention of f-HA formulation (10g/L). Instead, the membrane filled with HA had a fluid behavior with tendency to cross over at high frequencies (Figure 5d). Comparing these results with the MM distribution of f-HA in Table 1, we can infer that part of 10^5 Da fraction preferentially permeated was retained in the intestinal membrane.

Membrane perfused with saline



Membrane perfused with HA formulation

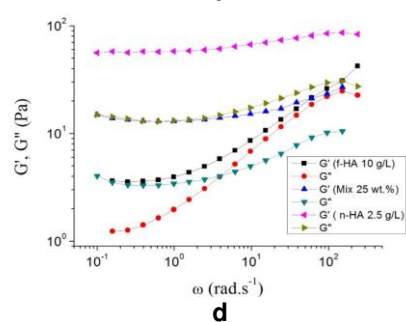
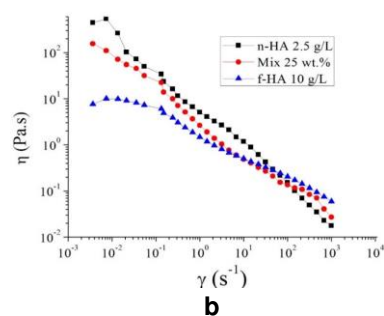


Figure 5. Profiles of shear viscosity and viscous and viscoelastic modulus of macerated of small intestine of rats emptied after perfusion with saline solution (control), and the HA formulations. Error bars represent the S.D. of $n=3$.

The retention of the HA fractions in mucus nanostructure yield anti-microbial protection due to obstruction of its pores (Hansen et al. 2017; Matricardi et., 2013). In addition, f-HA is a source of energy readily metabolized by the microbiota (Di Cerbo et

al., 2013; Koropatkin et al., 2012; Cockburn and Koropatkin, 2016) due to the large density of sites for hyaluronidase action.

3.2. *In Situ* Uptake and HA Absorption

Table 2 shows operating conditions, the permeated mass (%) in the intestinal mucosa of rats after 2h of continuous perfusion and the effective permeability coefficients (P_{eff}) calculated from the ingoing and outgoing concentrations (Eq. 2). These data characterize the HA intestinal uptake from the studied formulations in the small intestine wall of rats.

Table 2. Operating conditions and % mass permeated of HA formulations buffered 7.4 aqueous dispersion in intestinal mucosa of rats.

	HA Formulation		
	Free (10 g/L)	Nanoparticulate (2.5 g/L)	*Mixed (10 g/L)
Viscosity at 37°C (mPa. s)	349	1.8	0.7
Flow rate (mL/min)	0.5	0.2	0.2
Concentration inlet (g/L)	10 ± 0.05	2.5 ± 0.1	10 ± 0.07
Concentration outlet (g/L)	7.9 ± 0.02	0.5 ± 0.01	5.5 ± 0.01
% permeated	21 ± 3	80 ± 5	45 ± 4
P_{eff} (x 10⁻⁵ mm/min)	0.96 ± 0.12 ^a	2.62 ± 0.22 ^b	1.05 ± 0.02 ^a

*Mixture of f-HA with 25 wt. % of n-HA formulation.

Values of P_{eff} are expressed as means ($\cdot 10^{-5}$ mm/min.) ± S.D. ^bFor nanoparticulate HA vs free and mixed groups, $p < 0.05$.

The results show the structuring of HA in the different formulations generated tridimensional architectures that influenced its uptake in the intestinal mucosa of rats. The best uptake, P_{eff} 2.62 x 10⁻⁵ mm/min that correspond to 80 ± 5% permeated mass was obtained with the HA-ADH nanoparticles in n-HA formulation. Besides the stability of the crosslinked nanoparticles, the ability to permeate the

intestinal mucosa is also due to the nanoparticle size (Figure 3) which was in the range of the pore size of the mucin network (20-200nm).

The f-HA and mix-HA formulations were more poorly permeated, with P_{eff} 0.96×10^{-5} mm/min and 1.05×10^{-5} mm/min respectively. Despite non-statistical difference in P_{eff} s, the permeated masses were $21 \pm 3\%$ (f-HA) and $45 \pm 4\%$ (mix-HA), probably due to the differences in viscosity and flow rate (Table 2). From these data, it could be infer that the reduced uptake of the coiled and physically crosslinked structuring of free HA is due to its diffusion mechanism into the mucus controlled by chain interpenetration.

As described in literature, the enterocytes are sealed together by negatively charged tight junctions, forming an intercellular space of nanometer sized. Thus, paracellular transport of macromolecules larger than 250–300 kDa makes only a minor contribution to the overall intestinal permeation (Tavelin et al. 2003; Hisada et al, 2008). The quantitative importance of this route in the uptake of hydrophilic polymers is not fully clear, however its structuring in nanoparticles have been suggested to be largely absorbed (Fagerholm et al. 1999).

In addition, the negative zeta potential of free HA, -40 mV, (Figure 4) limits its passive transcellular diffusion (Devriendt et al, 2012). However, its active transcellular diffusion may be favored for HA nanoparticle structuring, both by its intermediate zeta potential, -20 mV, (Figure 4) and also because the nanoparticles can be substrates to TLR4 intestinal transporter protein in a carrier-mediated uptake of HA larger than 250–300 kDa (Asari et al. 2010; Lennernäs, 2007). Therefore, the n-HA formulation may be diffused by the paracellular and transcellular mechanisms, so benefiting its uptake into the intestinal mucosa.

After uptake, the TLR4 receptor delivery the intact HA to the Peyer's patches, following the lymphoid follicles to the systemic bloodstream (Tyrer et al., 2006). The levels of exogenous HA in the bloodstream cannot exceed the endogenous levels due to the deleterious effect on plasma even for low MM. Studies have shown that removal of exogenous HA from the bloodstream compartment occurs from 2 to 6 min after intravenous administration in rats and residual fractions were degraded in the

lymph nodes and excreted by the kidneys at a three-fold clearance to the urinary (Lebel, 1991).

Figure 6 shows that exogenous HA absorbed is rapidly removed from the bloodstream, never exceeding endogenous levels (normal saline group control). An analysis of bloodstream clearance time allows us to raise interesting questions. The clearance of n-HA occurred in minor time (0.5h). Barua and Mitragotri, (2014) reported that stable and smaller sizes (< 100 nm) from crosslinked HA permeated the vascular endothelium in less time due to higher rates of endocytosis and more rapid lymphatic transport.

Plasmatic clearance of f-HA structures occurred within 1h due to the slowest intestinal uptake, while the clearance of mix-HA started earlier (before 6 min), due to its smaller compositional fraction (25 wt. %) of nanoparticles, ending within 1.5h, due to the presence of f-HA. Concentration of HA in the blood tend to normalize after the period of clearance of exogenous HA, recovering homeostasis within 2h. These results indicate HA structuring plays an important role on transport mechanism in the vascular endothelium.

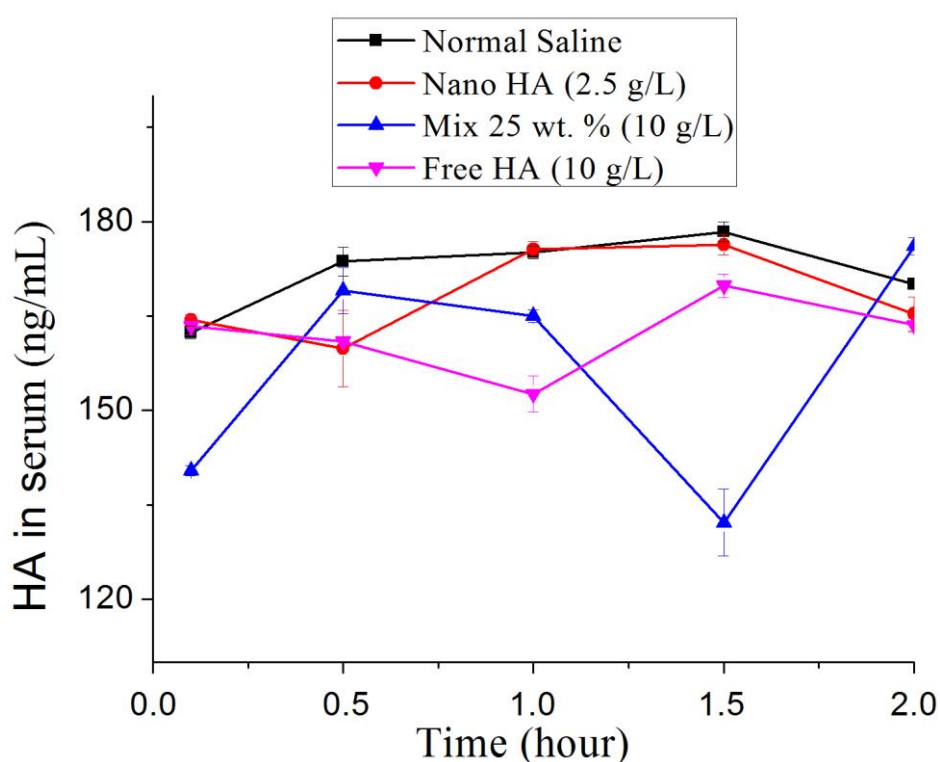


Figure 6. The cumulative exogenous HA in the serum pool during perfusion. Error bars represent the S.D. of $n=3$.

In this context, the nanoparticles present in mix formulation were the first class of particles to reach other tissues. Clearance of HA in the n-HA and f-HA formulations started at the same time, however, the nanoparticles were more readily absorbed to tissues due to rapid intestinal transit. Therefore, f-HA was the slowest formulation to reach other tissues.

Figure 7 summarizes the results obtained from uptake to absorption, bloodstream clearance and transport to other tissues, and classifies the studied HA formulations according to its total clearance time.

Analyzed together, these data point out to promising HA structuring for specific functions in oral formulations, such as: Because high molar mass (10^5 Da) free HA remain for a longer period of time attached to the intestinal mucosa, it is prone to pre-systemic metabolism such as cleavage/disintegration by variations of pH and hydrolysis by microbiota enzymes being promising to formulations for dysbiosis treatment. On the other hand, in order to reach other tissues, the formulations containing chemically crosslinked nanoparticles are better due to its uptake occurs in a shorter time.

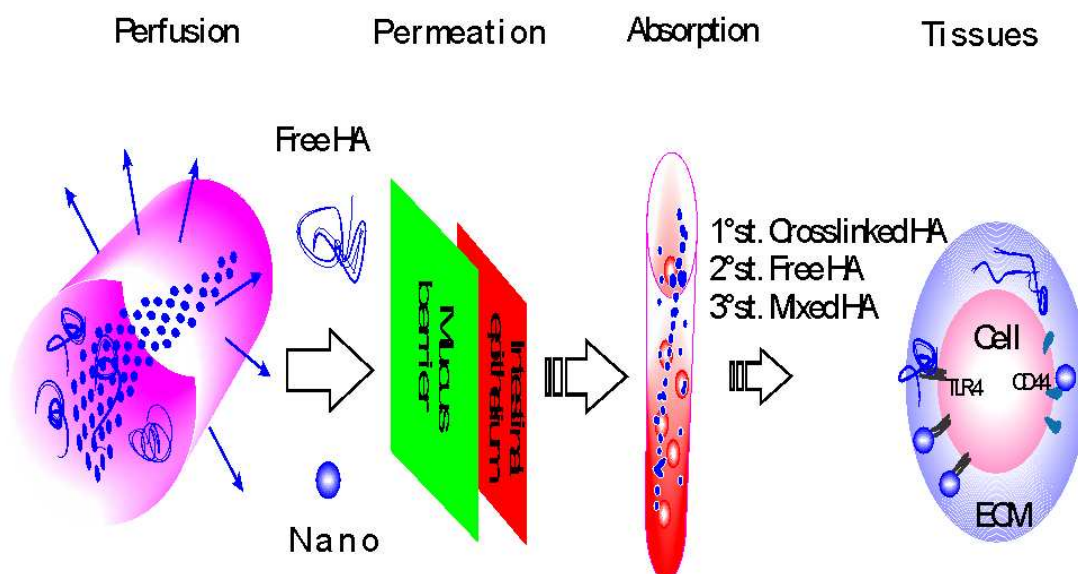


Figure 7. Schematic illustration of the main stages followed by the orally administered HA. The order of the clearance of HA in the blood is also indicated.

Conclusions

An accurate and sensitive assessment of the permeability and absorption of HA was obtained using the whole intestine of rats, in an improved single-pass intestinal perfusion. The HA structuring in the studied formulations was determinant of its transport in the steps of uptake, absorption and bloodstream clearance in the small intestine of rats. The best performance was obtained for the chemically crosslinked nanoparticles, followed by the free HA and the mixed formulation containing 25 wt. % nanoparticles and free HA. The precision and sensibility of the assay as well as the quantitative determinations have become compatible the kinetic behavior of HA intestinal uptake and its presence and clearance in the bloodstream. Finally, these results are relevant because shed light for the project of HA based formulations to oral administration.

Acknowledgements

This study was financed in part by the Coordination for the Improvement of Higher Educational Personnel (CAPES, Brazil), [grant number: 33003017034P8].

References

1. Abe, K., Ito, T. Qualitative and quantitative morphologic study of Peyer's patches of the mouse after neonatal thymectomy and hydrocortisone injection. *Am J Anat.* 1978,151(2):227-37.
2. Ahmad, A.B., Bennett, P.N., Rowland, M. Models of hepatic drug clearance: discrimination between the 'well stirred' and 'parallel-tube' models. *J Pharm Pharmacol.* 1983, 35(4):219-24.
3. Asari, A., Kanemitsu, T., Kurihara, H. Oral administration of high molecularweight hyaluronan (900 kDa) controls immune system via Toll-like receptor 4 in the intestinal epithelium. *J. Biol. Chem.* 2010, 285:24751–8.
4. Atuma, C., Strugala, V., Allen, A., Holm, L. The adherent gastrointestinal mucus gel layer: thickness and physical state in vivo. *Am J Physiol Gastrointest Liver Physiol.* 2001, 280(5):G922-9.
5. Barua, S., Mitragotri, S. Challenges associated with Penetration of Nanoparticles across Cell and Tissue Barriers: A Review of Current Status and Future Prospects. *Nano Today.* 2014, 9(2):223-243.
6. Berenbaum, F. Osteoarthritis as an inflammatory disease (osteoarthritis is not osteoarthrosis!). *Osteoarthritis Cartilage.* 2013, 21(1):16-21.
7. Bicudo, R.C., Santana, M.H. Effects of Organic Solvents on Hyaluronic Acid Nanoparticles Obtained by Precipitation and Chemical Crosslinking. *J Nanosci Nanotechnol.* 2012, 12(3):2849-57.
8. Bowers, W.H. Lubrication of human joints. Ch 18 in *The Musculoskeletal System. Basic Processes and Disorders*, 2nd ed., Wilson FC, Ed., JB Lippincott Company, Philadelphia. 1983, 225-230.
9. CDER/FDA, 2015. Guidance for industry: Waiver of in vivo bioavailability and bioequivalence studies for immediate release dosage forms based on a biopharmaceutical classification system. Center for Drug Evaluation and Research.
10. Chen, Y. H., Wang, Q. Establishment of CTAB Turbidimetric method to determine hyaluronic acid content in fermentation broth. *Carbohydr. Polym., Elsevier Ltd.* 2009, 78, 178–181.

11. Cockburn, D. W., Koropatkin, N. M. Polysaccharide Degradation by the Intestinal Microbiota and Its Influence on Human Health and Disease. *J. Mol. Biol.* pii: 2016, S0022-2836(16)30243-1.
12. de la Motte, C.A. Hyaluronan in intestinal homeostasis and inflammation: implications for fibrosis. *Am. J. Physiol. Gastrointest. Liver Physiol.* 2011, 301(6):G945-9.
13. Devriendt, B., De Geest, B.G., Goddeeris, B.M., Cox, E. Crossing the barrier: Targeting epithelial receptors for enhanced oral vaccine delivery. *J Control Release.* 2012, 160(3):431-9.
14. Di Cerbo, A., Aponte, M., Esposito, R., Bondi, M., Palmieri, B. Comparison of the effects of hyaluronidase and hyaluronic acid on probiotics growth. *BMC Microbiol.* 2013, 13: 243.
15. Fagerholm, U., Nilsson, D., Knutson, L., Lennernas, H. Jejunal permeability in humans in vivo and rats in situ: Investigation of molecular size selectivity and solvent drag. *Acta Physiologica Scandinavica.* 1999, 165:315-324.
16. Fukuda, K., Takayama, M., Ueno, M., Oh, M., Asada, S., Kumano, F., Tanaka, S. Hyaluronic acid inhibits interleukin-1-induced superoxide anion in bovine chondrocytes. *Inflamm. Res.* 1997, 46(3):114-7.
17. Grand View Research, Inc. 2016. Acessado < <https://www.grandviewresearch.com/>> em 18/02/19.
18. Han, X., Wang, Z., Wang, M., Li, J., Xu, Y., He, R., Guan, H., Yue, Z., Gong, M. Liver-targeting self-assembled hyaluronic acid-glycyrrhetic acid micelles enhance hepato-protective effect of silybin after oral administration. *Drug Deliv.* 2016, 23(5):1818-29.
19. Hansen, I. M., Ebbesen, M. F., Kaspersen, L., Thomsen, T., Bienk, K., Cai, Y., Malle, B. M., Howard, K. A. Hyaluronic Acid Molar Weight-Dependent Modulation of Mucin Nanostructure for Potential Mucosal Therapeutic Applications. *Mol Pharm.* 2017, 14(7):2359-2367.
20. Haserodt, S., Aytekin, M., Dweik, R.A. A comparison of the sensitivity, specificity, and molecular weight accuracy of three different commercially available Hyaluronan ELISA-like assays. *Glycobiology.* 2011, 21(2):175-83.
21. Hisada, N., Satsu, H., Mori, A., Totsuka, M., Kamei, J-I., Nozawa, T., Shimizu, M. Low-Molecular-Weight Hyaluronan Permeates through Human Intestinal Caco-2

- Cell Monolayers via the Paracellular Pathway. *Biosci. Biotechnol. Biochem.* 2008, 72 (4), 1111–1114.
22. Honary, S., Zahir, F. Effect of Zeta Potential on the Properties of Nano-Drug Delivery Systems - A Review (Part 2). *Tropical Journal of Pharmaceutical Research.* 2013, 12 (2): 265-273.
23. Hu, Z., Xia, X., Tang, L. 2006. Process for Synthesizing Oil and Surfactant-Free Hyaluronic Acid Nanoparticles and Microparticles. US Patent 20060040892A1. Available at <<http://www.freepatentsonline.com/20060040892.pdf>> (Accessed 09 November 2018).
24. Kawada, C., Yoshida, T., Yoshida, H., Matsuoka, R., Sakamoto, W., Odanaka, W., Sato, T., Yamasaki, T., Kanemitsu, T., Masuda, Y., Urushibata, O. Ingested hyaluronan moisturizes dry skin. *Nutr. J.* 2014, 13:70.
25. Kim, T. H., Paik, S. H., Chi, Y. H., Bulitta, J. B., Lee, D. Y., Lim, J. Y., Chung, S. E., Song, C. H., Jeong, H. M., Shin, S., Shin, B. S. Regional Absorption of Fimasartan in the Gastrointestinal Tract by an Improved in situ Absorption Method in Rats. *Pharmaceutics.* 2018,10(4). pii: E174.
26. Koropatkin, N. M., Cameron, E. A., Martens, E. C. How glycan metabolism shapes the human gut microbiota. *Nat. Rev. Microbiol.* 2012, 10:323– 335.
27. Lebel, L. Clearance of hyaluronan from the circulation. *Advanced Drug Delivery Reviews,* 1991, 7, 221–235.
28. Lennernäs, H. Human in vivo regional intestinal permeability: importance for pharmaceutical drug development. *Mol. Pharm.* 2014, 11, 12–23.
29. Lennernäs, H. Intestinal permeability and its relevance for absorption and elimination. *Xenobiotica.* 2007, 37(10-11):1015-51.
30. Li, M., Si, L., Pan, H., Rabba, A.K., Yan, F., Qiu, J., Li, G. Excipients enhance intestinal absorption of ganciclovir by P-gp inhibition: assessed in vitro by everted gut sac and in situ by improved intestinal perfusion. *Int. J. Pharm.* 2011, 403(1-2):37-45.
31. Lozoya-Agullo, I., Zur, M., Wolk, O., Beig, A., González-Álvarez, I., González-Álvarez, M., Merino-Sanjuán, M., Bermejo, M., Dahan, A. In-situ intestinal rat perfusions for human Fabs prediction and BCS permeability class determination: Investigation of the single-pass vs. the Doluisio experimental approaches. *Int. J. Pharm.* 2015, 480(1-2):1-7.

32. Martinez-Puig, D., Möller, I., Fernández, C., Chetrit, C. Efficacy of oral administration of yoghurt supplemented with a preparation containing hyaluronic acid (Mobilee™) in adults with mild joint discomfort: a randomized, double-blind, placebo controlled intervention study. *Mediterr. J. Nutr. Metab.* 2013, 6:63–8.
33. Matricardi, P., Di Meo, C., Coviello, T., Hennink, W.E., Alhaique, F. Interpenetrating Polymer Networks polysaccharide hydrogels for drug delivery and tissue engineering. *Adv. Drug Deliv. Rev.* 2013, 65(9):1172-87.
34. Necas, J., Bartosikova, L., Brauner, P., Kolar, J. Hyaluronic acid (hyaluronan): a review. *Veterinarni Medicina.* 2008, 53(8): 397–411.
35. Oe, M., Tashiro, T., Yoshida, H., Nishiyama, H., Masuda, Y., Maruyama, K., Koikeda, T., Maruya, R., Fukui, N. Oral hyaluronan relieves knee pain: a Review. *Nutrition Journal.* 2016, 15:11.
36. Rabba, A. K., Si, L., Xue, K., Li, M., Li, G. In Situ intestinal perfusion of irinotecan: application to P-gp mediated drug interaction and introduction of an improved HPLC assay. *J. Pharm. Pharm. Sci.* 2011, 14(2):138-47.
37. Round, A. N., Rigby, N. M., Garcia de la Torre, A., Macierzanka, A., Mills, E. M. C., Mackie, A. R. Lamellar structures of MUC2-rich mucin: a potential role in governing the barrier and lubricating functions of intestinal mucus. *Biomacromolecules.* 2012, 13:3253.
38. Sardi, B. 2004. How to live 100 years without growing old Hyaluronic Acid: Natures Healing Agent. Here and Now Books, 236p.
39. Schultz, R.H., Wollen, T.H., Greene, N.D., Brown, K.K., Mozier, J.O. 1989. Remote administration of hyaluronic acid to mammals. US 4,808,576.
40. Tavelin, S., Hashimoto, K., Malkinson, J., Lazorova, L., Toth, I., Artursson, P. A new principle for tight junction modulation based on occludin peptides. *Molecular Pharmacology.* 2003, 64:1530–1540.
41. Toole, B.P. Hyaluronan: from extracellular glue to pericellular cue. *Nat Rev Cancer.* 2004, 4(7):528-539.
42. Tyrer, P., Foxwell, A. R., Cripps, A. W., Apicella, M. A., Kyd, J. M. Microbial pattern recognition receptors mediate M-cell uptake of a gram-negative bacterium. *Infect Immun.* 2006, 74(1):625-31.
43. Zakeri-Milani, P., Barzegar-Jalali, M., Tajerzadeh, H., Azarmi, Y., Valizadeh, H. Simultaneous determination of naproxen, ketoprofen and phenol red in samples from

rat intestinal permeability: HPLC method development and validation. *J. Pharm. and Biom. Anal.* 2005, 39 624–630.

44. Zakeri-Milani, P., Valizadeh, H., Tajerzadeh, H., Azarmi, Y., Islambolchilar, Z., Barzegar, S., Barzegar-Jalali, M. Predicting human intestinal permeability using single-pass intestinal perfusion in rat. *J. Pharm. Pharm. Sci.* 2007, 10(3):368-79.

CAPÍTULO 4:
CONCLUSÕES E
SUGESTÕES PARA TRABALHOS FUTUROS

4 CONCLUSÕES E SUGESTÕES PARA PRÓXIMOS TRABALHOS

4.1. Conclusão geral

O transporte intestinal do AH é estrutura-dependente e as estruturas de AH mais adequadas para a preparação de formulações orais são as de AH livre com fração de MM intermediária (10^5 Da) predominante, ou de AH em nanopartículas para mais rápido trânsito sobre o epitélio intestinal e *clearance* sanguíneo.

4.2. Conclusões específicas

Neste trabalho foram preparadas e caracterizadas com sucesso 3 formulações de AH livre, de baixa, intermediária e alta fração de massa molar (MM) 10^4 , 10^5 e 10^6 Da, que compuseram as formulações L-MM, I-MM e H-MM respectivamente. Adicionalmente, estruturas reticuladas de AH compuseram uma formulação nanoparticulada e a combinação de I-MM com nanopartículas compuseram a formulação mista.

A caracterização das estruturas foi imprescindível para o entendimento fenomenológico da mucoadesão e de captação intestinal.

Nanopartículas e AH livre penetraram o muco por diferentes mecanismos. Partículas de diâmetro inferior ao poro de corte da rede mucina (< 200 nm) se beneficiaram da incorporação através dos poros, enquanto estruturas livres se beneficiaram das interações adesivas interpenetrantes das suas cadeias.

A combinação de estruturas livres e nanoparticuladas na formulação mista promoveu um efeito sinérgico sobre o trabalho de adesão porque combinou os dois fenômenos adsortivos (incorporação de nanopartículas com a interpenetração de cadeias de estruturas livres).

A perfusão intestinal mostrou que diferentes estruturas de AH permeiam a membrana intestinal a diferentes taxas (coeficientes de permeabilidade), modificando também o seu tempo total de *clearance* no sangue. O comportamento de permeabilidade foi compatível com o modelo qualitativo de adesão proposto.

4.3. Trabalhos Futuros

Determinar a mais adequada forma de administração do AH: suspensão em meio líquido, revestimento em cápsulas ou comprimido gastro-resistente.

Estudar os efeitos de variações de pH pré-prandial, durante a alimentação e pós-prandial sobre as estruturas de AH. Determinar o efeito de mudanças estruturais sobre a captação intestinal e sobre o tempo de *clearance* sanguíneo.

Estudar a dinâmica molecular interacional AH/receptores (TLR4 e CD44) sob a influência do ambiente intestinal e dimensionar os tamanhos de partículas ótimos para a interação. Caracterizar as vias de sinalização resultantes da interação molecular com estruturas otimizadas.

5 REFERÊNCIAS BIBLIOGRÁFICAS

1. Alberts, B., Johnson, A., Lewis, J., Morgan, D., Raff, M., Roberts, K., Walter, P. Molecular Biology of the Cell 6th Edition. November 18, 1464p. 2014.
2. Akasaka, H. S. S., Setu, M., Yanagi, M., Fukushima, S., Mitusui, T. J. Industrial production of hyaluronic acid by *Streptococcus zooepidemicus* [in Japanese]. Soc. Cosmet. Chem. Jpn. 22:35-42. 1988.
3. Asari, A., Kanemitsu, T., Kurihara, H. Oral administration of high molecular weight hyaluronan (900 kDa) controls immune system via Toll-like receptor 4 in the intestinal epithelium. J. Biol. Chem. 285:24751–8. 2010.
4. Balazs, E. A., Band, P. A. Therapeutic Use of Hyaluronan-Based Products. Carbohydrate Chemistry, Biology and Medical Applications. Pages 311-332. 2008.
5. Balazs, E. A., Denlinger, J. L. Clinical uses of hyaluronan. Ciba Found. Symp.143, 265–280. 1989.
6. Balogh, L., Polyak, A., Mathe, D., Kiraly, R., Thuroczy, J., Terez, M., Janoki, G., Ting, Y., Bucci, L. R., Schauss, A. G. Absorption, Uptake and Tissue Affinity of High-Molar-Weight Hyaluronan after Oral Administration in Rats and Dogs. J. Agric. Food Chem. 56, 10582–10593. 2008.
7. Barbucci, R., Lamponi, S., Borzacchiello, A., Ambrosio, L., Fini, M., Torricelli, P., Giardino, R. Hyaluronic acid hydrogel in the treatment of osteoarthritis. Biomaterials. 23, 4503–4513. 2002.
8. Barthe, L., Woodley, J., Houin, G. Gastrointestinal absorption of drugs: methods and studies. Fundam Clin Pharmacol. 13(2):154-68. 1999.
9. Benedini, L. J., Santana, M. H. A. Effects of soy peptone on the noculum preparation of *Streptococcus zooepidemicus* for production of hyaluronic acid. Bioresource Technol. 130, 798–800. 2013.
10. Boas, N. F. Isolation of hyaluronic acid from the cock's comb. J Biol. Chem. 181(2):573-5. 1949.
11. Bucci, L.R., Turpin, A.A. Will the real hyaluronan please stand up? Journal of applied nutrition. volume 54, number 1. 2004.
12. Canut, L., Zapatero, J., López, S., Torrent, A., Ruhí, R., Vicente, L. Genotoxicity, acute and subchronic toxicity studies in rats of a rooster comb extract rich in

- sodium hyaluronate. *Regulatory Toxicology and Pharmacology* 62, 532–541. 2012.
13. Cario, E., Podolsky, D. K. Differential Alteration in Intestinal Epithelial Cell Expression of Toll-Like Receptor 3 (TLR3) and TLR4 in Inflammatory Bowel Disease. *Infect. Immun.* 68(12):7010-7. 2000.
 14. Chong, B. F., Nielsen, L. K. Amplifying the cellular reduction potential of *Streptococcus zooepidemicus*. *Journal of Biotechnology*. v. 100, p. 33-41. 2003.
 15. Clark, K. L., Sebastianelli, W., Flechsenhar, K. R., Aukermann, D. F., Meza, F., Millard, R. L., Deitch, J. R., Sherbondy, P. S, Albert, A. 24 Week study on the use of collagen hydrolysate as a dietary supplement in athletes with activity-related joint pain. *Curr. Med. Res. Opin.* 24(5):1485-96. 2008.
 16. Dahiya, P., Kamal, R. Hyaluronic Acid: A Boon in Periodontal Therapy. *N Am J Med Sci.* 5(5): 309–315. 2013.
 17. de Goffau, M. C., Luopajarvi, K., Knip, M., Ilonen, J., Ruohtula, T., Härkönen, T., Orivuori, L., Hakala, S., Welling, G. W., Harmsen, H. J., Vaarala, O. Fecal microbiota composition differs between children with b-cell autoimmunity and those without. *Diabetes.* 62:1238–1244. 2013.
 18. de la Motte, C. A. Hyaluronan in intestinal homeostasis and inflammation: implications for fibrosis. *Am. J. Physiol. Gastrointest. Liver Physiol.* 301(6):G945-9. 2011.
 19. de la Motte, C. A., Kessler, S. P. 2015. The Role of Hyaluronan in Innate Defense Responses of the Intestine. *International Journal of Cell Biology*, ID 481301, 5p.
 20. Di Cerbo, A., Aponte, M., Esposito, R., Bondi, M., Palmieri, B. Comparison of the effects of hyaluronidase and hyaluronic acid on probiotics growth. *BMC Microbiol.* 13: 243. 2013.
 21. Fuji Keizai Co. Ltd., 2014. Acessado <<https://www.group.fuji-keizai.co.jp/en/>> em 21/02/19.
 22. Fukuda, K., Takayama, M., Ueno, M., Oh, M., Asada, S., Kumano, F., Tanaka, S. Hyaluronic acid inhibits interleukin-1-induced superoxide anion in bovine chondrocytes. *Inflamm. Res.* 46(3):114-7. 1997.

23. Gareau, M. G., Sherman, P. M., Walker, W. A. Probiotics and the gut microbiota in intestinal health and disease. *Nat. Rev. Gastroenterol. Hepatol.* 7(9):503-14. 2010.
24. Gerdin, B., Hallgren, R. Localisation of hyaluronan in the human intestinal wall. *Gut.* 32 (7): 760–762. 2016.
25. Hällgren, R., Gerdin, B., Tengblad, A., Tufveson, G. Accumulation of hyaluronan (hyaluronic acid) in myocardial interstitial tissue parallels development of transplantation edema in heart allografts in rats. *J. Clin. Invest.* 85(3):668-73. 1990.
26. Hascall, V. C., Laurent, T. C., Yanagishita, M. 1997. Hyaluronan: structure and physical properties In: *Hyaluronan Today*. <http://glycoforumgrip>.
27. Heenan, C., Adams, M., Hosken, R., Fleet, G. Growth medium for culturing probiotic bacteria for applications in vegetarian food products. *Food Sci Technol-Leb.* 35(2):171-176. 2002.
28. Jensen, G. S., Attridge, V. L., Lenninger, M. R., Benson, K. F. Oral Intake of a Liquid High-Molecular-Weight Hyaluronan Associated with Relief of Chronic Pain and Reduced Use of Pain Medication: Results of a Randomized, Placebo-Controlled Double-Blind Pilot Study, *Journal of Medicinal Food* 18 (1) 95–101. 2015.
29. Jones, D. S., Woolfson, A. D., Djokic, J., Coulter, W. A. Development and mechanical characterisation of bioadhesive semi-solid polymeric systems containing tetracycline for the treatment of periodontal diseases. *Pharm. Res.* 13 1732–1736. 1996.
30. Kalman, D. S., Heimer, M., Valdeon, A., Schwartz, H., Sheldon, E. Effect of a natural extract of chicken combs with a high content of hyaluronic acid (Hyal-Joint®) on pain relief and quality of life in subjects with knee osteoarthritis: a pilot randomized double-blind placebo-controlled trial. *Nutr. J.* 7. 2008.
31. Kawada, C., Yoshida, T., Yoshida, H., Matsuoka, R., Sakamoto, W., Odanaka, W., Sato, T., Yamasaki, T., Kanemitsu, T., Masuda, Y., Urushibata, O. Ingested AH moisturizes dry skin. *Nutr. J.* 13:70. 2014.
32. Keely, S., Talley, N. J., Hansbro, P. M. Pulmonary-intestinal cross-talk in mucosal inflammatory disease. *Mucosal Immunol.* 5(1):7-18. 2012.

33. Kogan, G., Soltés, L., Stern, R., Gemeiner, P. Hyaluronic acid: a natural biopolymer with a broad range of biomedical and industrial applications. *Biotechnol. Lett.* 29(1):17-25. 2007.
34. Koropatkin, N. M., Cameron, E. A., Martens, E. C. How glycan metabolism shapes the human gut microbiota. *Nat. Rev. Microbiol.* 10:323–335. 2012.
35. Ley, R. E., Turnbaugh, P. J., Klein, S., Gordon, J. I. Microbial ecology: human gut microbes associated with obesity. *Nature.* 444(7122):1022-3. 2006.
36. Li, X., Wang, C., Nie, J., Lv, D., Wang, T., Xu, Y. Toll-like receptor 4 increases intestinal permeability through up-regulation of membrane PKC activity in alcoholic steatohepatitis. *Alcohol.* 47(6):459-65. 2013.
37. Liu, J., Xing, J., Chang, T., Ma, Z., Liu, H. Optimization of nutritional conditions for nattokinase production by *Bacillus natto* NLSSE using statistical experimental methods. *Process Biochem.* 40(8) 2757-2762. 2005.
38. Martinez-Puig, D., Möller, I., Fernández, C., Chetrit, C. Efficacy of oral administration of yoghurt supplemented with a preparation containing hyaluronic acid (Mobilee™) in adults with mild joint discomfort: a randomized, double-blind, placebo controlled intervention study. *Mediterr. J. Nutr. Metab.* 6:63–8. 2013.
39. Meyer, K., Palmer, J. W. On glycoproteins II. The polysaccharides of vitreous humor and of umbilical cord. *J. Bio. Chem.*, 114, 689. 1936.
40. Meyer, K., Palmer, J. W. The polysaccharide of the vitreous humor. *Journal of Biological Chemistry*, 107, 629-634. 1934.
41. Möller, I., Martinez-Puig, D., Chetrit, C. Oral administration of Hyal-Joint for the treatment of knee OA with synovial effusion. *Clin. Nutr. Suppl.* 4, 171–172. 2009.
42. Moreland, L. W. Intra-articular hyaluronan (hyaluronic acid) and hylans for the treatment of osteoarthritis: mechanisms of action. *Arthritis Res. Ther.* 5(2):54-67. 2003.
43. Moriña, D., Solà, R., Valls, R. M., López de Frutos, V., Montero, M., Giralt, M., et al. Efficacy of a Low-fat Yogurt Supplemented with a Rooster Comb Extract on Joint Function in Mild Knee Pain Patients: A Subject-level Meta-analysis. *Ann. Nutr. Metab.* 63:1386. 2013.

44. Nagaoka, I., Nabeshima, K., Murakami, S., Yamamoto, T., Watanabe, K., Tomonaga A. et al. Evaluation of the effects of a supplementary diet containing chicken comb extract on symptoms and cartilage metabolism in patients with knee osteoarthritis. *Exp. Ther. Med.* 1:817–27. 2010.
45. Neo, H., Ishimaru, J. I., Kurita, K., Goss, A. N. The effect of hyaluronic acid on experimental temporomandibular joint osteoarthrosis in the sheep. *J. Oral Maxillofac. Surg.* 55(10):1114-9. 1997.
46. Oe, M., Tashiro, T., Yoshida, H., Nishiyama, H., Masuda, Y., Maruyama, K., Koikeda, T., Maruya, R., Fukui, N. Oral hyaluronan relieves knee pain: a Review. *Nutrition Journal*, 15:11. 2016.
47. Oliveira, R. C., Santana, M. H. A. Estudo da produção de ácido hialurônico utilizando peptonas de soja. São Paulo. Faculdade de Engenharia Química. Universidade Estadual de Campinas, 2014. 88 p. Dissertação (Mestrado).
48. O'Neill, L. A. Therapeutic targeting of Toll-like receptors for inflammatory and infectious diseases. *Curr. Opin. Pharmacol.* 3(4):396-403. 2003.
49. Patel, H., Mackintosh, D., Ayling, R., Nicholhas, R., Fielder, M. A. A novel medium devoid of ruminant peptone for high yield growth of *Mycoplasma ovipneumoniae*. *Vet Microbiol.* 127(3) 309-314. 2008.
50. Pinnix, C., Perkins, G. H., Strom, E. A, Tereffe, W., Woodward, W., Oh, J. L., Arriaga, L., Munsell, M. F., Kelly, P., Hoffman, K. E., Smith, B. D., Buchholz, T. A., Yu, T. K. Topical hyaluronic acid vs. standard of care for the prevention of radiation dermatitis after adjuvant radiotherapy for breast cancer: single-blind randomized phase III clinical trial. *Int. J. Radiat. Oncol. Biol. Phys.* 83(4):1089-94. 2012.
51. Pires, A. M. B., Santana, M. H. A. Metabolic effects of the initial glucose concentration on microbial production of hyaluronic acid. *Appl Biochem Biotech.* 162(6): 1751–1761. 2010.
52. Price, R. D., Berry, M. G., Navsaria, H. A. Hyaluronic acid: the scientific and clinical evidence. *Journal of Plastic, Reconstructive & Aesthetic Surgery* 60, 1110 e 1119. 2007.
53. Riehl, T. E., Ee, X., Stenson, W. F. Hyaluronic acid regulates normal intestinal and colonic growth in mice. *Am. J. Physiol. Gastrointest. Liver Physiol.* 303(3): G377–G388. 2012.

54. Santosh, Y, Dharmendra, J., Nataraj, V., Velankar, H., Kapat, A., Rangaswamy, V. Process for purification of high molecular weight hyaluronic acid. EP 2216412 B1. 2007.
55. Sardi, B. How to live 100 years without growing old Hyaluronic Acid: Nature's Healing Agent. Here and Now Books, 2004, 236p.
56. Sardi, B. Yuzurihara Reveals Its Secret: Hyaluronic Acid, The Molecule of Youth. HA UPDATE REPORT. Ed. 3, Vol. 2. 2007.
57. Sato, T., Iwaso, H. An Effectiveness study of hyaluronic acid Hyabest® (J) in the treatment of osteoarthritis of the knee on the patients in the United State. J New Rem.& Clin. 58:551–8. 2009.
58. Schultz, R. H., Wollen, T. H., Greene, N. D., Brown, K. K., Mozier, J. O. Remote administration of hyaluronic acid to mammals. US 4,808,576. 1989.
59. Schwartz, S. R., Park, J. Ingestion of BioCell Collagen®(®), a novel hydrolyzed chicken sternal cartilage extract; enhanced blood microcirculation and reduced facial aging signs. Clin Interv Aging. 7:267-73. 2012.
60. Smith, M. I., Yatsunencko, T., Manary, M. J., Trehan, I., Mkakosya, R., Cheng, J., Kau, A. L., Rich, S. S., Concannon, P., Mychaleckyj, J. C., Liu, J., Houpt, E., Li, J. V., Holmes, E., Nicholson, J., Knights, D., Ursell, L.K., Knight, R., Gordon, J. I. Gut microbiomes of Malawian twin pairs discordant for kwashiorkor. Science. 339:548–554. 2013.
61. Smith, M. M., Ghosh, P. The synthesis of hyaluronic acid by human synovial fibroblasts is influenced by the nature of the hyaluronate in the extracellular environment. Rheumatol. Int. 7(3):113-22. 1987.
62. Sousa, A. S., Guimarães, A.P., Gonçalves, C. V., Silva JR., I. J., Cavalcante JR, C. L., Azevedo, D. C. S. Purification and Characterization of Microbial Hyaluronic Acid by Solvent Precipitation and Size-Exclusion Chromatography. Separation Science and Technology, 44(4): 906-923. 2009.
63. Tashiro, T., Seino, S., Sato, T., Matsuoka, R., Masuda, Y., Fukui, N. Oral administration of polymer hyaluronic acid alleviates symptoms of knee osteoarthritis: a double-blind, placebo-controlled study over a 12-month period. Sci. World. 2012:167928. 2012.
64. Versantvoort, C. H. M., Rompelberg, C. J. M., Sips, A. J. A. M. Methodologies to study human intestinal absorption. A review. Research for man and

- environment. National Institute of Public Health and The Environment. RIVM report 630030 001, 1-55. 2000.
65. Yoshimura, M., Aoba, Y., Watari, T., Momomura, R., Watanabe, K., Tomonaga A, et al. Evaluation of the effect of a chicken comb extract-containing supplement on cartilage and bone metabolism in athletes. *Exp. Ther. Med.* 4:577–80. 2012.
66. Zheng, L., Riehl, T., Stenson, W. F. Regulation of Colonic Epithelial Repair in Mice by Toll-like Receptors and Hyaluronic Acid. *Gastroenterology.* 137(6): 2041–2051. 2009.

APÊNDICE

Definição de alguns termos usados nas áreas médicas e biológicas

- Homeostasia: Condição de estabilidade das funções desenvolvidas por determinado órgão para o equilíbrio do organismo.
- Disbiose: Estado de desequilíbrio populacional da flora microbiana intestinal em humanos.
- Prandial: Relativo à alimentação.
- Lamina propria: Epitélio de revestimento localizado entre as células epiteliais e o tecido conjuntivo constituído por colágeno do tipo IV, laminina, entactina e proteoglicanos.
- Fastidioso: Bactérias com elevados requerimentos nutricionais contendo nitrogênio, glicose e vitaminas, específicos para o seu desenvolvimento.

ANEXO I

Neste anexo é apresentado o parecer da Comissão de Ética em Uso de Animais (CEUA) da Universidade de Sorocaba (protocolo 091/2016).

UNIVERSIDADE DE SOROCABA
COMISSÃO DE ÉTICA NO USO DE ANIMAIS
CEUA-UNISO
PARECER

Protocolo nº 091/2016
Interessado (a): Marco Vinícius Chaud
Orientador (a): Marco Vinícius Chaud
Título do Projeto: Avaliação do trânsito transmural de hialuronato de sódio via TLR2 r TLR4 (Toll-Like Receptors) usando modelo animal
Título do Experimento: o mesmo

Apresentado à Comissão de Ética no Uso de Animais - CEUA para análise, segundo a Lei No. 11.794, de 8 de outubro de 2008, que regulamenta o inciso VII do parágrafo 1º do artigo 225 da Constituição Federal, foi considerado:

APROVADO.

APROVADO com RECOMENDAÇÃO, devendo o proponente encaminhar as modificações sugeridas em anexo para complementação do protocolo;

COM PENDÊNCIA, devendo o proponente readequar os itens do protocolo;

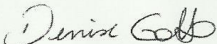
REPROVADO

Manifestação do Parecerista:

Diligências respondidas.

Nome: Denise Grotto

Coordenador da CEUA-Uniso

Assinatura: 

Data: 16/11/2016

* Encaminhar cópia deste parecer para o e-mail ceua@uniso.br e original assinado para a Seção Técnica Acadêmica

ANEXO II

Boletim técnico do hialuronato de sódio do fabricante Euflexxa.

Euflexxa®

Laboratórios Ferring

hialuronato de sódio

IDENTIFICAÇÃO DO MEDICAMENTO

Euflexxa®

hialuronato de sódio

APRESENTAÇÕES

Solução injetável de 10 mg/mL de hialuronato de sódio, disponível em embalagens contendo 1 ou 3 seringas preenchidas, embaladas individualmente em blister, com 2 mL cada.

VIA INTRA-ARTICULAR

USO ADULTO

COMPOSIÇÃO

Cada 1 mL de solução injetável contém:

Hialuronato de sódio 10 mg

Excipientes: cloreto de sódio, fosfato de sódio dibásico dodecaidratado, fosfato de sódio monobásico di-hidratado e água para injetáveis.

ANEXO III

Boletim técnico do hialuronato de sódio do fabricante Mapric.

ÁCIDO HIALURONICO - SOLUÇÃO 1%

INCI Name: Sodium Hyaluronate and water (1% solution).

DEFINIÇÃO:

O Ácido Hialurônico é obtido a partir da fermentação de substratos de plantas. A biossíntese é realizada por um *Streptococcus*. A solução é obtida pela simples dispersão do ácido hialurônico em pó na água deionizada.

ESPECIFICAÇÃO:

Parâmetros

Aparência	Líquido límpido
Cor	Incolor
Odor	Fraco, característico
pH direto	6,00 - 8,00
Densidade (g/cm ³)	0,900 – 1,100
Solubilidade	Solúvel em água; insolúvel em etanol e óleo mineral.